Functional characterization of an AMPA receptor auxiliary subunit GSG1L *in vivo*

By

Aichurok Kamalova

Dissertation

Submitted to the Faculty of the

Graduate School of Vanderbilt University

in partial fulfillment of the requirements

for the degree of

DOCTOR OF PHILOSOPHY

In

Neuroscience

December 12, 2020

Nashville, Tennessee

Approved:

Terunaga Nakagawa, M.D., Ph. D., Advisor

Roger Colbran, Ph.D., Committee Chair

Ege Kavalali, Ph.D.

Eric Delpire, Ph. D.

Sachin Patel, M.D., Ph. D

DEDICATION

to my Mama and Papa,
my constant source of love and support

ACKNOWLEDGEMENTS

This work would not have been possible without the guidance and support of many incredible people that I am so very lucky to have in my life.

First, I would like to thank my advisor and mentor, Dr. Teru Nakagawa, for his guidance throughout these years that shaped every aspect of my training. He has been extremely patient with me and showed by example the significance of critical thinking and rigorous science. I would not be writing this thesis if not for his constant guidance, mentoring, and support throughout these years. I also want to thank previous members of the Nakagawa lab, specifically Elena and Caleigh. Thank you for being supportive labmates and welcoming me into the lab.

I would also like to thank my thesis committee, Drs. Roger Colbran, Eric Delpire, Ege Kavalali, and Sachin Patel. Specifically, I would like to thank Dr. Roger Colbran for his constant support and mentoring during and after Vanderbilt International Scholars Program. Dr. Roger Colbran and Dr. Ege Kavalali, I also thank you for your support and guidance with navigating career opportunities. Thank you Dr. Eric Delpire for your help and guidance with establishing mutant mouse lines that I used throughout my studies.

Thank you to all my friends, who have made this whole journey a lot more exciting and fun. Thank you for always showing up, be it to eat at random hours, run races with me, or fly across the world on a Christmas day for our wedding.

I especially want to thank my Mom and Dad, who have been my biggest supporters and cheerleaders. My Dad, a scientist himself, has been and always will be my first and favorite mentor. My parents have been the pillars of support and love throughout these years.

I also want to thank my three amazing brothers, my baby nephew, and sisters in law- for always being there for me and for lifting me up when things were hard.

Lastly, I want to thank my husband, for making me laugh throughout these six years in graduate school. Thank you for being my best friend and biggest supporter. I wouldn’t have done this without you by my side.

Table of Contents

Page

LIST OF FIGURES

LIST OF ABBREVIATIONS

AD	Anterodorsal
AV	Anteroventral
AM	Anteromedial
AMPA	α-Amino-3-hydroxy-5-methyl-4-isoxazolepropionic acid
AMPAR	α-Amino-3-hydroxy-5-methyl-4-isoxazolepropionic acid receptor
ANOVA	Analysis of variance
Ca^{2+}	Calcium
CA1	*Cornu Ammonis* 1
CaMKII	Ca^{2+}/calmodulin-dependent kinase II
CKAMP	Cysteine-knot AMPAR modulating protein
CNIH	Cornichon homolog protein
CNS	Central nervous system
CP-AMPAR	Calcium-permeable AMPA receptor
CTZ	Cyclothiazide
CTD	C-terminal domain
C-tail	Cytoplasmic tail
DBS	Deep brain stimulation
DG	Dentate gyrus
ECD	Extracellular domain
EGL	External granule layer

EM	Electron microscopy
E/I	Excitation/inhibition balance
EPSCs	Excitatory postsynaptic currents
ER	Endoplasmic reticulum
ES	Embryonic stem cells
GABA	γ-aminobutyric acid
GABAA	γ-aminobutyric acid receptor A
GSG1L	Germ cell-specific gene 1 like protein
ID	Intellectual disability
i.p.	Intraperitoneal
KAR	Kainate receptor
KO	Knockout
KI	Knockin
lacZ	Encodes β-galactosidase
LD	Lateral dorsal nucleus
LTP	Long-term potentiation
LTD	Long-term depression
LBD	Ligand-binding domain
LC-MS/MS	Liquid chromatography-tandem mass spectroscopy
LRRTMs	Leucine-rich repeat (LRR)-containing transmembrane proteins
MAGUK	Membrane-associated guanylate kinase
mEPSCs	Miniature excitatory postsynaptic currents

MTR	Missense tolerance ratio
NMDA	*N*-methyl-D-aspartic acid
NMDAR	*N*-methyl-D-aspartic acid receptor
NBQX	2,3-dioxo-6-nitro-7-sulfamoyl-benzo[f]quinoxaline
NTD	N-terminal domain
NOR	Novel Object Recognition
P	Postnatal
PDZ	PSD-95, Drosophila disc large suppressor (Dlg1) and zonula occludens-1 protein (zo-1)
PICK1	Protein interacting with C kinase 1
PKC	Protein kinase C
PSD	Postsynaptic density
PSD-95	Postsynaptic density protein 95
PPR	Paired pulse ratio
SNP	Single nucleotide polymorphism
SynDig	Synapse differentiation-inducing gene protein
SWD	Spike-wave discharges
TARP	Transmembrane AMPA receptor regulatory protein
TM	Transmembrane helix
Tsc	Tuberous sclerosis complex
TTX	Tetrodotoxin
qEPSCs	Quantal excitatory postsynaptic currents
UPR	Unfolded protein response

X-gal	5-Bromo-4-Chloro-3-Indolyl β-D-Galactopyranoside

1. Introduction

Synaptic transmission is the main form of neuronal communication within the brain. The remarkable ability of synapses to change their strength and structure has profound effects on how information is processed. Ionotropic glutamate receptors are ligand gated ion channels that mediate the vast majority of excitatory synaptic transmission in the brain. Among these, α-amino-3-hydroxy-5-methyl-4-isoxazolepropionic acid receptors (AMPARs) mediate the majority of fast, moment-to-moment, neurotransmission. Changes in AMPAR density or gating properties are key determinants of synaptic plasticity, learning and memory (Huganir & Nicoll, 2013). Therefore, understanding the precise molecular mechanisms that contribute to and determine AMPAR biogenesis is key for better understanding of how information is stored in the brain and for better development of optimal therapeutic approaches.

The majority of AMPAR at the synapse are bound to a diverse structurally unrelated set of auxiliary subunits that fine tune the function and expression of AMPARs. Collective work over the past 20 years suggests that auxiliary subunits are critical for proper AMPAR function in synapses. Auxiliary subunits have distinct receptor regulatory properties including synaptic trafficking and regulation of biophysical properties of gating. As such, auxiliary subunits are essential for proper functioning of AMPARs, and hence for normal brain function. The composition of AMPAR complexes differ across brain regions, as well as during development, adding a layer of diversity to AMPAR functional profile within the CNS. The vast majority of known auxiliary subunits positively modulate AMPAR function. In contrast, GSG1L stands out for having a strong net receptor regulatory role.

The body of work in this dissertation will focus on characterizing the physiological role of this relatively new and under-studied auxiliary subunit, GSG1L. To put our findings in a better context, in this introductory Chapter 1, I will provide a brief overview of AMPAR regulation and detailed characterization of known AMPAR auxiliary subunits focusing on their roles in regulating AMPAR channel gating, trafficking, and synaptic plasticity. The majority of the work in this dissertation will be focused on characterizing the function of GSG1L primarily in one distinct brain region, the anterior thalamus. Therefore, the final parts of this Chapter will provide an overview of the circuitry and function of anterior thalamic nuclei.

1.1. Excitatory synaptic transmission

The mammalian brain is an intricate network comprising billions of neurons, each making thousands of connections, called synapses, with other neurons. Synapses are critical junctions where the electrical activity of a presynaptic neuron is generally transmitted through neurotransmitter release, which may either excite or inhibit a postsynaptic neuron. Synapses are functional units of complex brain circuits underlying all of our basic and higher-order brain functions, such as learning and memory. Dynamic changes in the strength of synaptic connections are postulated to underlie information storage essential for learning and memory (Huganir & Nicoll, 2013).

Glutamate is the principal excitatory neurotransmitter in the central nervous system (CNS) (Curtis *et al.*, 1959; Fonnum, 1984). Arrival of an action potential at a presynaptic neuron triggers the release of glutamate, which diffuses across the synaptic cleft and at the

postsynaptic site activates a family of ionotropic glutamate receptors (iGluRs) at excitatory central synapses, thereby underlying the majority of excitatory neurotransmission in the brain.

One of the key features of excitatory synapses is the functional specialization of a postsynaptic membrane, juxtaposed to presynaptic release sites, called postsynaptic density (PSD). The PSD is an electron-dense, thick morphological specialization packed with receptors, scaffolding proteins, cytoskeletal components, signaling enzymes, and other membrane proteins allowing for better coupling of receptor activation upon ligand binding with downstream signaling molecules (Kim & Sheng, 2004). Activation of glutamate receptors depolarizes the postsynaptic membrane initiating a cascade of signaling mechanisms activating downstream effectors (Niciu *et al.*, 2012). As a whole, iGluRs govern the vast majority of excitatory neurotransmission within the brain and their dysfunction is implicated in various neurological conditions, including Alzheimer's disease, motor neuron disease, and seizures (Bowie, 2008). Ionotropic glutamate receptors are pharmacologically classified into *N*-methyl-D-aspartic acid receptors (NMDARs), AMPAR, and kainate receptors (KARs), that all gate cations upon glutamate-induced activation (Traynelis *et al.*, 2010).

Early investigations determined that glutamate is abundantly present in the CNS (Berl & Waelsch, 1958) and was later shown to have powerful excitatory effect both depolarizing and increasing action potential firing of neurons in the spinal cord (Curtis *et al.*, 1959, 1960). Following this seminal discovery of glutamate as an excitatory neurotransmitter in the CNS, identification of the receptors at the postsynaptic site was not immediate. The iGluR members were first identified at the pharmacological level and were only later

cloned (Hollmann & Heinemann, 1994). GluR1 was the first AMPAR subunit that was cloned (Hollmann *et al.*, 1989) with subsequent cloning of GluR2-GluR4 (Keinanen *et al.*, 1990; Nakanishi *et al.*, 1990; Sakimura *et al.*, 1990; Puckett *et al.*, 1991; Potier *et al.*, 1992; Sun *et al.*, 1992). These core receptor subunits share 70% sequence homology and response to pharmacological application of AMPA (Lodge, 2009).

1.2. An overview of ionotropic glutamate receptor signaling

1.2.1. Ionotropic Glutamate Receptors

Among the iGluRs, AMPAR is the workhorse of fast excitatory neurotransmission transducing at a sub-millisecond timescale (Traynelis *et al.*, 2010; Huganir & Nicoll, 2013; Greger *et al.*, 2017). Activation of AMPARs in turn results in rapid depolarization of the postsynaptic membrane. In addition to fast activation and deactivation kinetics, AMPARs undergo rapid and pronounced desensitization while bound to glutamate, which in turn is critical for neuroprotection against overt excitotoxicity in the brain (Christie *et al.*, 2010). NMDARs, on the other hand, have significantly slower gating kinetics with activation and deactivation in tens and thousands of milliseconds and are subject to relatively weak or no desensitization (Traynelis *et al.*, 2010).

AMPAR induced postsynaptic depolarization allows the relieve of voltage-dependent Mg^{2+} block of the NMDAR, resulting in entry of Ca^{2+} ions and downstream signaling cascades (Mayer *et al.*, 1984; Huganir & Nicoll, 2013). The extent of AMPAR gating and the overall density of receptors are considered to be key determinants of synaptic

plasticity, learning and memory (Newpher & Ehlers, 2008; Huganir & Nicoll, 2013). Given its fundamental role for normal brain function, AMPAR dysfunction is associated with a wide range of neurological conditions, such as Rasmussen's encephalitis (Rogers *et al.*, 1994) and Alzheimer's disease (Hsieh *et al.*, 2006).

1.2.2. AMPARs mediate fast excitatory neurotransmission

AMPARs are homo- and heterotetramers of highly homologous subunits GluA1-4 (Collingridge *et al.*, 2009) (Figure 1.1). The functional identity of AMPARs at the synapse is defined by the channel pore-forming core subunits (Wenthold *et al.*, 1996), alternative splicing (Sommer *et al.*, 1990), RNA editing (Rueter *et al.*, 1995), posttranslational modifications (Lee *et al.*, 2003), and binding of various auxiliary subunits (Jackson & Nicoll, 2011).

While the majority of AMPARs in the brain contain GluA2, the absence of GluA2 subunit renders AMPARs calcium-permeable (CP-AMPARs). The vast majority of GluA2 subunits in the brain undergo RNA editing resulting in the modified receptor pore impermeable to calcium ions (Cull-Candy *et al.*, 2006). Following RNA editing, a key residue (glutamine) within the pore becomes an arginine resulting in calcium impermeability. In addition to being calcium permeable, CP-AMPARs have an inward rectifying current-voltage relationship and sensitivity to block by endogenous intracellular polyamines (Bowie & Mayer, 1995; Kamboj *et al.*, 1995; Koh *et al.*, 1995). Deficiency in the RNA editing at this key site within the channel pore is associated with lethality (Higuchi *et al.*, 2000).

AMPARs consist of four domains including the N-terminal domain (NTD), ligand-binding domain (LBD), membrane-embedded transmembrane domain (TMD), and a cytoplasmic C-terminal domain (CTD) (Figure 1.1). The N-terminal domain (NTD) in the extracellular space is most distantly positioned relative to the membrane. The function of the NTD is least understood, but it is critical for subunit assembly (Ayalon & Stern-Bach, 2001; Rossmann *et al.*, 2011) as well as receptor clustering and synaptic localization (Sia *et al.*, 2007; Garcia-Nafria *et al.*, 2016; Diaz-Alonso *et al.*, 2017; Watson *et al.*, 2017). Region C-terminal to the NTD forms a short linker that connects the NTD to the ligand-binding domain (LBD). Upon glutamate binding, the LBD undergoes conformational changes that result in channel gating (Armstrong *et al.*, 1998; Armstrong & Gouaux, 2000; Chen *et al.*, 2017; Twomey *et al.*, 2017b). The LBD connects to the transmembrane domain (TMD), which consists of three membrane spanning segments (M1, M3, and M4) and a re-entrant helix-loop (M2) (Hollmann *et al.*, 1994) (Figure 1.1.). Namely, in the primary structure the LBD is divided by the M1-3 of the TMD into two fragments, S1 and S2. The TMD forms an ion channel in the membrane that when open, conducts cations (Figure 1.1).

Finally, there is a cytoplasmic C-terminal domain (CTD) that regulates anchoring, signaling, and trafficking (Kim & Sheng, 2004; Huganir & Nicoll, 2013). The subunit composition of AMPARs is spatio-temporally regulated based on developmental stage and specific brain regions and cell-types within given brain structures (Henley & Wilkinson, 2016). In adult rodent brains, the majority of AMPARs consist of GluA1/GluA2 and GluA2/GluA3 containing heterotetrameric receptors (Wenthold *et al.*, 1996; Lu *et al.*, 2009; Zhao *et al.*, 2019). One of the contributing factors for the formation of primarily

heterotetramers, and fewer homomers, is the increased affinity of NTD of different GluA subunits relative to identical NTD subunits (Greger *et al.*, 2017).

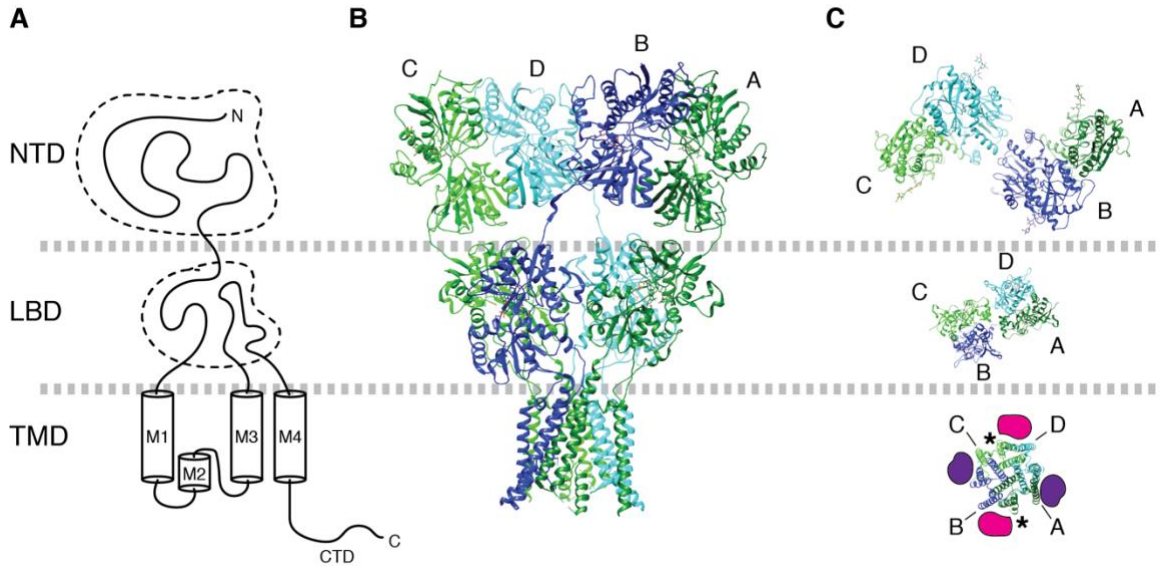

Figure 1-1. Architecture of AMPARs.

A. Domain organization of an AMPAR subunit. B. Architecture of tetrameric assembly of GluA subunits in the canonical 'Y' shape. Subunits are labeled as A (dark green), B (blue), C (green), and D (cyan). PDB model 3KG2 (Sobolevsky *et al.*, 2009) is displayed. C. The NTD, LBD, and TMD layers are viewed from top. The dimer pairs formed at NTD and LBD layer are different; A/B and C/D at NTD, whereas A/D and B/C at LBD. The TMD is pseudo four-fold symmetric. Labels A-D point to the M4 helix of each subunit. In the TMD, the A/B surface is equivalent to the C/D surface (magenta). Similarly, the B/D surface and A/D surface are equivalent. The locations indicated by magenta and yellow are the binding site for TARPs and CNIH3. The asterisk indicates the locations of lipids found in AMPAR/TARP γ-8 complex (Herguedas *et al.*, 2019). Adapted with permission from (Kamalova & Nakagawa, 2020).

1.2. An overview of AMPAR auxiliary subunits

1.3.1. Transmembrane AMPAR regulatory protein (TARP) family

The majority of the AMPARs in the brain form complexes with various auxiliary subunits that do not build the channel pore but physically interact with pore forming subunits (Jackson & Nicoll, 2011). AMPAR auxiliary subunits contribute to the modulation of almost every aspect of AMPAR biogenesis including trafficking of the receptor, localization within the synapse, channel gating, and pharmacology. Importantly, auxiliary subunits differ in their AMPAR modulation and also display a distinct spatio-temporal expression profile within the brain. The overall composition of AMPAR complexes may also differ among given synapses within a neuronal population. Therefore, a given homo- or heterotetrameric receptor core can acquire distinct functional properties by binding to specific class and subtype of auxiliary subunits. This in turn enriches the overall functional repertoire of AMPAR complexes and ultimately influences information processing in the brain.

AMPAR auxiliary subunits are structurally-unrelated transmembrane proteins that selectively interact with the core receptor and are essential for optimal receptor function (Figure 1.2) (Jackson & Nicoll, 2011). Stargazin is the founding member of AMPAR regulatory protein (TARP) family (Chen *et al.*, 2000; Tomita *et al.*, 2003; Kato *et al.*, 2008). Other auxiliary subunits include cornichon homologues 2 and 3 (CNIH2/3) (Schwenk *et al.*, 2009), CKAMP44 (Cysteine-knot AMPAR modulating protein of 44 kDA, also known as Shisa9) (von Engelhardt *et al.*, 2010), Shisa6 (Klaassen *et al.*, 2016), and GSG1L (Schwenk *et al.*, 2012; Shanks *et al.*, 2012). The two most abundant AMPAR auxiliary

subunits in the hippocampus, cortex, and striatum are predicted to be TARPs and CNIHs (Schwenk *et al.*, 2014a) . Other auxiliary subunits may be enriched in smaller populations of neurons within these regions.

The first AMPAR auxiliary subunit was identified through characterization of the *stargazer* mouse, which contained a spontaneous mutation in an inbred mouse line. The mutation caused prominent phenotype of dyskinesia, severe ataxia, characteristic head-tossing behavior, and prominent spike-wave dischargers (SWDs) analogous to absence epilepsy in human patients (Hashimoto *et al.*, 1999; Chen *et al.*, 2000). Positional cloning mapped the causative mutation in a tetraspanin protein that shared 23% sequence homology with the γ-1 subunit of 1,4-dyhydropyridine (DHP)-sensitive calcium channels in skeletal muscle and hence was named γ-2 (also known as stargazin) (Letts *et al.*, 1998). The hallmark of *stargazer* mutant mice is the complete loss of AMPAR-mediated synaptic currents at the mossy fiber to cerebellar granule cell synapses (Hashimoto *et al.*, 1999; Chen *et al.*, 2000).

Transfection of recombinant stargazin into cultured cerebellar neurons from *stargazer* mice rescues the mutant phenotype (Tomita *et al.*, 2003). Stargazin is essential for delivering AMPARs to the membrane in cerebellar granule cells and its distal PDZ-binding motif at C-terminal tail regulates synaptic clustering of AMPARs. In line with these results, subsequent studies demonstrated that stargazin directly binds to PSD-95, a major scaffold at excitatory postsynaptic site, as well as other members of membrane-associated guanylate kinase (MAGUK) family (Schnell *et al.*, 2002). Based on sequence homology and functional similarities, TARPs are subdivided into canonical type I stargazin (γ-2), γ-3, γ-4, and γ-8, and type II γ-5 and γ-7 (Tomita *et al.*, 2003). Type I TARPs contain

a canonical PDZ binding motif, whereas type II TARPs have an unconventional PDZ binding motif (Tomita *et al.*, 2003). Multiple sites in the C-tail of TARPs mediate binding to PSD-95, and the formation of the complex induces liquid phase separation, which in turn can affect AMPAR synaptic localization and ultimately influence synaptic transmission (Zeng *et al.*, 2019b). As a whole, TARPs share 60% sequence similarity with each other (Tomita *et al.*, 2003).

AMPAR auxiliary subunits are evolutionary conserved with TARP homologs identified in *Danio rerio, C.elegans, Apis mellifera, and Drosophila melanogaster* (Walker *et al.*, 2006; Wang *et al.*, 2008; Roy *et al.*, 2016). GLR-1, a *C elegans* AMPAR homolog, requires TARP homologs STG-1 or STG-2 and a structurally unrelated transmembrane auxiliary subunit SOL-1 for normal receptor function (Walker *et al.*, 2006). Additionally, a stargazin ortholog, Cacng2a, was identified in developing zebrafish. Cacng2a is critical for AMPAR function in zebrafish Mauthner cells since the knockdown of Cacng2a results in reduced AMPAR-mediated synaptic currents (Roy *et al.*, 2016). Therefore, TARPs appear to be evolutionary conserved gatekeepers of AMPAR function.

1.3.2. An overview of non-TARP classes of auxiliary proteins

Following the initial discovery and characterization of stargazin and other members of the TARP family, multiple proteomic screens and genetic data mining projects have been undertaken to uncover novel AMPAR interactors. CNIH2 and CHIN3 were identified through a proteomic analysis of AMPAR complexes from rat brains (Schwenk

et al., 2009). Recent structural investigations have shown that CNIHs consist of four hydrophobic helices (TM1-TM4) and an extracellular amino terminus (Nakagawa, 2019) (Figure 1.2. and 1.3.).

CKAMP44 (also known as shisa9) was also identified through a proteomic screen of purified AMPAR complexes from mouse brains (von Engelhardt *et al.*, 2010). Among all of the auxiliary subunits, CKAMP44 stands out for having a N-terminal cysteine-knot domain (Figure 1.2.). Further database search identified three other members of the CKAMP protein family, CKAMP39 (shisa8), CKAMP52 (shisa6), CKAMP59 (shisa7) which have also been shown to interact with AMPARs and modulate their function (Jacobi & von Engelhardt, 2018). Among these, the function of CKAMP39 in the brain has yet to be described. Furthermore, a recent study has shown that CKAMP59 may in fact be an auxiliary subunit of type A γ-aminobutyric acid (GABAA) receptors (Han *et al.*, 2019) . Therefore, further detailed studies are needed to determine the overall synaptic function of CKAMP39 and CKAMP59.

GSG1L was simultaneously and independently identified as a novel AMPAR auxiliary subunit with unique AMPAR regulatory functions (Schwenk *et al.*, 2012; Shanks *et al.*, 2012). Shanks et al., identified GSG1L through immunopurification of native AMPARs followed by shotgun liquid chromatography-tandem mass spectroscopy (LC-MS/MS) protein analysis. GSG1L was shown to be expressed in rat brain and co-purify with native AMPARs (Shanks *et al.*, 2012). GSG1L is a distant homolog of TARPs also belonging to an extended tetraspanin claudin superfamily (Figure 1.2.). Post embedding immunogold electron microscopy and immunocytochemistry showed that GSG1L co-

localizes with AMPARs in dendritic spines of cultured neurons (Shanks *et al.*, 2012; Schwenk *et al.*, 2014a). GSG1L is structurally similar to TARPs, with four

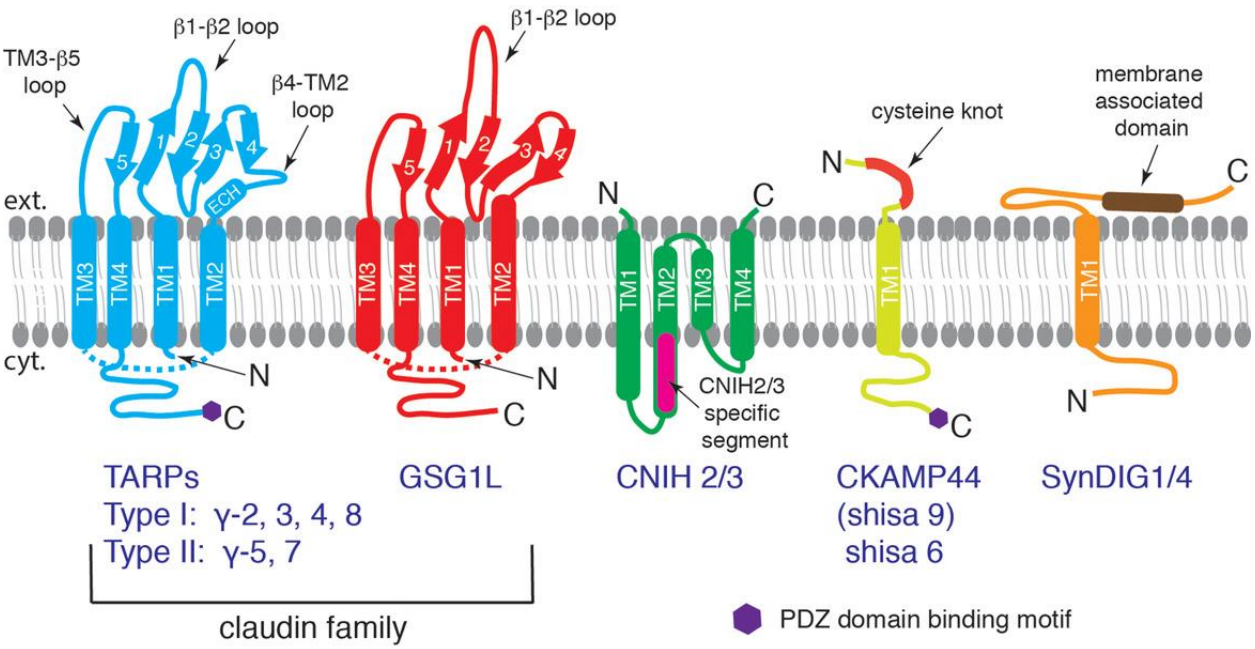

Figure 1-.2. Structurally unrelated classes of AMPAR auxiliary subunits.

TARPs (type I: γ-2, 3, 4, 8 with a canonical PDZ binding motif; type II: γ-5, 7 with an atypical PDZ binding motif) and GSG1L belong to the claudin superfamily. The α-helices (thick tubes) and β-strands (thick arrows) are depicted. Both subclasses contain four transmembrane domains, two extracellular loops and a cytoplasmic C-terminal tail. The β1–β2 loop is significantly longer in GSG1L. TM1~TM4 fold as a helical bundle, and therefore, the cytoplasmic TM2–TM3 loops of TARP and GSG1L (dashed lines) are shorter than how they are illustrated. CNIH is also a four-pass transmembrane protein, which is mostly embedded within the membrane. The N- and C-termini of CNIH are both extracellular. The CNIH2/3 specific segment, absent in CNIH1/4, is indicated (magenta). CKAMP44 (Shisa9) and Shisa6 have one transmembrane domain with an extracellular cysteine-knot motif and a long intracellular C-terminal tail with type II PDZ binding motif. SynDIG1 and 4 have one transmembrane domain and a long extracellular domain containing a membrane-associated domain. Adapted with permission from (Kamalova & Nakagawa, 2020).

transmembrane helices (TM1-TM4) with the N-terminus in the cytoplasm, immediately preceding TM1 (Figure 1.2.). TM1-TM4 of TARPs and GSG1L forms a twisted bundle in the membrane. The extracellular extensions that are connecting the transmembrane helices fold into an extracellular domain (ECD). The ECD is made of five β-strands (β1-5) and four flexible loops (β1- β2, β3- β4, β4-TM2, TM3- β5) (Figure 1.2.).

1.3.4. Structural characterizations of AMPAR-auxiliary subunit complexes.

The recombinant AMPAR-TARP complexes were studied extensively using cryo-EM, generating detailed information about their architectures (Twomey *et al.*, 2016; Zhao *et al.*, 2016; Chen *et al.*, 2017; Twomey *et al.*, 2017b; Herguedas *et al.*, 2019; Twomey *et al.*, 2019). The overall architecture of TARPs is similar to those of claudins (Suzuki *et al.*, 2014; Saitoh *et al.*, 2015; Nakamura *et al.*, 2019). The topology of TARPs comprises four transmembrane helices (TM1-4) with the N-terminus in the cytoplasm, immediately preceding TM1. TM1-4 forms a twisted bundle in the membrane. A cytoplasmic C-terminal tail (C-tail) extends from the TM4 and terminates with a PDZ domain ligand peptide. Consistently, the C-tail is unresolved in the available cryo-EM structures, possibly due to its flexibility or truncation from the constructs.

TARPs bind preferentially to the tetrameric AMPARs (Vandenberghe *et al.*, 2005; Shanks *et al.*, 2010), and consistently, the TARP binding site spans across adjacent subunits of AMPARs. Specifically, the M1 and M4 of adjacent GluA subunits interface with the TM3 and TM4 of TARPs The structurally confirmed stoichiometries of the complexes are four,

two, or one TARPs per tetrameric AMPAR (Twomey *et al.*, 2016; Zhao *et al.*, 2016; Chen & Gouaux, 2019; Herguedas *et al.*, 2019). Studies have compared functional signatures of neuronal AMPARs with heterologously expressed AMPAR-TARP complexes made of defined stoichiometry, by covalently linking TARPs and GluAs and titrating the number of bound TARPs, suggested the presence of AMPARs with two and four TARPs (Shi *et al.*, 2009; Dawe *et al.*, 2019).

Binding interfaces between AMPARs and TARPs proposed from structural studies are suggested to be functionally critical for gating (or modulation) (Chen *et al.*, 2017; Twomey *et al.*, 2017b). Indeed, receptors with mutations located at these interfaces exhibit abnormal gating behaviors, indicating the physiological relevance of these structurally defined interaction sites (Priel *et al.*, 2005; Tomita *et al.*, 2005a; Dawe *et al.*, 2016; Hawken *et al.*, 2017a; Riva *et al.*, 2017).

The residue contacts between the transmembrane helices of AMPAR and TARP are also critical for gating modulation, because the mutations in this region abolish slowing of desensitization imposed by TARPs (Ben-Yaacov *et al.*, 2017; Hawken *et al.*, 2017a). How this interaction regulates gating behavior remains elusive. The initial functional mappings of TARP γ-2 also suggested that the CTD is also critical for gating modulation (Priel *et al.*, 2005; Tomita *et al.*, 2005a; Milstein & Nicoll, 2009), but the underlying mechanism is unclear. Further investigations that combine structural biology, channel physiology, and molecular dynamic simulation, may provide information to improve our understanding of the mechanism of TARP action.

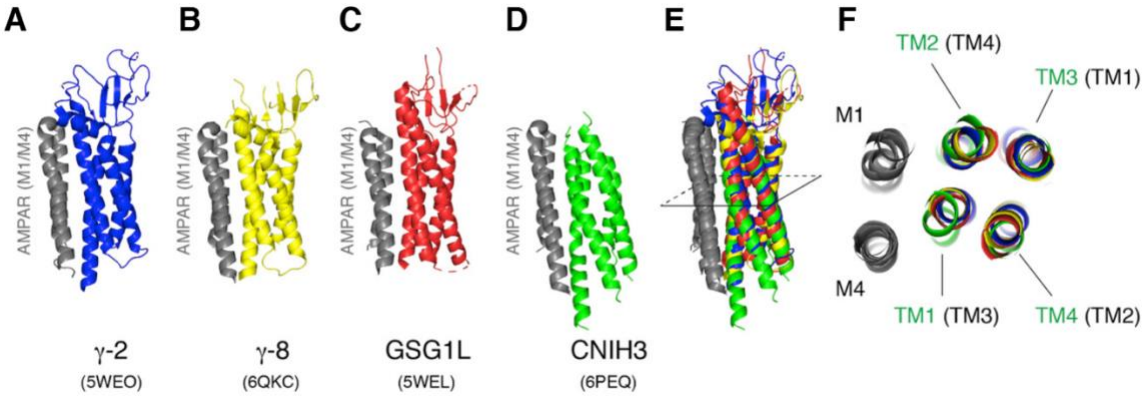

Figure 1-3. AMPAR-auxiliary subunit binding interface.

A-D. ribbon diagram of the M1 and M4 of AMPAR (grey) bound to various auxiliary subunits. The binding interface is viewed from the side in parallel to the membrane. A. TARP γ-2; B. TARP γ-8; C. GSG1L; D. CNIH3. E. Superposition of the structures in C–F. Specifically, when the M4 of AMPAR in *C–F* is aligned, the M1 and the transmembrane helices of the auxiliary subunits superimpose. The M1–M4 of AMPARs form the auxiliary subunit binding module for TARPs, GSG1L and CNIH3, and are geometrically conserved. F. Cross section at the slice shown in E. viewed from the top. The TM3 and TM4 (of TARP and GSG1L) interface with M1 and M4 of the adjacent subunit of AMPAR. In contrast, the TM1 and TM2 of CNIH3 interface with M1 and M4. TM1–TM4 of CNIH3 are labelled in green, and the corresponding TM in TARPs and GSG1L are labelled in black and in brackets. Adapted with permission from (Kamalova & Nakagawa, 2020).

Recent structural investigations have revealed that GSG1L folds like TARPs and binds to the same surface on the AMPAR to which TARPs bind (Twomey *et al.*, 2017c). Unlike TARPs, which were shown to be able to simultaneously bind up to four molecules per AMPAR tetramer, current cryo-EM structures contain only up to two GSG1L per AMPAR tetramer (Twomey *et al.*, 2017a, c). A notable difference between GSG1L and TARPs is the significantly longer β1- β2 loop in GSG1L. These structural differences contribute to the drastic functional differences between GSG1L and TARPs. Importantly, transplanting the β1- β2 loop of stargazin into the corresponding location in GSG1L is sufficient for GSG1L to acquire stargazin-like AMPAR modulatory characteristics (Riva *et al.*, 2017; Twomey *et al.*, 2017c). Remarkably, TARPs, CNIHs, and GSG1L all bind to identical surfaces on AMPARs.

1.4. Role of Auxiliary subunits in channel gating and trafficking

1.4.1. Auxiliary subunits positively regulate AMPAR channel function

The association of auxiliary subunits with the receptor core adds functional diversity to biophysical properties of channel gating and pharmacology in addition to receptor localization (Jackson & Nicoll, 2011). Furthermore, in addition to peak amplitude, the kinetics of AMPAR gating including rise time, deactivation and desensitization, and recovery from desensitization all contribute to determining to AMPAR gating and thus, have profound consequences on synaptic communication. As a whole, TARPs are considered to be positive modulators of AMPAR synaptic function through enhancement

in charge transfer and slowing the overall time course of synaptic current thereby increasing the size of postsynaptic currents (Jackson & Nicoll, 2011).

In vitro characterization determined that most auxiliary subunits slow deactivation rates of AMPARs, except for TARP γ-5 which significantly enhances the deactivation rate. In neurons, genetic deletion of TARP γ-8, CNIH2/3, CKAMP44, and shisa6 leads to decreased deactivation rates in the hippocampus (Rouach *et al.*, 2005; Herring *et al.*, 2013; Boudkkazi *et al.*, 2014; Klaassen *et al.*, 2016). Within Type I TARPs, there is a further sub-division into type-1b (TARP γ-4 and γ-8) and type-1a (TARP γ-2 and γ-3) subclasses. Type-1b TARPs slow desensitization and deactivation to a greater extent than type-1a TARPs do (Cho *et al.*, 2007; Milstein *et al.*, 2007).

In addition to TARPs, CNIH2/3 and CKAMP protein family also increase mean channel conductance of AMPARs (Jackson & Nicoll, 2011; Coombs *et al.*, 2012; Khodosevich *et al.*, 2014). TARPs and CNIHs also positively modulate the function of CP-AMPARs by increasing relative calcium permeability of CP-AMPARs (Tomita *et al.*, 2005a; Kott *et al.*, 2009; Coombs *et al.*, 2012). Furthermore, TARPs and CNIHs increase average single-channel conductance, slow desensitization and deactivation of CP-AMPARs (Tomita *et al.*, 2005a; Kott *et al.*, 2009; Coombs *et al.*, 2012). TARPs are also known to notably attenuate the intracellular polyamine block of CP-AMPARs (Soto *et al.*, 2007). Overall, TARPs and CHINs enhance the function of CP-AMPARs by increasing the net charge transfer by increasing the current amplitudes and the time course of currents.

1.4.2 GSG1L negatively regulates AMPAR channel function

As mentioned above, the majority of AMPAR auxiliary subunits positively modulate AMPAR function, by promoting synaptic trafficking and/or modifying gating towards increasing net charge transfer (Jackson & Nicoll, 2011). A subset of auxiliary subunits has mixed effects on gating. For example, CKAMP44 slows AMPAR deactivation, increasing net charge transfer during synaptic transmission, but also delays recovery from desensitization, making the channel not re-usable immediately (von Engelhardt *et al.*, 2010). Similarly, TARP γ-8 slows AMPAR desensitization and delays recovery from AMPAR desensitization of GluA2 and GluA3 specifically (Cais *et al.*, 2014). Among all of the auxiliary subunits, GSG1L stands out for having a strong net negative modulatory function (McGee *et al.*, 2015; Gu *et al.*, 2016; Mao *et al.*, 2017).

Although GSG1L also slows desensitization, it stabilizes the desensitized state (Twomey *et al.*, 2017c) and dramatically delays recovery from desensitization, over a magnitude slower than any other auxiliary subunit (Schwenk *et al.*, 2012; Shanks *et al.*, 2012). Additionally, GSG1L reduces mean single-channel conductance and calcium permeability of CP- AMPARs (McGee *et al.*, 2015). Consistently, overexpression of GSG1L decreases the amplitude of evoked excitatory postsynaptic currents (EPSCs) (McGee *et al.*, 2015; Gu *et al.*, 2016; Mao *et al.*, 2017). Dysregulation of CP-AMPARs has been previously hypothesized to contribute to cell damage after stroke and drug abuse (Cull-Candy *et al.*, 2006). Given the negative regulatory properties of GSG1L on CP-AMPAR function, it is intriguing to speculate its role, if any, in dynamically controlling CP-AMPAR function, thereby mitigating excitotoxic effects of excess calcium-entry

through the channel. In turn, it is possible that gain of function of GSG1L is protective against excess AMPAR activation, which otherwise results in excitotoxicity.

Despite its pronounced negative effect on AMPAR function, GSG1L expression in the brain is low compared to other auxiliary subunits (Schwenk *et al.*, 2014b) and it is unclear to what extent it is utilized *in vivo*. In particular, previous studies using GSG1L knockout (KO) rats reported a modest phenotype in the hippocampus and failed to identify synapses that express the signatures of GSG1L dependent AMPAR gating modulation, compounded by co-expression of another auxiliary subunit CNIH2 (Gu *et al.*, 2016).

Gu et al., showed that GSG1L overexpression in hippocampal CA1 neurons results in decreased AMPAR EPSCs, highlighting the negative effect on AMPAR function (Gu *et al.*, 2016). Interestingly, in striking contrast to results from heterologous systems, overexpression of GSG1L in CA1 pyramidal neurons fastened deactivation and desensitization kinetics and accelerated the recovery from desensitization. The authors speculated that the marked discrepancy with the heterologous system data is due to the presence and regulatory effects of other molecular players in a more physiologically relevant neuronal system. In order to further interrogate the physiological role of GSG1L, Gu et al. used a GSG1L KO rat model. Although there was no histological or biochemical evidence for robust GSG1L expression in hippocampal CA1 neurons, the results reveal increased AMPAR-mediated EPSCs and enhanced LTP in GSG1L KO CA1 neurons. Of note, in situ hybridization data also shows no GSG1L expression in CA1 neurons at the developmental stage used in this study (Lein *et al.*, 2007a).

Taken together, these previous investigations on the synaptic phenotypes of GSG1L KO rats in CA1 and DG neurons (Gu et al., 2016;Mao et al., 2017) were both conducted at

time points when the expression of the lacZ reporter for GSG1L promoter activity is low. Consistently, a previous study on GSG1L KO rat reported a substantial contribution of another auxiliary subunit, CNIH2, superimposed on the functional effect of GSG1L (Gu et al., 2016). The above findings suggest that more detailed description of spatial and temporal expression patterns of GSG1L is needed in order to also characterize the physiological role of GSG1L in regions of the brain where it is highly expressed.

1.4.3. Auxiliary subunits regulate AMPAR trafficking and synaptic localization

AMPAR auxiliary proteins regulate multiple aspects of the AMPAR lifecycle, including early biosynthetic pathways and receptor assembly. AMPARs are assembled in the endoplasmic reticulum (ER) and are subject to quality control mechanisms prior to exiting the ER (Traynelis *et al.*, 2010). Among AMPAR auxiliary subunits, TARPs and CNIHs were shown to be critical for exit from the ER of AMPARs (Jacobi & von Engelhardt, 2018). TARPs bind to AMPAR in the ER and facilitate their exit from ER by promoting receptor maturation. Consequently, the ratio of immature to mature AMPARs in the *stargazer* and γ-3 KO mice is significantly increased (Tomita *et al.*, 2003; Menuz *et al.*, 2008). Similarly, loss of CNIH-2 is associated with changes in AMPAR glycosylation patterns (Herring *et al.*, 2013).

Several mechanisms are proposed for reduced ER export in the absence of AMPAR auxiliary subunits (Jacobi & von Engelhardt, 2018). It has been proposed that binding TARPs to AMPAR in the ER may mask the ER-retention signal and thus aid in the exit

from the ER (Bedoukian *et al.*, 2006). *Stargazer* mutant mice also exhibit enhanced unfolded protein response (UPR) due to overall increase in the misfolded protein content in the ER (Tomita *et al.*, 2003; Vandenberghe *et al.*, 2005). However, future studies will be needed to definitively determine which auxiliary subunits and how they aid in the assembly and exit of AMPARs from the ER.

The PSD95-TARP interaction is particularly interesting, since AMPARs themselves have not been reported to directly interact with PSD95, suggesting that TARPs, through its interaction with PSD-95, may target AMPARs to synapses. In addition to TARPs, CKAMP44 and shisa6 also harbor PSD-95 binding PDZ motif (Karataeva *et al.*, 2014). The PDZ binding motif of shisa6 is critical for anchoring AMPARs at certain synaptic locations and decreasing overall mobility of AMPARs at the membrane (Klaassen *et al.*, 2016). GSG1L and CNIH2/3, on the other hand, do not contain a PDZ binding motif. TARPs and CKAMP44 are predicted to anchor AMPARs at the synapse through their interaction with PSD-95. The C-terminus of stargazin contains nine serine residues that upon phosphorylation are proposed to extend away from the negatively charged phospholipids within the plasma membrane enabling PSD-95 binding (Opazo *et al.*, 2010; Sumioka *et al.*, 2010; Hafner *et al.*, 2015). However, the effect of the phosphorylation on PSD-95 interaction and channel gating is still debated. More recent investigations have shown that phosphomimetic mutations have in fact diminished binding to PSD-95 (Zeng *et al.*, 2019b). Apparent differences in these findings could be due to different experimental approaches between these studies. Nevertheless, future investigations may be needed

1.4.4 Post-translational modification of AMPAR auxiliary subunits

AMPAR-auxiliary subunit complexes may be subject to tight trafficking regulation. Potential posttranslational modifications are candidate mechanisms that could drive this process. For instance, TARPs γ-2 and γ-8 are differentially phosphorylated by protein kinase-C (PKC) (Inamura *et al.*, 2006). CKAMP44, on the other hand, is phosphorylated by PKC and protein interacting with C kinase 1 (PICK1) (Kunde *et al.*, 2017). Glycosylation of TARP γ-8 partially affects surface expression of AMPARs (Zheng *et al.*, 2015). Other auxiliary subunits also have predicted posttranslational modification sites, which have yet to be functionally validated and characterized.

Phosphorylation of TARPs also has consequences on AMPAR synaptic clustering. AMPARs undergo lateral diffusion within the plasma membrane and phosphorylation of stargazin by CaMKII results in clustering of AMPARs (Opazo *et al.*, 2010). Furthermore, AMPAR diffusion is increased following desensitization and it has been hypothesized that unbinding of stargazin is important for the recovery from desensitization (Constals *et al.*, 2015). C-terminus is likely to be unstructured and traditional approaches may not be feasible for structural characterization.

1.4.5. Functional co-expression of auxiliary subunits

In many cases, multiple auxiliary subunits function within a given neuronal population (Tomita *et al.*, 2003; Fukaya *et al.*, 2005; Lein *et al.*, 2007b; Schwenk *et al.*, 2014a). An

exception are the cerebellar granule cells, in which stargazin is the only predominant Type I auxiliary subunit; loss of γ-2 is equivalent to inactivation of granule cell function, which leads to ataxia in *stargazer* mice. The prevailing model suggests that γ-2 is a prominent auxiliary subunit in granule cells and its absence is associated with loss of AMPAR phenotype. However, subsequent studies claimed that type II TARP γ-7 is functionally co-expressed in cerebellar granule cells, where it inhibits the trafficking of calcium- impermeable AMPARs (CI-AMPARs) and enhances the expression of CP-AMPARs (Studniarczyk *et al.*, 2013). Interestingly, knockdown of TARP γ-7, in fact, rescued synaptic AMPAR current as a result of loss of inhibition on CI-AMPARs. However, an independent study showed that γ-7 does not have a postsynaptic function in cerebellar granule cells and that γ-7/ γ-2 double KO exhibit similar lack of synaptic AMPARs as *stargazer* mutant mice (Yamazaki *et al.*, 2015). Apparent discrepancies in these findings could be due to the differences in the experimental approach. Nevertheless, further investigations will be needed to further characterize the function of γ-7 in cerebellar granule cells.

On the other hand, behavioral deficits are not obvious in other TARP knockout models possibly due to functional redundancy among the TARPs (Letts *et al.*, 1998; Hashimoto *et al.*, 1999; Chen *et al.*, 2000; Rouach *et al.*, 2005; Menuz *et al.*, 2008; Menuz *et al.*, 2009). For example, due to co-expression of both proteins, neither single KO of γ-3 or γ-2 is sufficient to elicit deficits in AMPAR function in cerebellar Golgi cells; double KO is necessary to induce severe phenotypes (Menuz *et al.*, 2008; Menuz *et al.*, 2009). A similar functional synergy is observed between γ-8 and γ-2, which are differentially localized within a given hippocampal CA1 neuron (Rouach *et al.*, 2005; Yamazaki *et al.*,

2015). In the cerebellar Purkinje cells, γ-7 and γ-2 TARP exhibit compensatory roles (Yamazaki *et al.*, 2010; Yamazaki *et al.*, 2015).

Functional interactions were also observed across different classes of AMPAR auxiliary subunits. CKAMP44 and TARP γ-8 are co-expressed in the dentate gyrus (DG) granule cells (von Engelhardt *et al.*, 2010). Genetic deletion of TARP γ-8 or CKAMP44 results in the overall reduction in the density of somatic AMPARs—deletion of both results in an even further decrease (Khodosevich *et al.*, 2014). The two have opposing effects on the recovery from AMPAR desensitization, with CKAMP44 significantly slowing this parameter in DG neurons. AMPAR desensitization itself is known to contribute to short-term plasticity (Chen *et al.*, 2000). Consistently, the paired pulse ratio (PPR) of AMPAR mediated EPSCs was increased in CKAMP44 KO mice and decreased in γ-8 KO mice (Khodosevich *et al.*, 2014). Interestingly, γ-8 slows the recovery from desensitization in HEK cells of GluA2 and GluA3 specifically (Cais *et al.*, 2014). This discrepancy between heterologous cells and mouse slice data could be due to other co-existing auxiliary subunits or differing composition of GluA subunits in the same neuron.

While multiple studies have identified functional interactions between auxiliary subunits at the synapse, the signaling pathways that control auxiliary subunit composition remain largely unknown. Gating properties of AMPARs could change significantly if dynamic switching of an auxiliary subunit takes place within the synapse, although currently there is no evidence in support of this hypothesis. Functionally, co-expression of multiple auxiliary subunits with AMPAR leads to composite gating phenotypes in HEK cells. It is becoming clear that more than one type of auxiliary subunit could simultaneously bind to an AMPAR (Kato *et al.*, 2010; Gill *et al.*, 2011; Khodosevich *et al.*, 2014; Zhao *et al.*,

2019). Revealing the regulation of AMPAR complexes in the context of biogenesis may provide critical information. A specialized set of proteins interacts with AMPARs in the early biogenic pathway (Schwenk *et al.*, 2014a; Erlenhardt *et al.*, 2016; Schwenk *et al.*, 2019). Whether and how the assembly is regulated is an important question to address in the future.

1.5. Role of AMPAR auxiliary subunits in synaptic plasticity

1.5.1. Role of auxiliary subunits in short-term plasticity

Gating modulation imposed by auxiliary subunits contribute to short-term plasticity mechanisms in some neurons. While most commonly seen mechanisms for short-term plasticity are presynaptic (Zucker, 1999), postsynaptic mechanisms, such as changes in the rate of desensitization, also occur in the brain (Chen *et al.*, 2002; Kielland & Heggelund, 2002). The overall ultrastructure of the synapse and the presence of neighboring release sites may allow for glutamate to spillover from active to non-active release sites and the overall rate of glutamate clearance from the cleft is slower relative to other synapses due to very low glial ensheathment (Chen *et al.*, 2002). As such, these circumstances allow for AMPARs to enter the desensitized state and desensitization itself can contribute to synaptic transmission, as it was shown for retinogeniculate synapses (Chen *et al.*, 2002).

AMPAR auxiliary subunits can contribute to short-term plasticity by altering the rate of recovery from AMPAR desensitization. In turn, auxiliary subunits affect short-term

plasticity in a complex manner. For example, members of the CKAMP family of proteins, CKAMP44 and Shisa6, slow recovery from desensitization in HEK cells, and thus one would expect that both affect short term plasticity in a similar way. However, genetic deletion studies show opposing effects on short-term plasticity in the hippocampus. CKAMP44 KO mice show decreased short-term depression at the lateral perforant path to DG granule cell synapses (Khodosevich *et al.*, 2014). Shisa6 KO mice, on the other hand, have increased synaptic depression at Schaffer collateral-CA1 synapses (Klaassen *et al.*, 2016). It is predicted that this effect is due to Shisa6 slowing down the entry into the desensitized state. Another possible explanation for the discrepancy between results in HEK cells and neurons could be the presence of other auxiliary subunits or other unknown factors specific to the neuronal cell types. Shisa7, another member of CKAMP family, also slows the recovery from desensitization. However, it has been shown not to regulate short-term plasticity in CA1 neurons (Schmitz *et al.*, 2017; Han *et al.*, 2019). In fact, there is evidence that it may be an auxiliary subunit of GABAARs (Han *et al.*, 2019)

A more recent study established how changes in short term dynamics imposed by an auxiliary subunit, CKAMP44, directly affects *in vivo* firing during behavior (Chen *et al.*, 2018). Retinogeniculate synapses exhibit high release probability and pronounced short-term depression, which is partly due to AMPAR desensitization (Chen & Regehr, 2000; Chen *et al.*, 2002). CKAMP44 regulates short-term depression in these synapses by slowing the recovery from desensitization. CKAMP44 KO mice have increased spike probability and *in vivo* firing of dorsal lateral geniculate neurons (Chen *et al.*, 2018).

Future structural analyses of AMPAR/CKAMP44 complex may produce new functional insights into their role in synaptic AMPAR regulation.

Among all of the auxiliary subunits, GSG1L stands out for having the strongest effect on slowing the recovery from AMPAR-desensitization in HEK cells (Schwenk *et al.*, 2012; Shanks *et al.*, 2012). However, overexpression of GSG1L in CA1 hippocampal neurons speeds the recovery from desensitization (Gu *et al.*, 2016). It is predicted that this discrepancy is due to innate properties specific to neuronal systems, such as AMPAR subunit composition and the presence of other auxiliary subunits including CNIH2 (Gu *et al.*, 2016). Association of GSG1L with AMPARs prevents CNIH2 regulation in heterologous systems (Gu *et al.*, 2016). The functional competition between GSG1L and CNIH2 is in agreement with structural data indicating that the two bind to the same location on AMPARs (Twomey *et al.*, 2017c; Nakagawa, 2019).

Short-term plasticity of AMPAR-mediated currents is not only determined by presynaptic mechanisms or postsynaptic changes in the rate of recovery from desensitization, but can also be affected by fast lateral diffusion of the receptors within membrane (Constals *et al.*, 2015). It has been shown that lateral diffusion of AMPARs allows for exchange of desensitized receptors with non-desensitized “naïve” receptors, and thus recovery from desensitization could be in part due to this exchange of receptor pools at the synapse (Heine *et al.*, 2008). TARPs and shisa6 have been shown to reduce the AMPAR diffusion and mobility by anchoring the receptors via their interactions with PSD-95 (Opazo *et al.*, 2010; Klaassen *et al.*, 2016). Glutamate binding induces an increase in AMPAR diffusion due to enhanced mobility of desensitized AMPARs relative to non-desensitized receptors (Constals *et al.*, 2015). It has been proposed that desensitization

is associated with an unbinding of stargazin resulting in increased mobility of AMPARs and replacement of desensitized receptors with non-desensitized receptors, which in turn allows for faster recovery from receptor desensitization (Constals *et al.*, 2015).

1.5.3. Role of auxiliary subunits in long-term plasticity

A seminal discovery by Bliss and Lomo first established that brief high frequency stimulation of hippocampal synapses results in long-lasting increase in the strength of the synaptic response lasting for days (Bliss & Lomo, 1973). This provided the first experimental evidence of long-term potentiation (LTP). While LTP has been studied at multiple brain regions (Malenka & Bear, 2004), Schaffer collateral-CA1 synapses have been best characterized. LTP induction at Schaffer collateral-CA1 synapses requires NMDAR activation, as the application of APV, a selective NMDAR antagonist, blocked LTP (Collingridge *et al.*, 1983). Influx of Ca^{2+} ions through NMDARs, in turn, was also shown to activate Ca^{2+}/calmodulin-dependent protein kinase (CaMKII), which is predicted to be necessary for LTP (Lisman *et al.*, 2012). Among all of the downstream substrates of CaMKII (Shonesy *et al.*, 2014), GluA1 subunit of AMPARs has been a focus of multiple investigations. CaMKII- dependent phosphorylation of GluA1 at Ser831 site has been shown to be associated with LTP (Barria *et al.*, 1997). However, more recent investigations suggest that AMPARs lacking the C-terminal tail containing Ser831 do not present with deficits in basal trafficking of AMPARs or LTP at CA1 synapses (Granger *et al.*, 2013). Furthermore, knock-in mice lacking the entire C-

terminal domain of GluA1 have normal LTP and performance in spatial memory tasks, such as Morris water maze (Diaz-Alonso *et al.*, 2020).

Changes in synaptic AMPAR trafficking resulting in the accumulation of AMPARs at the synapse is one of the primary mechanisms for synaptic plasticity (Huganir & Nicoll, 2013), as it is accompanied with an activity-dependent exocytosis of AMPARs (Lledo *et al.*, 1998; Lu *et al.*, 2001). Since the initial discovery of AMPAR auxiliary subunits, numerous studies have looked at their potential involvement in long-term plasticity including LTP and long-term depression (LTD). TARP γ-8 and CNIH2/3 are co-expressed in hippocampal CA1 cells and each contributes to regulating AMPAR mediated response (Rouach *et al.*, 2005; Herring *et al.*, 2013). In the hippocampus, removal of γ-8 or CNIH2/3 results in reduced AMPAR-mediated synaptic transmission and attenuated LTP (Rouach *et al.*, 2005; Herring *et al.*, 2013).

One of the key roles of γ-8 in hippocampal CA1 is to mediate molecular interaction via its cytoplasmic C-tail with synaptic scaffold protein PSD-95, whereby facilitating recruitment of γ-8 containing AMPAR complexes into synapses (Sumioka *et al.*, 2011). This interaction is dispensable for LTP, as LTP was normal in knock in (KI) mice that lack the PDZ domain ligand of the γ-8 (Sumioka *et al.*, 2011). Instead of the PDZ domain interaction phosphorylation of the C-tail of γ-8 by CaMKII plays a critical role, as LTP was impaired in KI mice whose phospho-substrate residues in the C-tail of γ-8 were mutated to alanine (Park *et al.*, 2016). The events downstream of the phosphorylation remain unclear. In one view, phosphorylation releases the C-terminal from the membrane and facilitates its interaction with PSD-95 (Park *et al.*, 2016), but such mechanism appears unimportant for LTP (recall that interaction of γ-8 with PSD-95

is dispensable for LTP). On the other hand, based on quantitative binding assay between the C-tail of γ-8 and the PDZ domain of PSD-95, introducing phosphomimetic mutation to the phospho-substrate residues in the C-terminal tail of γ-8 was shown to decrease the affinity (Zeng *et al.*, 2019b). In two recent studies, which used molecular replacement at the cellular resolution, the interaction between the C-tail of γ-8 and PSD-95 was suggested to be critical for LTP in CA1 cells (Sheng *et al.*, 2018; Zeng *et al.*, 2019b), which is a completely opposite model from what was described previously. Zeng et al. also found that loss of TARP- PSD-95 interaction disrupts LTP in hippocampal neurons. The different conclusions may be due to the use of different experimental systems in these studies.

Phosphorylation of stargazin also has functional consequences on LTP and LTD. The C-terminus of stargazin contains nine serine residues that upon phosphorylation extend away from the negatively charged phospholipids in the plasma membrane facilitating PSD-95 binding (Opazo *et al.*, 2010; Sumioka *et al.*, 2010; Hafner *et al.*, 2015). Phosphorylation of the stargazin C-terminus is required for hippocampal LTP and dephosphorylation for cerebellar and hippocampal LTD (Tomita *et al.*, 2005b; Nomura *et al.*, 2012). However, as mentioned above, a more recent study determined that phosphomimetic mutation diminishes stargazin binding to PSD95 and decreases AMPAR EPSCs (Zeng *et al.*, 2019a). This is also in agreement with phosphomimetic mutants having no effect on potentiation in hippocampal neurons (Kessels *et al.*, 2009). Similarly to aforementioned γ-8 studies, the discrepancy in the results among these studies could be due to the very different experimental approaches and further studies will be needed to solidify these results.

In hippocampal CA1 cells, CNIH2/3 regulates the number of synaptic heteromeric AMPARs that contain GluA1 (Herring *et al.*, 2013). However, as described earlier, the residues in GluA1 and GluA2 critical for binding CNIH2/3 are fully conserved, and thus it is unclear how CNIH2 can distinguish between GluA1 and GluA2. Considering that γ-8 and CNIH2/3 bind to the same site on AMPAR (Herguedas *et al.*, 2019; Nakagawa, 2019) and co-assemble (Kato *et al.*, 2010; Gill *et al.*, 2011; Schwenk & Fakler, 2019; Zhao *et al.*, 2019), it will be important to evaluate in more detail the functional contribution of each auxiliary subunit belonging to the same AMPAR complex (containing both TARP and CNIH).

Among CKAMP family of proteins, genetic deletion of CKAMP59 abolishes LTP in CA1 neurons (Schmitz *et al.*, 2017). In addition to LTP and LTD regulation, AMPAR auxiliary subunits have also been implicated in other forms of plasticity such as inflammatory-pain induced plasticity (Sullivan *et al.*, 2017). Stargazin is expressed in the lamina II of the spinal cord horn and is essential for CP- AMPAR plasticity following inflammatory hyperalgesia. In fact, previous studies have shown that knockdown of stargazin in the spinal cord is associated with decreased pain following inflammation and postoperative pain (Tao *et al.*, 2006; Guo *et al.*, 2014).

LTP at hippocampal CA1 synapses was enhanced in GSG1L KO rats at P13-P19 (Gu *et al.*, 2016). However, GSG1L overall has a very low expression in the hippocampus (Schwenk *et al.*, 2014a). *In situ* hybridization data also shows that the hippocampal expression is minimal and is only present in adult mice starting at P60 (Lein *et al.*, 2007b). Therefore, the observed phenotypes in the GSG1L KO rats could be due to the loss of GSG1L elsewhere in the brain or due to the presence of other auxiliary subunits,

such as CNIH2. More studies looking at the direct postsynaptic role of GSG1L are needed to determine its physiological function.

1.6. Disease relevant mutations in native AMPAR complexes and diseases

Mutations in the core AMPAR subunits have been linked to various neurological diseases. Namely, mutations in GluA2 (encoded by GRIA2) are linked to intellectual disability (ID) (Tzschach *et al.*, 2010; Hackmann *et al.*, 2013; Salpietro *et al.*, 2019). In addition, multiple GluA3 (encoded by GRIA3) mutations are also associated with ID (Chiyonobu *et al.*, 2007; Wu *et al.*, 2007; Bonnet *et al.*, 2009; Philippe *et al.*, 2013). For instance, a missense A653T mutation within the ion conduction pore of GluA3 is associated with sleep dysregulations as well as ID.

Additionally, missense tolerance ratio (MTR) analysis, which is a measure of intolerance to genetic variation, indicates GluA2 and GluA3 are highly intolerant to genetic variation. The A653T mutation in GluA3 has an MTR of 0.33 thereby indicating the relevance of MTR scores to disease states (Figure 1.4). Missense mutation G833R in the M4 of GluA3 is associated with cognitive impairments (Wu et al. 2007). Mutations in the neighbouring residues within the M4 of GluA2 are known to disrupt receptor tetramerization (Amin et al. 2017). Interestingly, the region immediately preceding M1 (pre-M1: GVFSFLDPLAYE) in GluA2, where lipids are predicted to bind (Herguedas et al. 2019), and M1 (WMCIVFAYIGVSVVL), where TARPs and CNIHs are predicted to bind, are highly intolerant of variation (MTR = 0). Mutations in the pre-M1 of NMDARs

are also linked to epilepsy and developmental delay (Ogden et al. 2017). Overexpression of these mutants results in prolonged EPSCs and excitotoxicity, which can be attenuated by the NMDAR inhibitor memantine (Ogden et al. 2017). In AMPARs the pre-M1 region may also tune gating (Shi et al. 2019).

The disease associated mutations are not limited to core AMPAR subunits but can also be found in auxiliary subunits. A missense *de novo* mutation in the TM3 of TARP γ-2 (V143L) is associated with ID (Hamdan *et al.*, 2011). The V143L mutation reduces AMPAR- γ-2 interaction, as well as mEPSC amplitude and frequency in cultured hippocampal neurons. *De novo* deletion of CNIH2 has also been linked to ID (Floor *et al.*, 2012). In general, TARPs γ-3 and γ-2 have been identified as susceptibility loci for a subpopulation of patients with childhood absence epilepsies and schizophrenia respectively (Everett *et al.*, 2007; Liu *et al.*, 2008). MTR analysis indicates that AMPAR auxiliary subunits contain multiple regions that are mildly intolerant to genetic variation (as shown in Figure 1.4.) Within the TARP sub-family, γ-3 has the highest degree of intolerance. Interestingly, the cysteine knot domain in the CKAMP44 is also intolerant to variation. Among all of the auxiliary subunits, CNIH2 stands out for having a stretch of amino acids that are highly intolerable to missense variation (Figure 1.4.)

Dysregulation of AMPAR function has been associated with a myriad of neurological diseases (Chang *et al.*, 2012). However, due to their ubiquitous expression and essential function, the pore forming subunits of AMPAR are not optimal targets for therapeutic compounds; such drugs may cause substantial off-target effects such as

dizziness and sedation (Rogawski, 2011). On the other hand, because of their rich spatiotemporal diversity of expression, auxiliary subunits are potential targets for therapeutic compounds that could control AMPAR function in a region specific manner (Azumaya *et al.*, 2017; Maher *et al.*, 2017). Compounds specific for AMPARs associated with TARP γ-8 are being developed and proven to work in animal models of epilepsy (Gardinier *et al.*, 2016; Kato *et al.*, 2016; Lee *et al.*, 2017). While the residues critical for drug action have been mapped, current structural data suggests that the proposed binding pocket is too small for drug binding (Herguedas *et al.*, 2019). Establishing the structural basis for AMPAR-auxiliary subunit action is expected to reveal new information about strategies to control functions of AMPAR-auxiliary subunit complexes in various disease states.

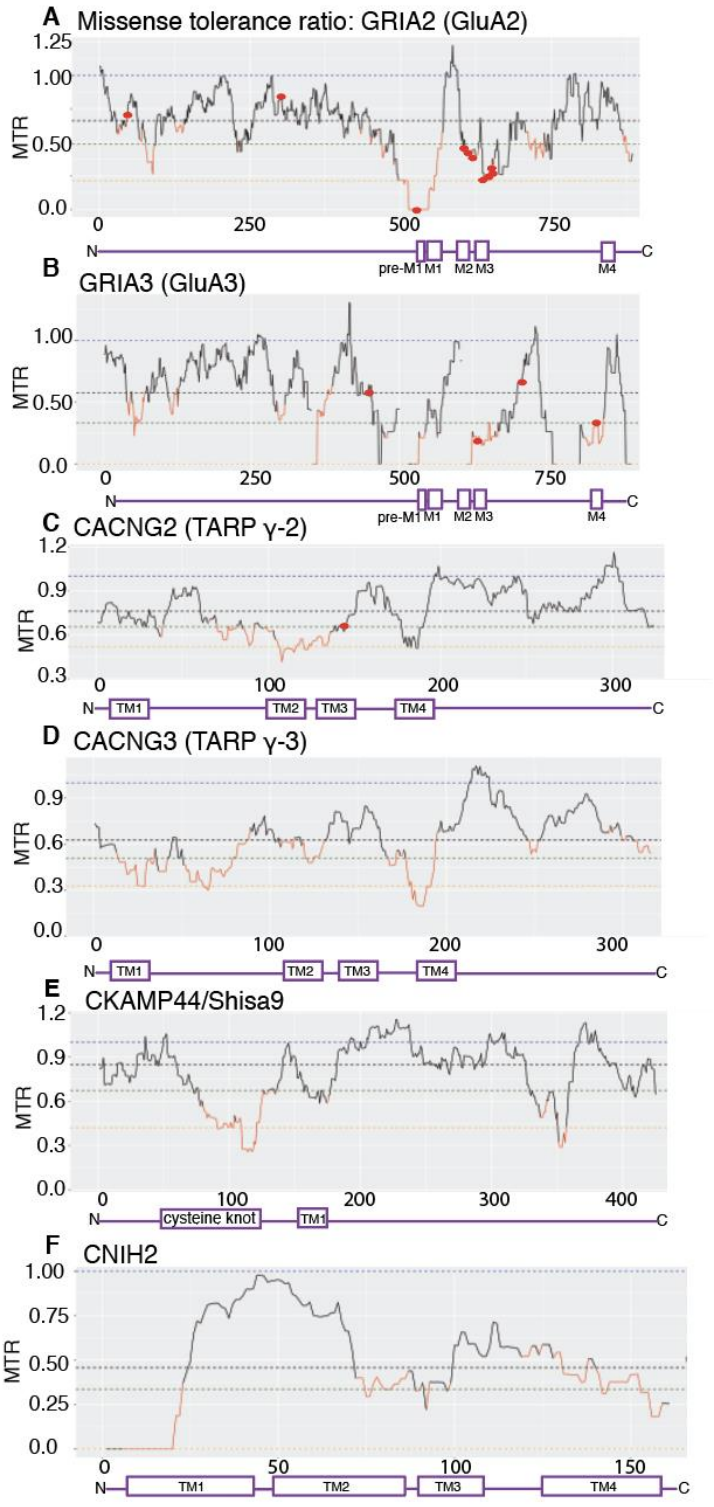

Figure 1-4. Intolerance of AMPAR complexes to missense mutations.

Missense tolerance ratio (MTR) is an estimate of the extent of purifying selection or the removal of deleterious alleles (Traynelis *et al.*, 2017). An MTR=1 indicates neutrality and the ratios below the 10th percentile (in red) are under purifying selection. AMPAR auxiliary subunits have varying degrees of tolerance for missense mutations (i.e. low MTR scores).
A. GRIA2, which encodes GluA2 subunit, has regions with MTR=0 (pre-M1 and part of M1), no tolerance to variation. Missense mutations associated with neurodevelopmental disorders (G47E, D302G, P528T, Q/R607G/E, G609R, D611N, A639S, F644L, T646L, V647L) are indicated with red dots (Salpietro *et al.*, 2019).
B. GluA3 subunits also has multiple regions with MTR=0, highly intolerant to variation. The locations of mutations associated with cognitive impairment (G833R, M706T, R631S, R450Q) are indicated as red dots (Wu *et al.*, 2007).
C. MTR distribution for γ-2 shows multiple regions of high intolerance (in red) including TM2. Missense mutation V143L associated with ID is indicated as a red dot.
D. Among TARPs, γ-3 has the highest number regions of intolerance including TM1, TM2, and TM4.
E. Cysteine knot domain within CKAM44 is highly intolerable to genetic variation. F. CNIH2 has a stretch of amino acids that are highly intolerable to genetic variation. This region is mapped as the critical AMPAR binding site. Adapted with permission from (Kamalova & Nakagawa, 2020).

1.7. The overview of Anterior thalamic nuclei

The major focus of the current dissertation work is the investigation of the synaptic function of GSG1L. GSG1L is highly expressed in the anterior thalamic nuclei and has an important role in regulating a subset of synapses in an input-specific manner, which will be extensively discussed in subsequent chapters. I would, therefore, like to introduce the circuitry and function of anterior thalamic nuclei to put our work in a better context.

1.7.1. The circuitry of anterior thalamic nuclei

Neurons in the anterior thalamus, located within the medial diencephalon, share reciprocal projections with the hippocampus with important implications for spatial navigation as well as memory formation (Jankowski *et al.*, 2013). The anterior thalamus is comprised of three distinct nuclei: anterodorsal (AD), anteroventral (AV), and anteromedial (AM) nuclei (Figure 1.6). Although there are some differences between AD and AV nuclei, the two share progenitor origin (Shi *et al.*, 2017), expression profile of neurotransmitter receptors (Phillips *et al.*, 2019), as well as afferent and efferent projections (Jankowski *et al.*, 2013). Compared to other thalamic nuclei, such as lateral geniculate nucleus (LGN), the synaptic properties of anterior thalamus are less well understood.

Anterior thalamic nuclei (ATN) receive dense projections from the subiculum, mammillary bodies, and retrosplenial cortex (Jankowski *et al.*, 2013). Interestingly, almost every neuron within the mammillary bodies projects to the ATN via the mammillothalamic tract (Vann *et al.*, 2007; Aggleton *et al.*, 2010). Anatomical tracing studies have shown that cells from layer V and VI of the postsubiculum share reciprocal projections with the ATN (Wright *et al.*, 2010). On the other hand, the ATN project to layers I, III, and IV of the retrosplenial cortex and receive dense projections from pyramidal cells primarily from layer VI of the retrosplenial cortex (Shibata, 1998).

Interestingly, axons of hippocampal projection neurons or cortical neurons to the mammillary bodies and ATN can reach their targets via the fornix fiber tract (Shibata, 1998; Aggleton *et al.*, 2010). Analogous to the sensory thalamic relay circuits (Sherman

& Guillery, 2004), the inputs to the AD/AV neurons are classified into driver and modulator inputs. Specifically, mammillary bodies inputs drive the firing of the AD/AV neurons, whereas cortical and subiculum inputs modulate the action of the mammillary bodies inputs (Petrof & Sherman, 2009). However, more recent investigations suggest that corticothalamic inputs into ATN may have some characteristics of a driver pathway (Vantomme *et al.*, 2020).

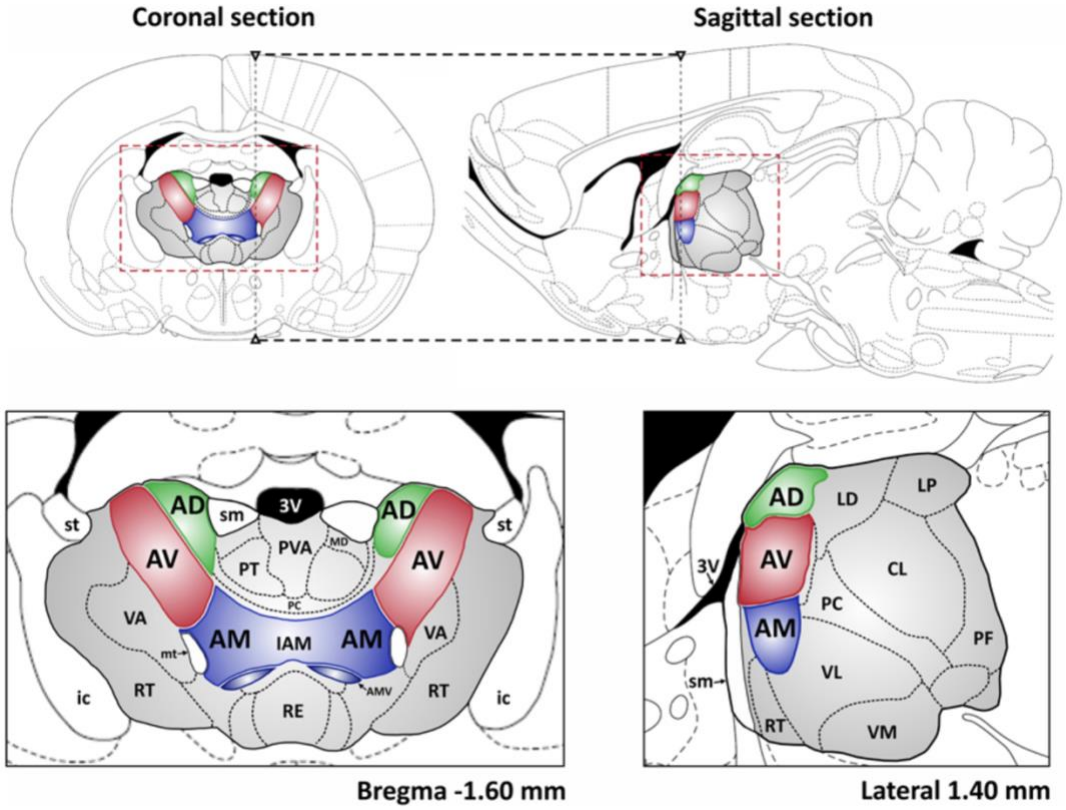

Figure 1-5. Anatomical localization of anterior thalamic nuclei.

Coronal and sagittal sections of rat brains showing the localization of anterior thalamic nuclei: anterodorsal (AD), anteroventral (AV), and anteromedial (AM) nuclei. The dashed lines represent the extent of sections. Adapted from (Jankowski *et al.*, 2013).

1.7.2. Function of anterior thalamic nuclei

Similar to the hippocampus, the intactness of the anterior thalamus is vital for memory. Anterior thalamus is at the core of the extended hippocampal-diencephalic network with crucial roles in memory (Aggleton & Brown, 1999). Experimental evidence at the behavioral, anatomical, and physiological levels suggest that interactions between ATN, cortex, and hippocampal formation are critical for spatial memory. For instance, previous studies have shown that alcoholic patients with Korsakoff's psychosis developed a pronounced anterograde episodic memory loss (Harding *et al.*, 2000). In these studies, postmortem analysis revealed that atrophy of ATN was associated with amnesia in Korsakoff's psychosis. Similarly, patients with a localized infarct in ATN exhibit anterograde memory impairment with an overall delayed recall deficit (Ghika-Schmid & Bogousslavsky, 2000). Interestingly, lesions in the hippocampus, fornix, ATN, and the mammillary bodies in rats manifest in similar deficits in spatial learning (Aggleton *et al.*, 2010). Therefore, multiple lines of compelling evidence suggest that ATN, similar to the hippocampus, is critical for the memory system as its damage is associated with anterograde amnesia (Ghika-Schmid & Bogousslavsky, 2000; Gold & Squire, 2006).

ATN also contain neurons that sense head direction during spatial navigation (Clark & Taube, 2012). Similar to the postsubiculum, ATN contain head direction cells that fire as a function of the animal's head orientation and independent of overall location in space (Taube, 1995). In the ATN, the majority of head direction cells are located within the AD nucleus and with a smaller proportion in AV nucleus. These cells fire when an animal's head is positioned in a certain direction. Outside of postsubiculum and ATN, head

direction cells have also been found in retrosplenial cortex, medial entorhinal cortex, and the lateral mammillary nucleus and dorsal tegmental nucleus of Gudden, with latest being the main input to the mammillary bodies from the brainstem (Clark & Taube, 2012). The head direction system of the ATN may contribute to the function of place cells, which discharge as a function of the location in the environment, in the hippocampus, since lesion of the AD nucleus resulted in place fields with altered properties (Calton *et al.*, 2003).

Besides their critical role for the memory system, ATN have also been implicated in seizure initiation and/or propagation (Mirski & Ferrendelli, 1984; Kerrigan *et al.*, 2004). Interestingly, deep brain stimulation (DBS) of ATN showed therapeutic relieve for patients with intractable epilepsy (Hodaie *et al.*, 2002). Clinical studies have also shown that DBS of ATN has positive effect on intractable epilepsy through reduction in the seizure frequency (Lee *et al.*, 2012). While there is experimental evidence for DBS of ATN providing therapeutic effect in epilepsy patients, the underlying mechanism is currently unknown. It is proposed that DBS of ATN affects has network level changes in multiple brain region as it was associated with changes in motor excitability (Jankowski *et al.*, 2013). Similarly, in rodents, bilateral electrical stimulation ATN reduced seizure activity in pilocarpine epilepsy rat model (Hamani *et al.*, 2004). Whereas in humans, bilateral stimulation of ATN reduced seizures by 50% during a two-year clinical study (Fisher *et al.*, 2010). Taken together, it has been well confirmed experimentally that ATN is associated with seizure states. However, further studies are needed to determine the underlying cellular and circuit-level mechanisms. It is currently unknown how the anterior thalamus is associated with seizure states.

1.8. Overview of the work to be presented in this thesis

The main goal of the current dissertation work was to determine the synaptic function of a relatively less studied and unique auxiliary subunit, GSG1L. Among all of the currently known auxiliary subunits, GSG1L stands out for having a strong net negative AMPAR regulatory role. However, the impact of this negative regulation on synaptic transmission and animal behavior has not been fully chacaterized.

Aim 1 of my thesis work, presented in Chapter 3, was to determine the synaptic function of GSG1L using GSG1L KO mouse line. To study GSG1L synaptic function, it was first important to determine its expression within the brain. We performed a comprehensive spatio-temporal expression profile characterization of GSG1L within the brain using a transgenic reporter KO rat line. Out of all the various brain regions that had GSG1l expression, the anterior thalamic nuclei stood out for having the most sustained expression of GSG1L at all the developmental time-points that were tested.

In Chapter 3, I will present the findings that establish the postsynaptic role of GSG1L specifically in the anterior thalamus, where it regulates AMPAR activity in an input-specific manner. We found that GSG1L has a strong impact on short-term plasticity through the slowing of the recovery from AMPAR desensitization specifically in corticothalamic synapses. Consistent with its negative regulatory role, AMPAR activity is enhanced in GSG1L KO mice. Additionally, we discovered that stargazin is co-expressed in the anterior thalamus, but it is functionally inactive in corticothalamic synapses and is a dominant auxiliary subunit at mammillothalamic and subiculum-

thalamic synapses. Additionally, we showed that there is functional competition of GSG1L and stargazin *in vivo* using GSG1L and stargazin double KO mice.

Aim 2 of my dissertation work was to determine the whole-animal and behavioral changes associated with GSG1L KO mice. To address this, the work presented in Chapter 4 will demonstrate that loss of negative AMPAR regulation in GSG1L KO mice is associated with enhanced hyperexcitability, seizure susceptibility, and cognitive deficits.

In the final Chapter 5, I will discuss the major findings of our studies and future directions and unanswered questions of the current dissertation work.

2. Materials and Methods

2.1. Rodent models

For all of the experiments in this dissertation, male and female mice and rats were used. To summarize the ages of animals used in a given experiment, here is a brief overview. For short-term plasticity experiments comparing the three pathways, GSG1L KO and WT mice at postnatal ages of 21 to 33 (P21-P33) were used. For short-term plasticity experiments of AD only, AD/AV combined, NMDAR-dependent, and CTZ recordings were done at P15-P30. For mEPSCs, sEPSCs, qEPSCs and current clamp recordings of GSG1L KO and WT mice at P15-P30 were used. For mEPSCs and sEPSCs of γ-2 KO and WT (and GSG1L/ γ-2 dKO) mice at P15-P22 were used. For behavioral experiments, GSG1L KO and WT mice at 9-10 month old were used. LacZ staining of GSG1L KO rat and WT control littermates was done as indicated in the figures: P14, P21, P60, and P180.

Below, I will provide a brief overview of the transgenic rat and mouse lines that were used in our studies.

GSG1L knockout reporter rat line

A transgenic GSG1L KO rat line in the background of SD strain was among the mutants generated through transposon-based mutagenesis by Kent Hamra at UT Southwestern (Izsvak *et al.*, 2010). The mutant rat line was purchased and maintained in house. Animal housing and handling during experiments were in agreement with the NIH and Vanderbilt University guidelines for the care and use of Laboratory animals.

The original transgenic animal had been confirmed to have a lacZ insertion in the GSG1L gene but information on whether additional insertions were present was unknown. A detailed genomic Southern analysis in our laboratory revealed that a total of three lacZ cassettes were integrated into the rat genome. Using inverse PCR we identified that one of the insertions was at the GSG1L locus (chromosome 1q36) and the second one at the Piccolo locus (chromosome 4q12). For the third lacZ cassette, the inverse PCR revealed the genomic sequence immediately outside of the insertion site. The BLAST search to this sequence only returned data that are homologous but not identical to some of the L1 repeats in other species. Based on these observations we suggest that the third lacZ is located at an L1 repeat non-coding region that was not determined in the rat genome project.

By mating the heterozygotes with wild-type rats for several generations we bred out the Piccolo mutation. The LacZ in the L1 repeat was tightly linked to GSG1L and not separable after one year of continuous breeding. However, due to its location in the non-coding region the expression of LacZ from this insertion is unlikely. Consistently, in the GSG1L KO rat the X-gal (5-Bromo-4-Chloro-3-Indolyl β-D-Galactopyranoside) staining in the brain was consistent with *in situ* hybridization data of GSG1L in Allen brain atlas. We therefore suggest that the LacZ reporter expression in the GSG1L KO rat provides a strong tool in determining populations of GSG1L expressing neurons in various brain regions.

GSG1L knockout mouse line

A GSG1L KO transgenic mouse line was generated by targeting exon 4 of GSG1L gene in 129/SvEvTac embryonic stem (ES) cells. Two independent clones were shown by Southern blot analysis and PCR to have undergone proper homologous recombination and germline transmission was confirmed from chimeras derived from clone 2H2. To remove the pGK-neo cassette, the 3-loxP mouse was crossed with FlpE line (Rodriguez *et al.*, 2000) that ubiquitously expresses Flp recombinase, generating a 2-loxP animal. Finally, by crossing with EIIa-cre mice (JAX: Stock 003724, which was back crossed with C57BL6/J over 10 generations) that expresses cre-recombinase in the one cell zygote, we obtained the 1-loxP heterozygotes. All strains were backcrossed with C57BL6/J mice for 8 generations. All KO animals were viable with no overt issues with breeding and/or development.

The mice were genotyped by boiling the 5mm tail snips in at 50°C in 200 µl Solution A (250 µl of 10N NaOH + 40 µl of 0.5N EDTA+ 100 ml H_2O) for 25 minutes and neutralized in 200 µl Solution B (4ml of 1M Tris pH 5.0+ 96 ml H_2O). The mixture was spun at 13K rpm for 10 minutes and 200 µl supernatant was saved and used for the polymerase chain reaction (PCR). The primers for genotyping GSG1L 1loxp line were as follows, TN 21: AAACAGACAACATGGCCCTCAGACTC; TN 22: AAACCAGAGTCCCAGCTGGTTGTG.

The PCR mix (25 µl total) contained 19.8 µl of sterile water, 2.5 µl 10X Buffer, 0.5 µl of 10 mM dNTPs, 0.5 µl primer 1, 0.5 µl primer 2, and 0.2 µl Taq Polymerase. Per PCR mix, 1.2 µl of tail DNA was used. The PCR was done with the following program: 95°C, 2:00; 95°C, 0:30; 58°C, 0:30; 72°C, 1:00; GOTO step 2, 30X; 72°C, 10:00; 4°C.

Resulting PCR products were resolved on a 2% agarose gel electrophoresis. The GSG1L 1loxp WT is indicated by a band size of 567 bp and KO at 273 bp.

CACNG2 knockout mouse line

The γ-2 KO mouse was generated as follows: A 20 bp sequence (TGAAACCAGCAAGAAGAACG) followed by AGG as proto-spacer adjacent motif (PAM), was selected within exon 1 of the CACNG2 (encoding γ-2) mouse gene to create a target-specific guide RNA molecule. The sequence flanked by *BbsI* sites was ligated in pX330, a vector expressing the guide RNA under a strong U6 promoter and cas9 under a hybrid chicken beta-actin (Cbh) promoter. The vector was injected alongside a 195 base repair single stranded oligonucleotide into 314 mouse embryos. The repair oligo contained 90 bp homology arms, a codon substituting lysine residue 53 to a stop codon, a unique *AgeI* restriction site, and a few additional third base mutations to prevent targeting of cas9 to the repaired DNA. Out of 314 embryos injected, 267 were transferred to 11 pseudo-pregnant females to generate 16 pups. At weaning, genotyping was done by amplifying a 926 bp fragment followed by sequencing. Out of 15 pups (one died prior to weaning), only one animal (female #12) carried the designed mutation. After several backcrossing to C57BL6/J mice to eliminate any possible off target events, heterozygote mice were crossed to generate homozygous KO animals.

For genotyping of CACNG2 KO mice, the tail DNA was obtained in a similar way as described above. The PCR genotyping was performed with Expand Long Template PCR system containing in 25 µl reaction: 14.23 µl water, 2.5 µl Buffer 1, 2.5 µl CAC9

primer, 2.5 µl CAC10 primer, 0.9 µl of 10mM dNTPs, 0.375 µl polymerase enzyme, and 2 µl of DNA. The PCR was perfomed under following conditions:

95°C, 2:00; 93°C, 0:10; 60°C, 0:30; 68°C, 0:45; GOTO step 2, 9X; 93°C, 0:03; 60°C, 0:30; 68°C, 0:45; +10s per cycle; GOTO Step 6, 24X; 68°C; 8:00.

Obtained PCR product was further digested with AgeI restriction enzyme: 15 µl water, 2 µl Cut Smart buffer, 2 µl water, 1 µl AgeI enzyme- at 37°C for 1 hour.

Resulting products were resolved on a 2% agarose gel electrophoresis. The CACNG2 WT is indicated by a band size of 926 bp and KO at 542 and 380 bp.

2.2. Histology

Whole brain staining

P14, P24, P42, and 4mo GSG1L KO rat brains and corresponding wild-type (WT) rat brains were anesthetized with sodium pentobarbital (Nembutal). The animals were then perfused with normal Rat Ringer solution for 2 minutes for complete perfusion, followed by 4% paraformaldehyde in 0.1M phosphate buffer for 4 minutes. The brains were then removed and permeabilized with 0.01% Sodium deoxycholate and 0.02% triton X-100 in PBS buffer for 2 hours. Following permeabilization, the tissue samples were incubated with X-gal staining solution containing 5mM $K_3[Fe(CN)_6]$, 5mM $K_4[Fe(CN)_6]$, 2mM $MgCl_2$, 0.02% triton X-100, and 0.1% X-gal in PBS buffer at 37°C for 8 hours in the dark. Stained brains were imaged the following day (MULTIZOOM AZ100M, Nikon).

Histology using fixed brain sections

P14, P21, P60, and P180 GSG1L KO rat brains with corresponding WT rat brains were anesthetized with sodium pentobarbital (Nembutal). Each animal was then perfused with normal Rat Ringer solution for 2 minutes for complete perfusion, followed by 4% paraformaldehyde in 0.1M phosphate buffer for 4 minutes. Obtained brains were further fixed for 15 minutes. Fixed brains were subsequently sectioned to generate 300 µm-thick coronal sections using a vibratome (Leica VT 1200). The sections were then permeabilized with 0.01% Sodium deoxycholate and 0.02% triton X-100 in PBS buffer for 2 hours. Following permeabilization, 300 µm-thick coronal sections were incubated with X-gal staining solution containing 5mM $K_3[Fe(CN)_6]$, 5mM $K_4[Fe(CN)_6]$, 2mM $MgCl_2$, 0.02% triton X-100, and 0.1% X-gal in PBS buffer at 37°C for 8 hours in the dark. Stained brains were imaged (MULTIZOOM AZ100M, Nikon) the following day (1 day post staining) and then left for 1 week at 4°C to enhance the lacZ staining due to residual x-gal in the tissue.

2.3. Confirming the absence of targeted proteins in the KO animals

Immunoprecipitation of protein complexes were performed as previously described (Nakagawa *et al.*, 2005). Briefly, mouse (or rat) brains were homogenized in 20 mM HEPES pH 7.4, 320 mM sucrose, 5 mM EDTA, 5 mM EGTA, 30 µM NBQX supplemented with protease inhibitors 1 mM PMSF, 10 µg/ml aprotinin, 10 µg/ml leupeptin, 1 µg/ml pepstatin, and 500 µM benzamidine. Brain homogenates were spun

down at 3000 g for 15 min and the obtained supernatant was further spun at 38,400 g for 15 min resulting in a membrane pellet. The membrane pellet was resuspended in a buffer containing 20 mM HEPES pH 7.4, 1 M KI, 5 mM EDTA, 5 mM EGTA, and 30 µM NBQX. To wash off the KI, membranes were washed with wash buffer containing 20 mM HEPES pH 7.4, 5 mM EDTA, 5 mM EGTA, and 30 µM NBQX. The final membrane pellet was solubilized in a resuspension buffer containing 20 mM HEPES pH 7.4, 100 mM NaCl, 5 mM EDTA, 5 mM EGTA, 1% CHAPS, 30 µM NBQX and the protease inhibitors for two hours at 4°C. To validate GSG1L 3-loxP KO, GSG1L was immunoprecipitated with previously described anti-GSG1L Ct2 antibody (2mg/ml) and eluted with the epitope peptide CKVFEQGYREEPTFIDPEAIKYFR (Shanks *et al.*, 2012).

To validate GSG1L 1-loxP KO, GSG1L was immunoprecipitated with anti-GSG1L Ct1 antibody (2mg/ml) and eluted with the epitope peptide CRSSAHEAAELNRQCWVLGHWV (Shanks *et al.*, 2012). Immunoprecipitated GSG1L from the brain lysates of 3-loxP KO and 1-loxP KO GSG1L was then subjected to western blot analysis with anti-GSG1L Ct1 antibody and Ct2 antibody, respectively. Of note, long and short isoforms of GSG1L transcripts are listed in the mouse genome database. The short isoform is predicted to lack the Ct2 epitope, and thus we were only able to confirm the KO of 43kDa long isoform of GSG1L. The short isoform lacks the TM4, which is essential for binding AMPAR from the cryo-EM structure (Twomey *et al.*, 2017c), and unlikely to have a role in regulating AMPAR. The folding of TM1-TM4 is highly conserved among the tetraspanins and therefore loss of TM4 is likely to cause a substantial misfolding in the short isoform. Specifically, if the short isoform exists, it

would have an extracellular C-terminal, whose topology is completely different from the long isoform with a cytoplasmic C-terminal.

Moreover, our targeting design does not permit efficient transcription of the shorter isoform given that exon 4, upstream of the putative splice site, is targeted. Collectively, we suggest that the short isoform is unlikely to exist and only the long isoform is relevant in the current study. We also note that the observed differences in the non-specific band patterns is a consequence of using different polyclonal antibodies for detection. Note that the band immediately below GSG1L in 1loxp KO blot is due to nonspecific binding. For validating γ-2 KO, AMPAR complexes were pulled down with anti-GluA2 antibody (EGYNVYGIESVKI). Immunoprecipitated stargazin was probed with anti-stargazin antibody (Millipore, AB9876).

2.4. Immunoprecipitation of GSG1L during development

Wild-type cortices were dissected from four P17, 2mo, 4mo, and 6mo mouse brains. The tissue was processed as described above. In brief, the tissue was homogenized 20 mM HEPES, pH 7.4, 320 mM sucrose, 5 mM EDTA, 5 mM EGTA, 30 uM NBQX supplemented with protease inhibitors (1 mM PMSF, 10 µg/ml aprotinin, 10 µg/ml leupetin, 1 µg/ml pepstatin, and 500 µM benzamidine). Supernatant is then obtained by centrifuging the homogenate at 3000g for 15 min and further at 38,400 g for 15min to obtain a membrane pellet P2. P2 is then resuspended in SB1 (20 mM HEPES, pH 7.4, 1 M KI, 5 mM EDTA, 5 mM EGTA, and 30 µM NBQX) and ultracentrifuged at 50,000 rpm. Obtained membrane fraction is washed in SB2 (20 mM HEPES, pH 7.4, 4 M urea,

5 mM EDTA, 5 mM EGTA, 30 µM NBQX) and ultracentrifuged at 50,000 rpm. The final membrane fraction is solubilized in RB (20 mM HEPES, pH 7.4, 100 mM NaCl, 5 mM EDTA, 5 mM EGTA, 1% CHAPS, 30 uM NBQX, with protease inhibitors) for 2 hours at 4C and ultracentrifuged at 50,000 rpm to remove insoluble fraction. The supernatant is incubated overnight with precoupled anti-GSG1L Ct-1 antibodies to Protein A-Sepharose beads overnight and applied to the column. The column was washed 3 times with WB (20mM HEPES pH 7.4, 150mM NaCl, 5mM EDTA, 5mM EGTA, 1% CHAPS) and eluted with 0.5 mg/ml GSG1L Ct-1 peptide (CRSSAHEAAELNRQCWVLGHWV) in WB.

2.5. Electrophysiology in acute slices

For all electrophysiology experiments that were done in the anterior thalamus, mice of both sexes aged were used. Using the stria medullaris (sm) and the hippocampus as anatomical landmarks, we unambiguously identified AD/AV in 300 µm-thick coronal sections. For short-term plasticity experiments, the corticothalamic synapses were isolated in a coronal slice configuration and the cortical inputs were stimulated outside of AD/AV. Mammillothalamic synapses were isolated in 300 µm-thick sagittal brain sections. The prominent mammillothalamic tract and the hippocampus were used as anatomical landmarks to identify the AD/AV. To stimulate this synapse, the stimulating electrode was placed directly on the mammillothalamic tract. The subiculumt-thalamic synapse was isolated in 300 µm-thick sagittal brain sections. The mammillothalamic

tract and the hippocampus were used as landmarks to isolate the AD/AV and the electric stimulator was placed on the subiculum inputs directly below the hippocampus.

Mice were decapitated and the brains were rapidly removed and placed in ice-cold *N*-methyl-D-glucamine (NMDG) cutting solution containing 92 mM NMDG, 2.5 mM KCl, 30 mM $NaHCO_3$, 1.25 mM NaH_2PO_4, 11 mM Glucose, 0.5 mM $CaCl_2$, 10 mM $MgCl_2$, 20 mM HEPES, 2 mM thiourea, 5 mM Na-ascorbate, 3 mM Na-pyruvate, with pH adjusted to 7.4 with HCl. Acute 300 µm-thick slices were prepared using a vibratome (Leica VT 1200). Slices were then left to recover for 1 hr in artificial cerebro-spinal fluid (aCSF) solution containing 119 mM NaCl, 2.5 mM KCl, 26 mM $NaHCO_3$, 1 mM NaH_2PO_4, 11 mM Glucose, 1 mM $MgCl_2$, 2 mM $CaCl_2$, at pH 7.4 and 310 mOsm, saturated with 95%O_2/ 5% CO_2.

For AMPAR-mediated mEPSCs recordings, the aCSF was supplemented with tetrodotoxin (TTX, 0.5 µM) in order to suppress spontaneous excitation. To specifically isolate AMPAR-mediated mEPSCs at a holding potential of -70mV, GABA-A receptor activity was blocked with 100 µM picrotoxin (Tocris). For AMPAR-mediated sEPSCs recordings, the aCSF was supplemented with 100 µM picrotoxin to isolate the AMPAR component at -70 mV. Pipettes were filled with the internal solution containing 115 mM Cs methanesulfonate, 20 mM CsCl, 10 mM HEPES, 2.5 mM $MgCl_2$, 4 mM Na_2ATP, 0.4 mM Na_3GTP, 10 mM Na phosphocreatine, and 0.6 mM EGTA. The osmolarity was adjusted to 295 mOsm and the pH was adjusted to 7.25 with CsOH. The patches were formed with borosilicate glass pipettes (3-5 MΩ tip resistance). Recordings were made using Multiclamp 700B Amplifier (Axon Instruments) operated by pCLAMP10 software,

low-pass filtered at 10 kHz and digitized at 20 kHz using Digidata1440A (Axon Instruments).

Obtained mEPSCs and sEPSCs events were detected and analyzed with NeuroMatic event detection software (IGOR-pro, Wavemetrics) and correct event detection was confirmed by manual visual inspection, while errors were corrected by manual inspection of the traces. All the recordings and analysis were done in a blind manner, with the experimenter blind to the genotype during data acquisition and analysis. Significance was determined with Mann-Whitney U-test or a two-way analysis of variance (Two-Way ANOVA) with Sidak's multiple comparison *post hoc* test when applicable.

To evoke asynchronous quantal EPSCs (qEPSCs), Ca^{2+} was replaced with Sr^{2+} (4 mM $SrCl_2$). In order to avoid the multiquantal events, we only analyzed the qEPSCs that occurred >10 ms following the stimulation with the total sweep duration of 360 ms. Obtained qEPSC events were detected and analyzed with NeuroMatic event detection software (an extension to the IGOR-pro, Wavemetrics) and correct event detection was confirmed, while errors were corrected by manual inspection of the traces. The kinetic analysis of qEPSCs and mEPSCs were also done using NeuroMatic and IGOR-pro. From each corresponding cell, all isolated events with flat baseline were used for analysis. Typically, from each cell 15-30 representative events with monotonic rise and distinct decay were selected and averaged. The decay time of averaged qEPSCs was determined by fitting to double exponential function. The weighted decay time constant was further calculated as sum of slow and fast time constants and weighted by fractional amplitudes (Hawken *et al.*, 2017b).

For short-term plasticity experiments, whole-cell recordings AD/AV neurons were achieved in response to electrical stimulation of mammillothalamic tract, subiculum, or the cortical inputs at a holding potential of -70 mV. For M-T recordings, 300 µm-thick acute sagittal slices with AD/AV and visible mammillothalamic tract were obtained. The mammillothalamic tract was electrically stimulated, and current changes were recorded in response to 5-pulse stimulation at 20 Hz and 50 Hz. For S-T recordings, 300 µm-thick acute sagittal slices with AD/AV were obtained. Similarly, the subiculum inputs (as depicted in Figure 2) were stimulated at 20 Hz and 50 Hz. For C-T recordings, 300 µm thick acute coronal slices with AD/AV were obtained and the cortical inputs (as depicted in Figure 2) were electrically stimulated at 20 Hz and 50 Hz. Slices were perfused with aCSF supplemented with 100 µM picrotoxin. To isolate the effect of CTZ on short-term plasticity, we bath applied aCSF supplemented with 100 µM CTZ (Tocris). NMDAR currents were recorded as aforementioned, but at a holding potential of +40mV and in the presence of 10 µM NBQX and 100 µM picrotoxin. Statistical significance was assessed using a two-way analysis of variance (Two-Way ANOVA) with Sidak's multiple comparison *post hoc* test.

Intrinsic excitability properties were analyzed in current clamp recording mode. The recordings were done using potassium-based internal solution containing: 115mM K methanesulfonate, 20 mM KCl, 10 mM HEPES, 2.5 mM $MgCl_2$, 4 mM Na_2ATP, 0.4 mM Na_3GTP, 10 mM Na phosphocreatine, 0.6 mM EGTA,, The osmolarity was adjusted to 295 mOsm and the pH was adjusted to pH 7.25 with KOH In order to measure the intrinsic excitability properties, the neurons were held at -70 mV and current was

injected in 10 pA increments (from -20 to 160 pA) for 200 ms. The rheobase was determined as a minimal current injection required to elicit an action potential firing. The firing rate was determined as the number of action potentials fired at 150 pA injection. The input resistance was determined by calculating the slope of current-voltage plot (-20 to 20 pA). The firing frequency of spiking GSG1L KO neurons was determined, by calculating the frequency of fired action potentials during a 50 msec recording period.

2.6. Fast glutamate application from outside out patches

TetON HEK cells were plated on a coverglass coated with poly-D-lysine (37.5 µg/ml in H_2O) for 15 min. Excess coating material was removed by washing in D-PBS three times. Cells were plated and incubated on a coverglass until they were adherent (typically within 12 hrs) and transfected with a plasmid (DualpTREt-GluA2i(Q)+GSG1L) that DOX dependently express GluA2flip(Q) and GSG1L. After transfection, 30 µM NBQX and 5 µg/ml doxycycline (DOX) were added. Cells were used for recording 24-36 hr after induction. Ligand (1mM glutamate) was applied via theta tubing glass capillary mounted on a piezo actuator (P-830.30, Physik Instrumente) controlled by an LVPZT amplifier (E-505, Physik Instrumente), DAQ device (NI USB-6221, National Instruments), and LabView software (National Instruments). Recording was done using a single channel of a Multiclamp700B Amplifier (Axon Instruments) operated by pCLAMP10 software.

Signals were digitized using Digidata1440A (Axon Instruments) at a sampling rate of 50 kHz and low pass filtered at 2kHz. Borosilicate glass capillaries (O.D. 1.5 mm, I.D. 0.86

mm, Sutter) were pulled to manufacture electrodes with pipette resistances of 4-5 MΩ. Internal solution was (in mM) 110 NaCl, 10 NaF, 5 EGTA, 0.5 $CaCl_2$, 1 $MgCl_2$, 10 Na_2ATP, 5 HEPES, adjusted to pH 7.3 with CsOH and 295 mOsm. External solution was (in mM) 145 NaCl, 2.5 KCl, 1.8 $CaCl_2$, 1 $MgCl_2$, 5 HEPES, 10 glucose, adjusted to pH 7.3 with NaOH and 301 mOsm. Standard solution without ligand was the external solution. The ligand solution contained 1mM glutamate in external solution, supplemented with 2mM glucose and 3 mM NaCl to facilitate the visualization of the interface of the two solutions and recording liquid junction potential after breaking the patch. A protocol for four 1ms glutamate pulses at 20Hz was programmed using LabView. The 20-80% rise time of liquid junction potential, measured after breaking the patch, was ~300 µs.

2.7. Behavioral experiments

Seizure behavior

To investigate seizure susceptibility behavior, GSG1L KO and WT littermates of both sexes (9-10 month old) were administered an intraperitoneal (i.p.) injection of kainic acid monohydrate (Sigma) dissolved in 0.9% saline solution at 15 mg/kg or 25 mg/kg body weight. Seizure susceptibility was determined immediately following the kainate injections. Seizure activity was video recorded for 2 hrs and scored for severity using a previously described seizure severity scale in a blind manner, with the experimenter blind to the genotype during scoring (Morrison *et al.*, 1996; Wu *et al.*, 2005; Bateup *et al.*, 2013). Seizure severity was assessed at a five-minute interval.

The severity of seizures was assigned based on the following chart:

0, no abnormality;

1- immobility, cessation of normal behavior;

2- rigid posture with extended tail or forelimbs;

3- repetitive behaviors including head nodding, head bobbing, twitching, or scratching;

4- Forelimb clonus with partial or intermittent rearing;

5- continuous forelimb clonus/rearing or repeated rearing and falling;

6- loss of posture, generalized tonic-clonic whole body convulsions or hyperactivity/jumping behavior;

7- mortality.

Novel object recognition task

GSG1L KO and WT littermates of both sexes (9-10 month old) were habituated for 10 min in an empty novel object recognition arena ($40 \times 64 \times 33\,cm^3$) on day 1. The following day, the mice were placed in the novel object recognition arena that contained two identical objects and were allowed to explore the space for 10 min. Following the habituation phase, mice were placed back into their homecage for 1 hr. During probe phase, one of the familiar (previously exposed) objects was replaced with a novel object. The exploration behavior was recorded for 10 min. Time spent exploring familiar and novel objects was scored blindly and the recognition index was identified as (time exploring novel object)- (time exploring familiar object)/total time exploring both objects.

Rotarod

Motor coordination and balance were measured by placing the mice on an accelerating rotating rod (Ugo Basile model 7650; Stoelting Co., Wood Dale, IL, USA). The initial rotations per minute (rpm) were set at 4rpm, which gradually increased to 40 rpm. The performance of each animal was recorded over the course of 300 s. The time taken for a mouse to fall off the rod was recorded by an observer blinded to the mouse genotype. The test was conducted over the course of three days with three independent trials per day.

Elevated Zero Maze

Anxiety was measured using elevated zero maze (San Diego Instruments, CA). The device is an elevated ring-shaped platform with four equal chambers (two open arms and two closed arms). Light levels in the closed arms were at approximately 100 lux and 200 lux in open arms. Mice were placed in the center of an open arm and allowed to explore the maze for 5 min. The activity was video-recorded and analyzed using ANY-maze software (Stoelting, Wood Dale, Illinois, USA).

Grip strength

Grip strength was measured using a Grip Strength Test Apparatus (San Diego Instruments, CA). The grip strength was measured by a digital gauge over 7 independent trials. The average grip strength was calculated as an average of 7 trials (in Newtons).

3. GSG1L has a negative AMPAR regulatory postsynaptic function in a subset of AD/AV synapses

Adapted from Kamalova et al., “AMPA receptor auxiliary subunit GSG1L suppresses short-term facilitation in corticothalamic synapses and determines seizure susceptibility” (Kamalova *et al.*, 2020)

3.1. Introduction

As introduced in Chapter 1, the regulation of excitatory synaptic transmission is essential for synaptic plasticity, learning, and memory. AMPARs play a key role in this process by mediating most fast excitatory neurotransmission in the brain (Bowie, 2008; Traynelis et al., 2010; Huganir and Nicoll, 2013). At the synapses, GluA1–GluA4 are the pore-forming subunits of AMPARs that assemble into functional ligand-gated ion channels consisting of homo- and heterotetramers (Greger et al., 2017). The canonical structural units of native AMPARs are complexes composed of the core tetramers of GluA subunits and their auxiliary subunits (Nakagawa et al., 2005; Schwenk et al.,2012; Zhao et al., 2019).

The most extensively studied among these are the stargazin/TARPs (Tomita et al., 2003). Other auxiliary subunits include CNIH2/3 (Schwenk et al., 2009), CKAMP44 (also known as Shisa9) (von Engelhardt et al., 2010), Shisa6 (Klaassen et al., 2016), SOL-1 (Zheng et al., 2004), and GSG1L (Schwenk et al., 2012; Shanks et al., 2012). Each class of auxiliary subunits is structurally unrelated to the others except for GSG1L and TARPs, which are both claudin homologs. Modulation of AMPARs by auxiliary subunits is predicted to substantially affect brain function (Jackson and Nicoll, 2011). As discussed in Chapter 1, mutations in one or more AMPAR auxiliary subunits lead to

neurological and cognitive deficits in both mice and humans (Everett et al., 2007; Hamdan et al., 2011; Floor et al., 2012).

Most AMPAR auxiliary subunits positively modulate AMPAR function by promoting synaptic trafficking and/or modifying gating toward increasing net charge transfer (Jackson and Nicoll, 2011). A subset of auxiliary subunits has mixed effects on gating. For example, CKAMP44 slows AMPAR deactivation, increasing net charge transfer during synaptic transmission, but also delays recovery from desensitization so that the channel is not immediately re-usable (von Engelhardt et al., 2010). Similarly, TARP γ-8 slows AMPAR desensitization and delays recovery from AMPAR desensitization of GluA2 and GluA3 specifically (Cais et al., 2014).

Among all auxiliary subunits, GSG1L stands out for having a strong negative modulatory function (McGee et al., 2015; Gu et al., 2016; Mao et al., 2017) . Although GSG1L also slows desensitization, it stabilizes the desensitized state (Twomey et al., 2017b) and dramatically delays recovery from desensitization, over a magnitude slower than other auxiliary subunits (Schwenk et al., 2012; Shanks et al., 2012). In addition, GSG1L reduces single-channel conductance and calcium permeability of calcium-permeable AMPARs (McGee et al., 2015). Consistently, overexpression of GSG1L decreases the amplitude of evoked EPSCs in (McGee et al., 2015; Gu et al., 2016; Mao et al., 2017).

The extent of this negative regulation *in* vivo and slowing of the recovery from AMPAR desensitization phenotype has yet to be shown in synapses. Overall GSG1L expression in the brain is low (Schwenk *et al.*, 2014b), but it is possible that it is enriched in distinct brain regions. Despite its pronounced negative AMPAR regulatory role, it is unclear to what extent GSG1L is utilized *in vivo.* Previous studies have looked at phenotypes of GSG1L KO rats and failed to identify GSG1L-dependent postsynaptic modulation in synapses due to co-expression of another auxiliary subunit CNIH2 (Gu *et al.*, 2016). Therefore, further investigations will be needed to identify GSG1L-dependent regulation in synapses where it is functionally expressed.

In this chapter, I will demonstrate that GSG1L is enriched in the AD and AV nuclei in the anterior thalamus. As discussed in the previous chapter, the anterior thalamus is important for memory formation (Aggleton & Brown, 1999; Wolff *et al.*, 2006), encoding head direction information during spatial navigation (Clark & Taube, 2012), as well as seizure initiation and propagation (Mirski & Ferrendelli, 1984; Hamani *et al.*, 2004; Takebayashi *et al.*, 2007; Bittencourt *et al.*, 2010). However, the molecular mechanisms that regulate synaptic function of the anterior thalamus remain largely unexplored compared to other thalamic nuclei such as LGN. In our investigations, we find that GSG1L has a postsynaptic role in regulating short-term plasticity in synapses that receive inputs from the cortex, but not from the subiculum or the mammillary bodies. Importantly, we also determine that GSG1L and stargazin are co-expressed in the AD/AV. We find that these two auxiliary subunits are sequestered into distinct synapses. Among the synapses in the AD/AV neurons formed by three distinct input projections,

cortico-thalamic synapses are controlled by GSG1L, but not by stargazin. Finally, similar to reports from *in vitro* heterologous systems, we discover that GSG1L and stargazin compete *in vivo*.

3.2. GSG1L has a high and persistent expression in AD and AV throughout development

In order to unambiguously determine the synaptic function of GSG1L, we first needed to know its expression pattern within the brain. While our house made polyclonal antibodies against GSG1L work well for detecting protein levels using western blotting; unfortunately, none of them worked for immunohistochemistry (data not shown). We were able to circumvent this problem by using a transgenic rat that expresses a lacZ reporter under the control of GSG1L promoter, which allowed us to determine detailed spatio-temporal expression pattern of GSG1L over the course of 8 months (Figure 3.1A-B). This was achieved by using lacZ expression as proxy for GSG1L expression during development.

The homozygous GSG1L KO rats were viable and did not present with any apparent early developmental or behavioral deficits while housed in their home cages. To confirm the loss of GSG1L protein in KO rats, we probed GSG1L with a polyclonal antibody (Shanks *et al.*, 2012) on anti-GluA2-CT co-precipitates since the anti-GSG1L antibody was not sensitive enough for direct detection from whole brain extracts. Taking this approach, we confirmed that GSG1L was co-immunoprecipitated only from the wildtype lysate, consistent with the disruption of GSG1L gene at exon 3-4, while equal amounts of GluA2 were pulled down from WT and KO rat brains (Figure 3.1B). We also found no significant

difference in co-immunoprecipitation of stargazin (TARP γ -2), as assessed by anti-panTARP antibody generated against the C-terminal peptide of stargazin (Nakagawa *et al.*, 2005).

To systemically analyze lacZ expression in whole brains, homozygous GSG1L KO rats at P14, P24, P42, and P120 were compared with corresponding WT littermates taken as negative controls. The chromogenic reaction by X-gal produced blue stain reporting the expression of lacZ, which was dynamic across the developmental time points that were tested (Figure 3.1C). No staining was observed in WT controls. Strong lacZ expression was observed in the external granular layer (EGL) of cerebellum at P14 (Figure 3.1C). The EGL contain precursors of granule cells that migrate and differentiate by P20 into the internal granular layer of the cerebellum (Silbereis *et al.*, 2010). Indeed, at later developmental time points, we observe high lacZ expression in the granular layer of cerebellum (Figure 3.1C). The striated staining pattern in the adult rats is consistent with a signal emerging from the mature granule cell layer, with no expression in the molecular layer. We further observe strong lacZ expression in olfactory bulbs and the pons at P17 and P21 (Figure 3.1C). Taken together, the whole brain X-gal staining of the GSG1L KO showed that the expression levels increase during development except for limited brain regions where expression remain persistent.

Next, we generated 300 μm-thick coronal sections from P14, P21, P60, P180, and P240 GSG1L KO and WT brains, and stained with X-gal post-sectioning to maximize dye penetration into the inner brain structures. Notably, lacZ staining in the hippocampus is undetectable in young animals (P14 and P21). At P60, lacZ staining is apparent in the dentate gyrus (DG) but overall, it is low in the CA and CA3. The expression persists and

increases as the animal ages at P180 and P240 (Figure 3.2C, top). This is further corroborated by the *in situ* hybridization data from the Allen Brain Atlas (Figure 3.2D, top).

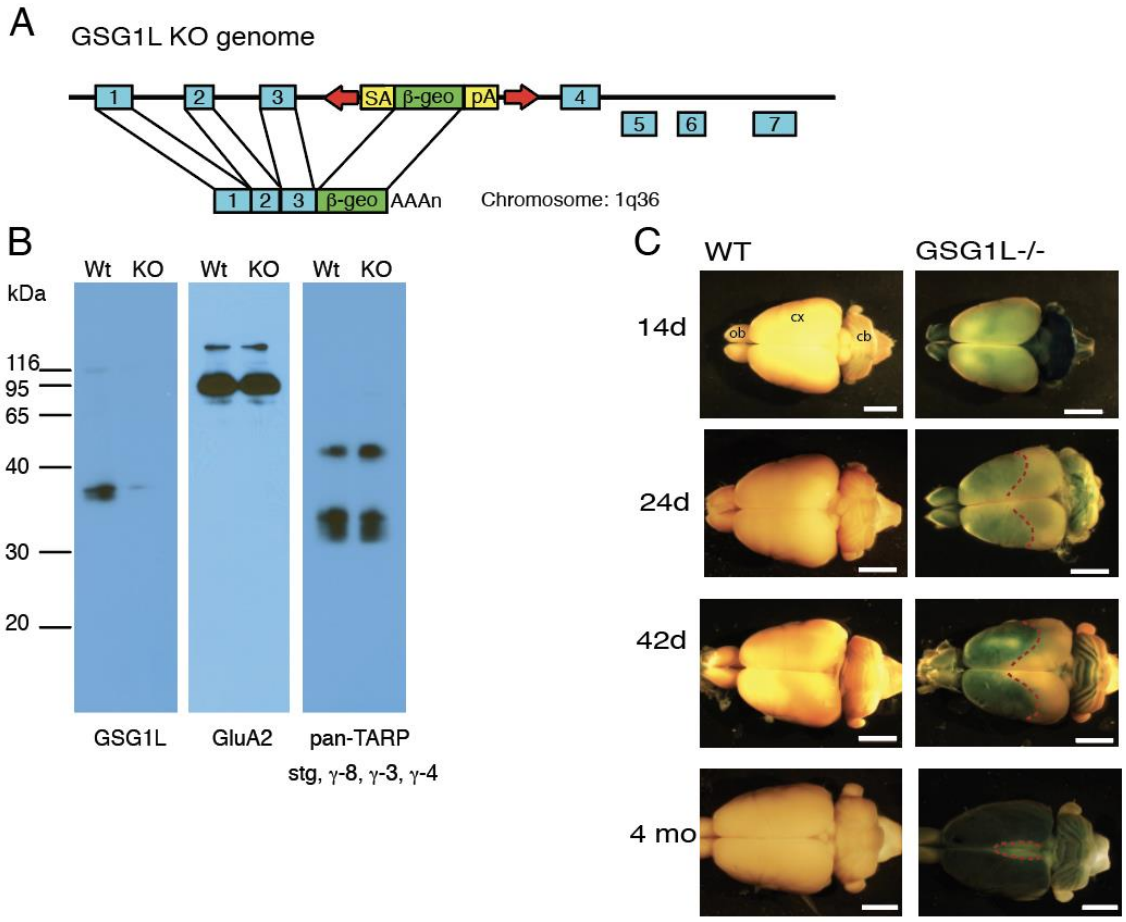

Figure 3-1. Characterization of transgenic GSG1L KO rat expressing lacZ under the control of endogenous GSG1L promoter.

A. A lacZ containing transposon is inserted after exon 3 thereby disrupting the normal splicing event. B. Western blot of immunoprecitate of anti-GluA2CT antibody from 1% CHAPS-extracted total brain membrane. GSG1L KO homozygotes lack GSG1L immunoprecitation. GluA2 and TARP levels, detected with anti-panTARP antibody, are unchanged in GSG1L KO relative to WT. C. Whole brain lacZ staining of P14, P24, P42, and 4mo GSG1L KO brains. LacZ staining is dynamic with increased levels in adult animals. Cortical staining is restricted as shown by dashed red lines.

Although gene KO could potentially influence GSG1L promoter activity in transgenic GSG1L KO rats, we suggest that LacZ expression represents the endogenous expression patterns of GSG1L. In support of this, the lacZ signals in heterozygotes were weaker but the distribution was overall identical to that of homozygotes (data not shown). Furthermore, in situ hybridyzation data from Allen Brain Atlas is consistent with our lacZ analysis.

LacZ expression is an indirect way of looking at GSG1L expression and it is based on the overall promoter activity. Therefore, to further confirm GSG1L expression dynamics at the protein level, we examined the developmental changes in GSG1L protein expression in the cortex using westernblots in mouse, which paralells the results from rats (Figure 3.2.). To this end, we pulled down GSG1L from WT mouse cortices at various developmental time points such as P17, 2mo, 4mo, and 6mo. Importantly, GSG1L uniquly increases expression in mature animals, while this trend that was not observed for stargazin and CNIH2. We predict that the abudance of GSG1L containing AMPAR complexes increases with aging due to an overall decrease in AMPAR subunits, GluA1, GluA2, and GluA4 (Figure 3.2).

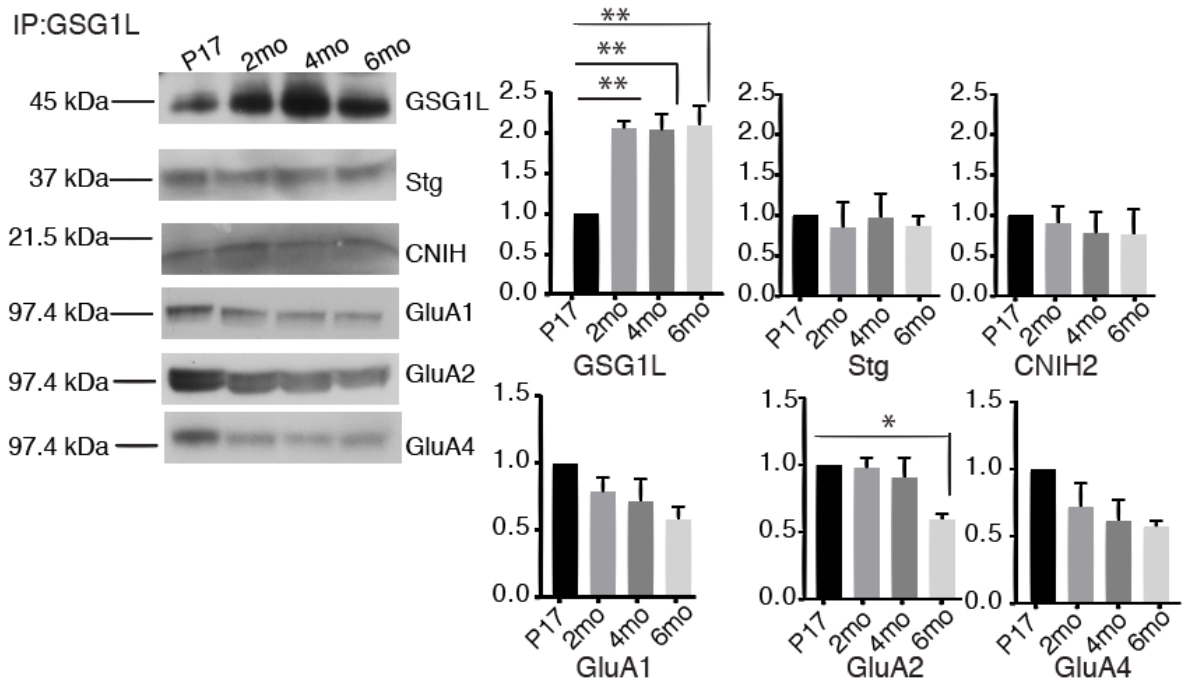

Figure 3-2. GSG1L protein levels in the mouse cortex increase during development.

Western blot showing increased cortical GSG1L protein levels in adults. WT mouse cortices were dissected out from P17, 2mo, 4mo, and 6mo WT animals (4 brains each). GSG1L was immunoprecipitated, with anti-GSG1L Ct-1 antibodies, from 1% CHAPS-extracted membrane fraction. GSG1L protein levels increase in the cortex from P17 to 6mo.

GSG1L has an age-dependent increase in expression in most brain regions, with an overall increase at about 2 months. Out of all brain regions that we examined, AD and AV nuclei of the anterior thalamus stood out and had the most persistent lacZ expression at all the developmental time points we tested. High expression of GSG1L was found in the anterior thalamus throughout development (Figure 3.3A, bottom). GSG1L is restricted to AD and AV, but absent in anteromedial (AM) or lateral dorsal nuclei (LD), in agreement with *in situ* hybridization data from the Allen Brain Atlas (Figure 3.3D, bottom) (Lein *et al.*, 2007a).

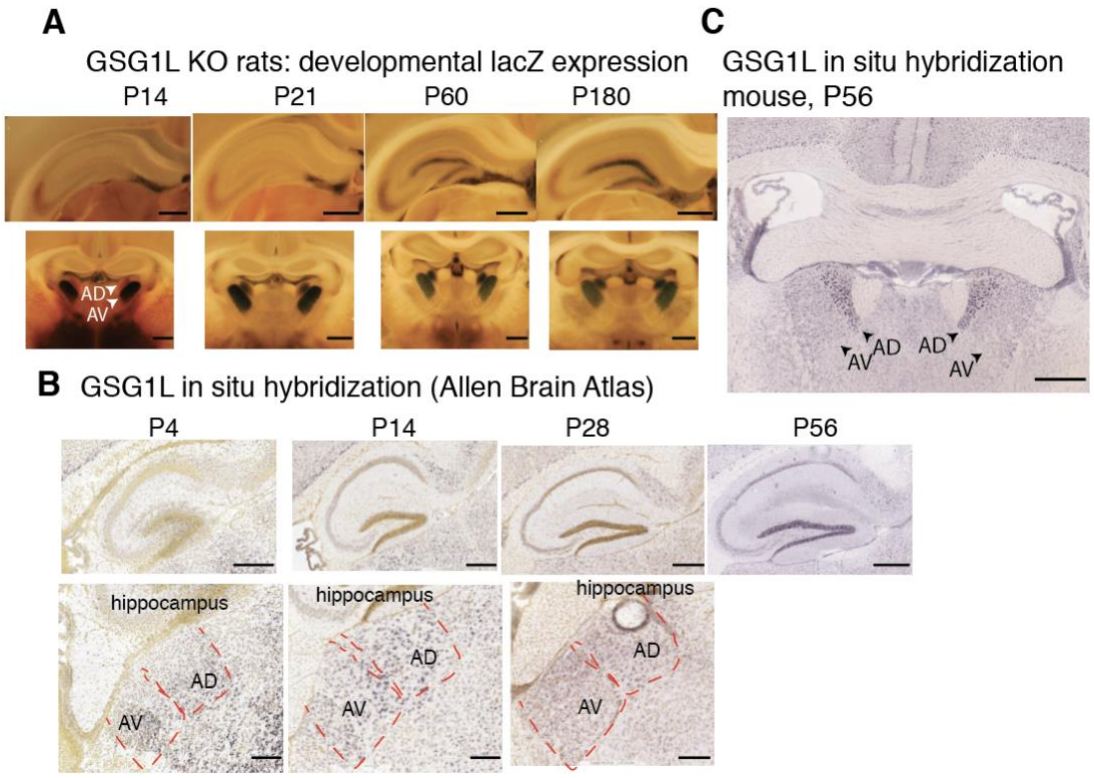

Figure 3-3. High expression of GSG1L in AD/AV nuclei.

A. GSG1L KO rat brains at P-14, 21, 60, and 180, lacZ expression is represented by dark blue stain (scale bar- 1000 µm). (Top=hippocampus) The expression in the DG is minimal at P14 and P21, but increases at P60 and further at P180 . The expression in CA3 is very low, whereas the expression in CA1 is minimal throughout. (Bottom=AT) The intensity of lacZ staining is substantially greater in AD/AV than the signal in the hippocampus at P14, P21, and P60 (scale bar- 1000 µm). B. *In situ* hybridization data from the Allen Brain Atlas in the hippocampus (top) and AD/AV (bottom) is consistent with our LacZ staining pattern (scale bar- 420 µm). C. *In situ* hybridization data (from Allen Brain Atlas) shows GSG1L expression in AD and AV nuclei (scale bar- 420 µm).

3.3. GSG1L is sufficient to induce short-term depression *in vitro*

To determine the synaptic function of GSG1L, we aimed to look at GSG1L-dependent "signature" modulations. The most significant action of GSG1L *in vitro* is the slowing of AMPAR recovery from desensitization (Figure 3.4A) (Schwenk *et al.*, 2012; Shanks *et al.*, 2012). Furthermore, GSG1L has been shown to negatively regulate the amplitude of AMPAR-mediated EPSCs (Figure 3.4A) (McGee *et al.*, 2015; Gu *et al.*, 2016).

Given the strong effect on the recovery from AMPAR desensitization, we predict that, in synapses in which AMPARs desensitize, GSG1L should prevent immediate re-use of AMPARs during repetitive activation and as a result promote short-term depression or attenuate short-term facilitation. Conversely, elimination of GSG1L should relieve short-term depression, or in an extreme case, convert to short-term facilitation.

Consistent with this hypothesis, GSG1L was sufficient to induce short-term depression in a reconstituted system (Figure 3.4B-E). Indeed, we found that outside-out patches pulled from HEK293 cells that co-express GSG1L and GluA2 (flip splice variant with unedited Q-pore) show significantly depressing currents in response to 1 mM glutamate pulses of 1 ms at 20 Hz, while in the absence of GSG1L the amplitudes remained constant (Figure 1B-E). These findings show that presence of GSG1L in recombinant systems is sufficient to induce short-term depression in response to repetitive stimulation.

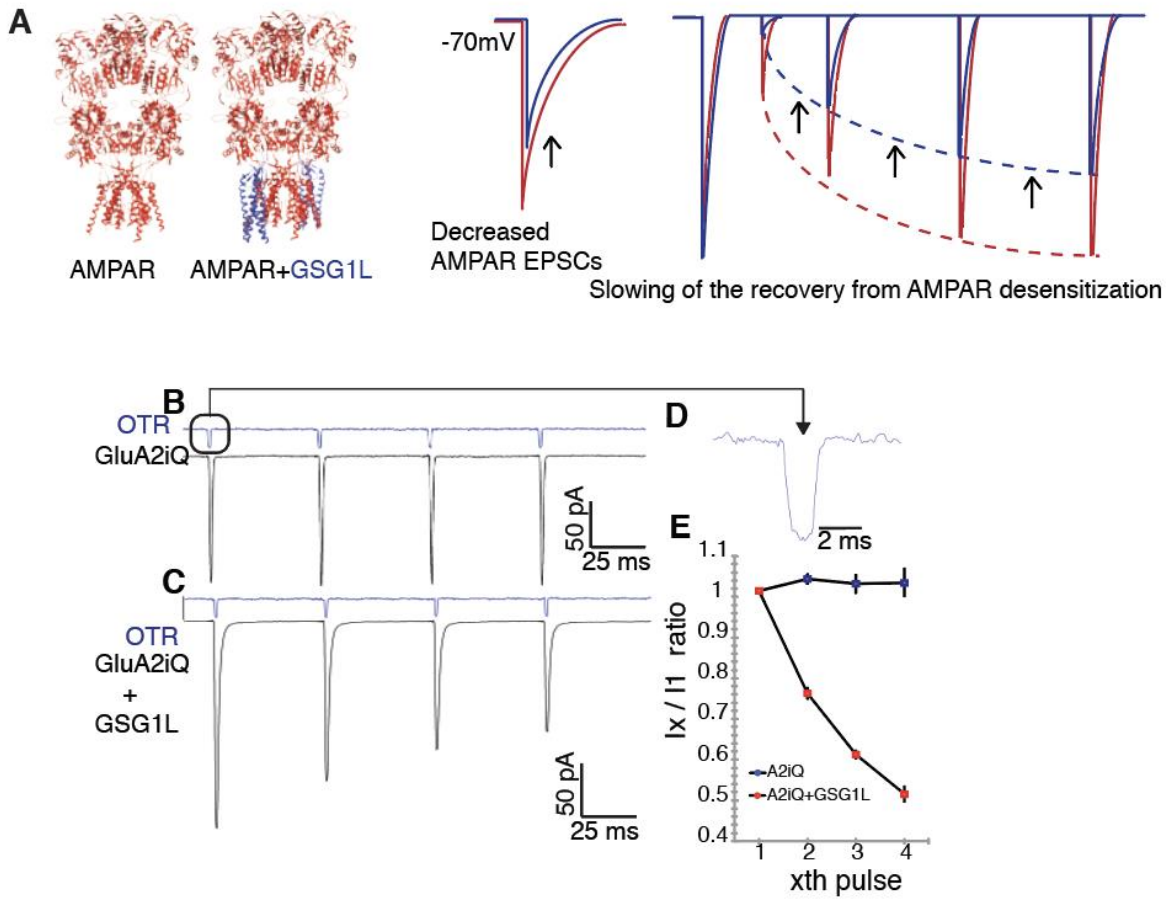

Figure 3-4. GSG1L is sufficient to induce short-term depression *in vitro*.

A**.** Ribbon diagram of GluA2 (red) with or without GSG1L (blue), PDB 5WEK (Twomey *et al.*, 2017a). Schematic drawing summarizing the effects of GSG1L, emphasized with black arrows (right). AMPAR+GSG1L (blue lines) exhibits decreased amplitude and slower recovery from desensitization compared to AMPAR alone (red lines). B-E. Recordings from outside out patches. Representative averaged traces for B. GluA2iQ (i.e. flip/Q-pore) alone, and C. GluA2iQ+GSG1L. OTR=open tip response. D. A magnified view of the OTR. E. The ratio of each pulse over the first pulse (Ix/I1, where x=2, 3, and 4). A2iQ(n=5), A2iQ+GSG1L(n=4) ($p<0.001$ for pulse #2-4, Two-Way ANOVA).

3.4. Input-specific modulation of short-term plasticity by GSG1L

Having established that presence GSGL is sufficient to induce short-term depression through slowing of the recovery from receptor desensitization in recombinant systems, we next aimed to determine whether GSG1L also slows this parameter in AD/AV neurons. While we attempted to measure the recovery from desensitization directly, AD/AV neurons appear to have not enough somatic receptors to perform outside-out patch recordings (data not shown). An alternative possibility is to look at the potential contribution of the recovery from AMPAR desensitization to short-term plasticity. While the two most common mechanisms of short-term plasticity are both presynaptic, recovery from AMPAR desensitization is one of the postsynaptic mechanisms that can occur in certain brain regions (Chen *et al.*, 2002).

The AD and AV share progenitor origin (Shi *et al.*, 2017), expression profile of neurotransmitter receptors (Phillips *et al.*, 2019), as well as afferent and efferent projections (Jankowski *et al.*, 2013). Therefore, we will treat the two as single nuclei, AD/AV, in our investigation. The AD/AV nuclei receive dense projections from the retrosplenial cortex, the subiculum, and the mammillary bodies via the mammillothalamic tract (Wright *et al.*, 2010) (Figure 3.6A-B). Through directly stimulating each afferent, we can selectively record evoked postsynaptic responses from individual inputs (see methods and Figure 1I) (Petrof & Sherman, 2009; Oh *et al.*, 2014).

Analogous to the sensory thalamic relay circuits (Sherman & Guillery, 2004), the inputs to the AD/AV neurons are classified into driver and modulator inputs. Specifically, mammillary bodies inputs drive the firing of the AD/AV neurons, whereas cortical and

subiculum inputs modulate the action of the mammillary bodies inputs (Petrof & Sherman, 2009). However, recent findings suggest that cortical inputs to AD/AV may have characteristics of a driver pathway (Vantomme *et al.*, 2020).

In order to study the synaptic function of GSG1L in a model organism with a wealth of latest genetic tools, we generated a mutant mouse with global and a conditional null of GSG1L (Figure 3.5). We chose to delete exon 4 because the nucleotide base pairs of exon 1-3 are all multiples of 3, and thus deleting them will not induce codon frame shift, potentially resulting in an expression of an aberrant protein. The exon 4 encodes 3rd and 4th TMD that we have determined by co-IP to be essential for interacting with AMPARs (data not shown). Furthermore, when deletion mutant of GSG1L were generated and expressed in primary hippocampal neurons, constructs that do not have all four intact TMD did not localize to the synapse (data not shown). Therefore, even if a fragment of GSG1L encoding exon 1-3 is present in the mutant mice it would have minimal effect on AMPAR function.

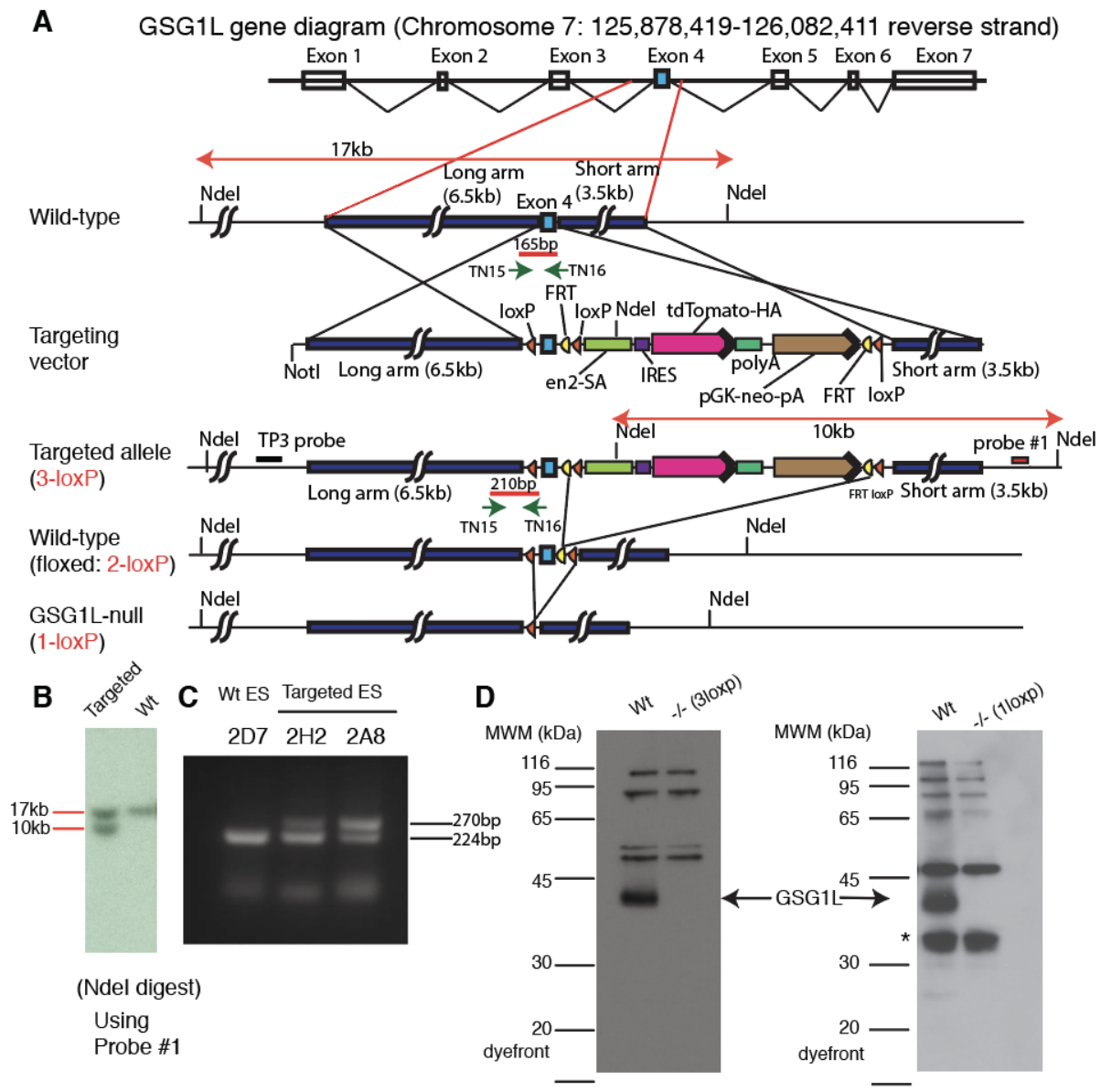

Figure 3-5. Characterization of GSG1L KO mouse line.

A. Targeting strategy. B. A representative genomic Southern blot demonstrating an ES clone with band pattern consistent with homologous recombination. C**.** PCR based genotyping demonstrating 2 bands in targeted ES clones and only one band in wild type. **D.** Western blot demonstrating absence of GSG1L in 3-loxP and 1-loxp homozygote brains. Note: lower band in 1loxp KO blot is nonspecific (denoted with *).

Inputs to AD/AV neurons undergo varying degrees of short-term plasticity upon repetitive stimulation (Petrof & Sherman, 2009). Given the high expression of GSG1L in the AD/AV neurons, we wondered if GSG1L is responsible for short-term plasticity. To address this, the extent of short-term plasticity in AD/AV neurons was compared between GSG1L KO and WT mice.

Sagittal sections were used to record from mammillothalamic and subiculum-thalamic synapses, whereas coronal sections were used to obtain corticothalamic synapses . We electrically stimulated the mammillary bodies inputs (i.e. the mammillothalamic tract) at 20 Hz and 50 Hz, while whole-cell recording from AD/AV neurons (Figure 3.6C-E, Figure 3.7A-C). The degree of synaptic depression in the mammillothalamic synapses was quantified by taking amplitudes ratios of the first (S1) and following four (S2–5) responses. There was no statistical difference between GSG1L KO and WT control littermates (Figure 3.6C-E, Figure 3.7A-C). Similar results were obtained when inputs from the subiculum, the subiculum-thalamic synapses, were examined at 20 Hz and 50 Hz (Figure 3.6F-H, Figure 3.7D-F). In contrast, stimulation of the corticothalamic pathway of GSG1L KO, at both 20 Hz and 50 Hz, resulted in enhanced synaptic facilitation, relative to WT control and heterozygous littermates (Figure 3.6I-K, Figure 3.7G-I). Importantly, similar findings were obtained when only the AD synapses were examined, consistent with the close cellular pedigree of neurons in the AD and AV nuclei (Figure 3.7J-M) (Shi *et al.*, 2017).

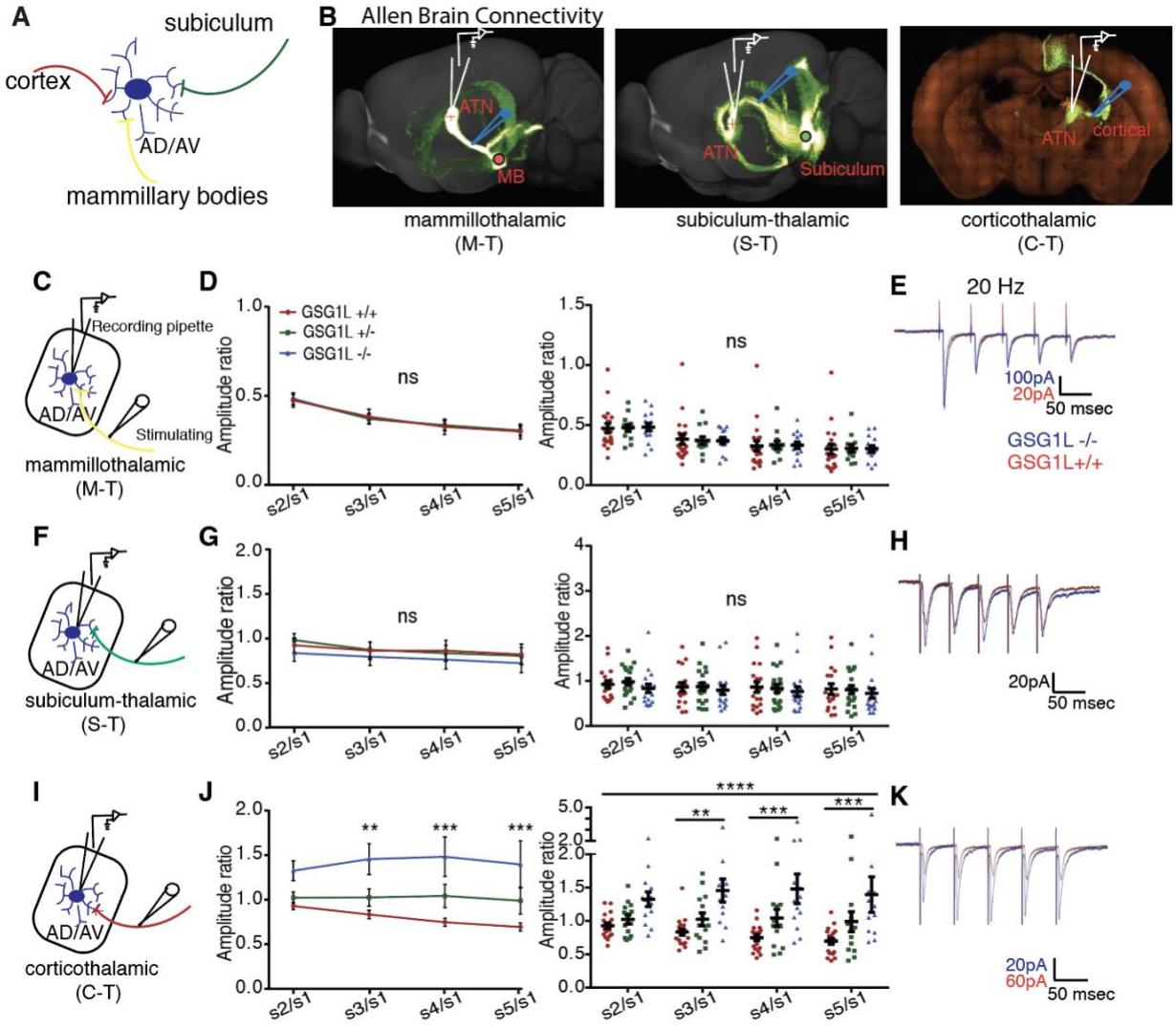

Figure 3-6. GSG1L input-specifically regulates short-term plasticity at cortico-thalamic synapses in AD/AV.

A. Inputs received by AD/AV. B. Input dependent stimulation paradigm of AD/AV (scale bar-420 µm). Brain images were derived from Allen Brain Connectivity (Oh *et al.*, 2014). C, F, and I**.** Schematic illustrations of the pathways**.** D**.** Pulse-ratios of electrically evoked EPSCs from AD/AV neurons at a holding potential of -70 mV of GSG1L KO (P21-P33, n=15 cells, N=6 mice), Het (n=13, N=5), and WT (n=20, N=8). S1-5 are amplitudes of each stimulus in a train of five stimuli (p=0.9956,Two-Way ANOVA). S(n)/S1, where n=2,..,5, is the paired pulse ratio of 2-5th pulse divided by the 1st pulse. E,H,K. Superimposed sample traces of whole-cell recordings of

currents in AD/AV in response to mammillary bodies, subiculum, or cortical stimulation. G. No changes in pulse ratios between GSG1L KO (P21-P33, n=18, N=6), Het (n=20, N=6), WT (n=18, N=7) (p=0.7288, Two-Way ANOVA) in response to subiculum stimulation at 20 Hz. J. Pulse ratios are significantly different between GSG1L KO (P21-P33, n=13, N=6), Het (n=14, N=6) and WT (n=19, N=7) at 20 Hz (p<0.0001, Two-Way ANOVA) in response to cortical stimulation. *Post hoc* Sidak comparisons: ** *p<0.01, *** p<0.001, **** p<0.0001.*

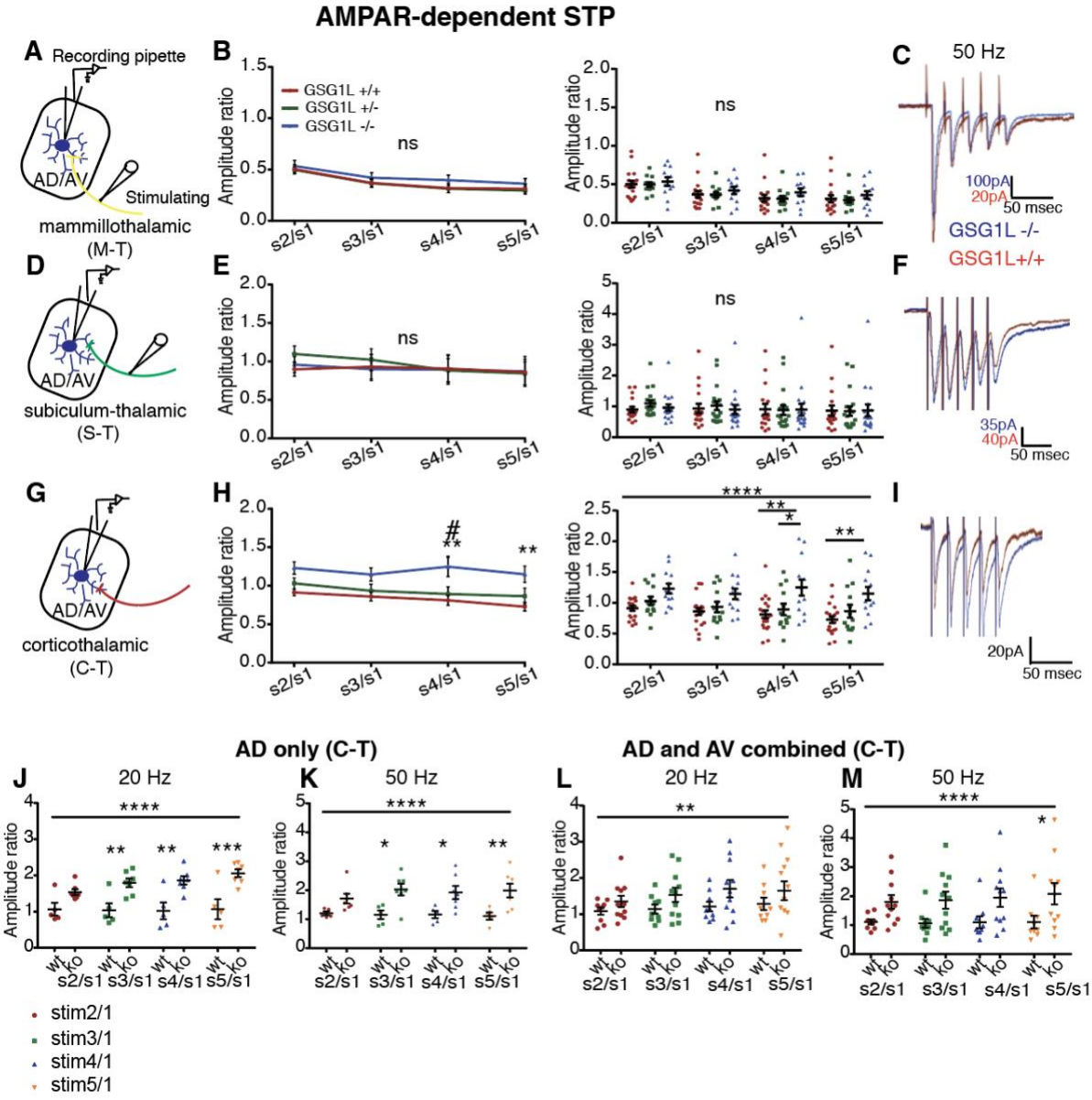

Figure 3-7. GSG1L input specifically regulates short-term plasticity at cortico-thalamic synapses. A, D, and G,. Schematic illustrations of the pathways. B. Pulse-ratios of electrically evoked EPSCs from AD/AV neurons at a holding potential of -70 mV of GSG1L KO (P21-P33, n=12 cells, N=6 mice), Het (n=13, N=5), and WT (n=17, N=8). S1-5 are amplitudes of each stimulus in a train of five stimuli. S(n)/S1, where n=2,…,5, is the paired pulse ratio of 2-5th pulse divided by the 1st pulse. Pulse-ratios (PPR) at 50 Hz in response to mammillary bodies stimulation (p=0.1402,Two-Way ANOVA). C, F, and I. Superimposed sample traces of whole-cell recordings of currents in AD/AV in response to mammillary bodies, subiculum, or cortical stimulation. E. No differences in PPR between GSG1L KO (P21-P33, n=17, N=6), Het (n=18,

N=6), WT (n=18, N=7) (p=0.8159, Two-Way ANOVA) in response to subiculum stimulation. H. PPR is significantly different between GSG1L KO (P21-P33, n=13, N=6), Het (n=13, N=6) and WT (n=19, N=7) (p<0.0001, Two-Way ANOVA) in response to cortical stimulation at 50 Hz. J, and K. Pulse-ratios of electrically evoked EPSCs from AD neurons of GSG1L KO (P15-30, n=5, N=3) and WT (n=7, N=3). Both At 20 Hz (p<0.0001, Two-Way ANOVA) and 50Hz (p<0.0001, Two-Way ANOVA) the PPR is enhanced in GSG1L KO. L, and M. Pulse-ratios of electrically evoked EPSCs from AD and AV neurons at a holding potential of -70 mV of GSG1L KO (P15-30, n=11, N=5) and WT (n=9, N=3). Both at 20 Hz (p=0.0063,Two-Way ANOVA) and 50 Hz C stimulation (p<0.0001,Two-Way ANOVA), the PPR is enhanced in AD/AV corticothalamic synapses in GSG1L KO. *Post hoc* Sidak comparisons: * *p<0.05,* ** *p<0.01,* *** *p<0.001,* **** p<0.0001). Data in L-M are collected from a different set of animals from those used in H-I, thus there is no re-use of data points.

Given that two most common mechanisms for presynaptic plasticity are both presynaptic, it is important to establish that the genotype effect we observed is due to a postsynaptic mechanism. Changes in the presynaptic glutamate release would affect both AMPARs and NMDARs. If short-term plasticity were mediated by a presynaptic mechanism, one would expect to find the effect of the genotype in both AMPAR-mediated and NMDAR-mediated EPSCs. Therefore, to exclude the possibility of a presynaptic effect, we examined short-term plasticity of NMDAR mediated EPSCs in the corticothalamic synapses in response to 20 Hz and 50 Hz stimulations (Figure 3.8A-E).

We found no differences between GSG1L KO and control littermates indicating that the effect is postsynaptic and AMPAR-dependent. Input-specific stimulation of the corticothalamic pathway unveiled the postsynaptic role of GSG1L, where its deletion is associated with enhanced synaptic short-term facilitation. Collectively, these results

suggest that GSG1L input-specifically regulates synaptic plasticity at the AD/AV by likely slowing the recovery from AMPAR desensitization.

3.5. AMPAR desensitization occurs at corticothalamic synapses of AD/AV neurons

If GSG1L indeed regulates cortico-thalamic synapses by altering the rate of recovery from desensitization of postsynaptic AMPARs, desensitization of AMPAR must be occurring during synaptic transmission. A simple way to test this is to examine sensitivity of evoked EPSCs to cyclothiazide (CTZ), a blocker of AMPAR desensitization. In GSG1L WT mice, whole-cell recordings from AD/AV neurons detected a significant increase in the degree of synaptic facilitation upon addition of 100 µM CTZ, while stimulating the cortical inputs at 20 Hz and 50 Hz in the presence picrotoxin, a blocker of GABA-A receptors. Interestingly, we find that AMPAR desensitization contributes to short-term plasticity at all three synapses at AD/AV nuclei (data not shown). The degree of synaptic depression and facilitation was attenuated in mammillothalamic, subiculum-thalamic, and corticothalamic synapses in C57BL6/J mice in the presence of CTZ. Importantly, CTZ sensitivity in corticothalamic synapses requires GSG1L, as it is absent in GSG1L KO (Figure 3.8F-J). This further substantiates our hypothesis that GSG1L affects short-term plasticity in these synapses through a postsynaptic mechanism of slowing the AMPAR recovery from desensitization.

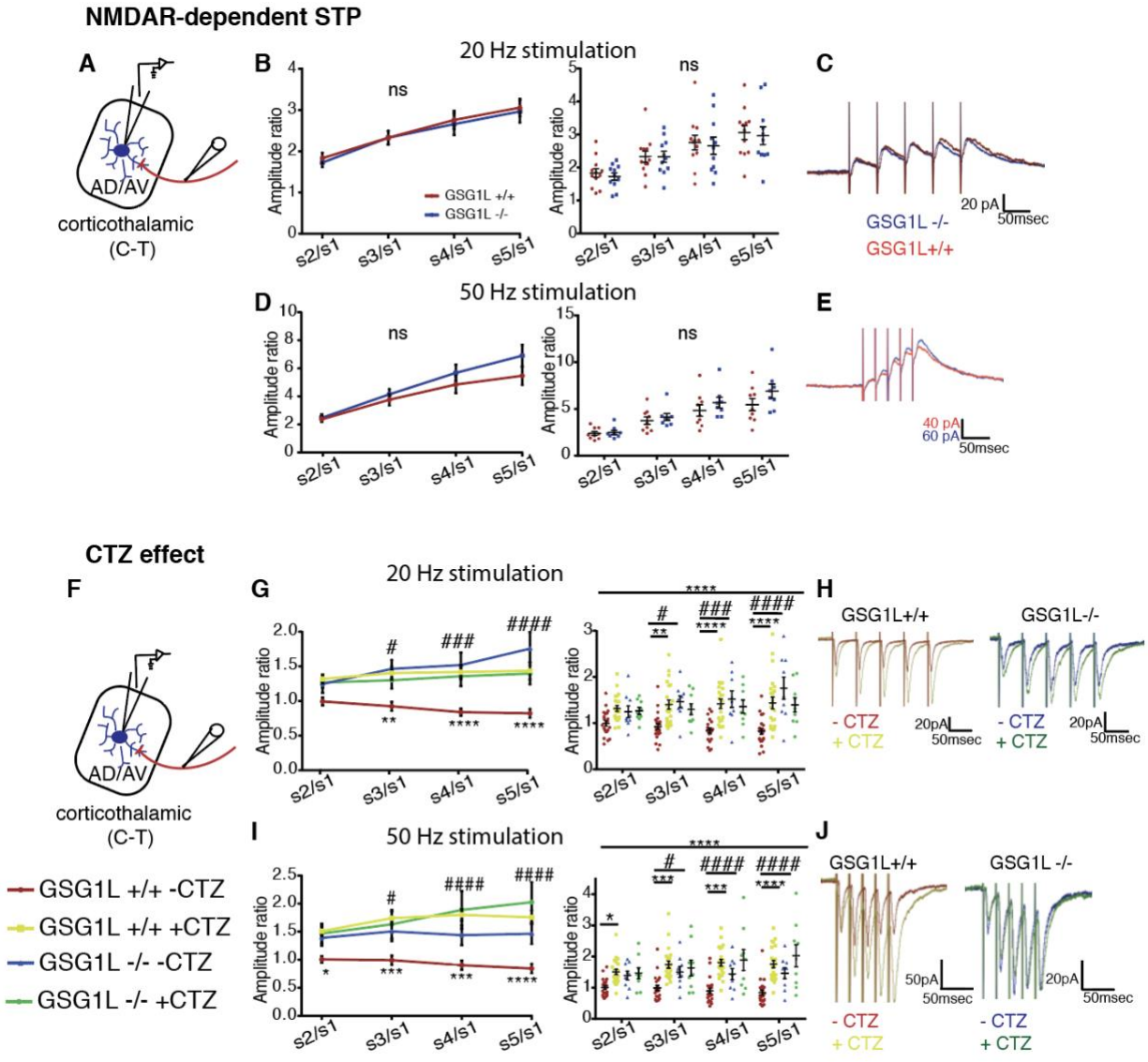

Figure 3-8. The effect of GSG1L on short-term plasticity is postsynaptic.

A. Schematic illustrations of the C-T pathway. B and D. GSG1L does not have a presynaptic effect with no changes in NMDAR component. Pulse-ratios of electrically evoked EPSCs from AD/AV neurons at a holding potential of +30 mV in the presence of NBQX and picrotoxin, of GSG1L KO at 20 Hz (P15-P30, n=11, N=3) and WT (n=12, N=3) (p=0.5940, Two-Way ANOVA) and 50 Hz (p=0.0623, Two-Way ANOVA). C and E. Superimposed sample traces of whole-cell recordings of NMDAR currents of AD/AV in response to C stimulation at 20 Hz and 50 Hz. **F.** Schematic illustrations of the C-T pathway. G and I. Bath application of 100 bath application of

100 of the C-T pathway. Recordings of NMDAR currents of AD/AV in response to C stimulation at 20 Hz and mice (n=9, N=6) (*p<0.0001,*for both 20 and 50 Hz, Two-Way ANOVA) at 20 Hz and at 50 Hz. H and J. Superimposed sample traces of whole-cell recordings of currents of AD/AV GSG1L WT in response to C stimulation at 20 Hz and 50 Hz before (red) and after (yellow) CTZ application. GSG1L KO before (blue) and after (green) CTZ application. *Post hoc* Sidak comparisons: * p<0.05, ** p<0.01, *** p<0.001, **** p<0.0001 (symbol * denotes comparison of GSG1L WT –CTZ and WT +CTZ; # WT-CTZ and KO-CTZ; & WT-CTZ and KO +CTZ).

3.6. GSG1L modulates basal synaptic transmission at corticothalamic synapses

Another predicted signature of synapses regulated by GSG1L is the reduction of the amplitude of AMPAR mediated responses (Figure 3.4A) (McGee *et al.*, 2015). Thus, we next investigated whether GSG1L also regulates basal AMPAR-mediated synaptic transmission by recording AMPAR-mediated miniature EPSCs (mEPSCs) in AD/AV neurons from GSG1L KO and WT mice (Figure 3.9A-D). Interestingly, we found no significant differences in the average amplitude nor the frequency of AMPAR mediated mEPSCs. However, upon careful inspection, we found that there was a subset of GSG1L KO neurons with enhanced amplitude of mEPSCs (Figure 3.9C). This is in agreement with GSG1L functionally regulating a subset of synapses, specifically those formed by corticothalamic inputs.

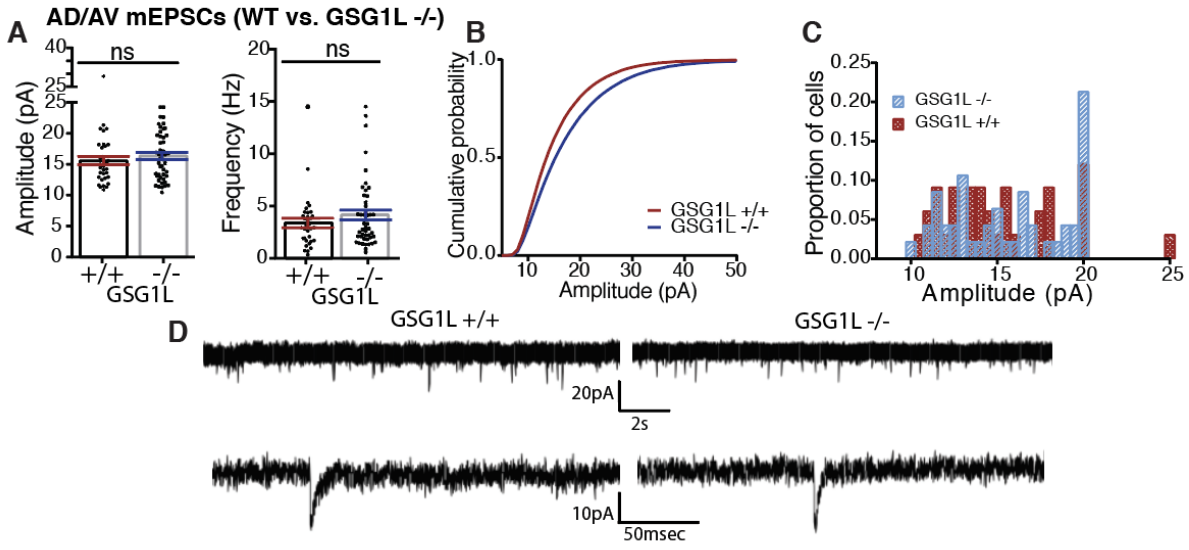

Figure 3-9. No changes in AMPAR-mediated mEPSCs at AD/AV nuclei.

A. Mean amplitude and frequency of AMPAR-mediated mEPSCs in the AD/AV of GSG1L KO and GSG1L WT (p=0.3082, p=0.4054 respectively, Mann Whitney U test) ; GSG1L KO (P15-P30, n=47, N=4; GSG1L WT n=33, N=3). B. Cumulative plot of the amplitude distribution (p=0.0041, Kolmogorov-Smirnov, K-S, test,). C. Histogram of amplitudes of individual cells**.** D. Representative traces of AMPAR-mediated mEPSCs in each genotype.

To directly test whether GSG1L regulates basal synaptic transmission at corticothalamic synapses, we recorded asynchronous quantal EPSCs (qEPSCs) evoked in the presence of strontium (4 mM $SrCl_2$) (Figure 3.10A-D). Synaptic responses produced by isolated asynchronous quantal events represent postsynaptic AMPAR activity in the evoked pathway (Goda & Stevens, 1994). This experimental paradigm would allow us to directly examine the postsynaptic AMPAR activity specifically in corticothalamic synapses comparing GSG1L KO and WT.

Indeed, we found that the amplitude of asynchronous qEPSCs is enhanced in GSG1L KO animals relative to WT control (Figure 3.10A-D). The frequency of qEPSCs was also higher in GSG1L KO corticothalamic synapses, most likely due to increase in apparent detection sensitivity caused by increase in the amplitudes. Additionally, consistent with GSG1L's role in modulating AMPAR gating kinetics in heterologous systems (Schwenk *et al.*, 2012; Shanks *et al.*, 2012), the kinetics of corticothalamic qEPSCs are accelerated in GSG1L KO relative to WT control. While the difference in the rise time of qEPSCs was not significant ($p=0.0900$), the decay time was significantly reduced in GSG1L KO consistent with GSG1L slowing the deactivation kinetics *in vitro* (Figure 3.10E-H).

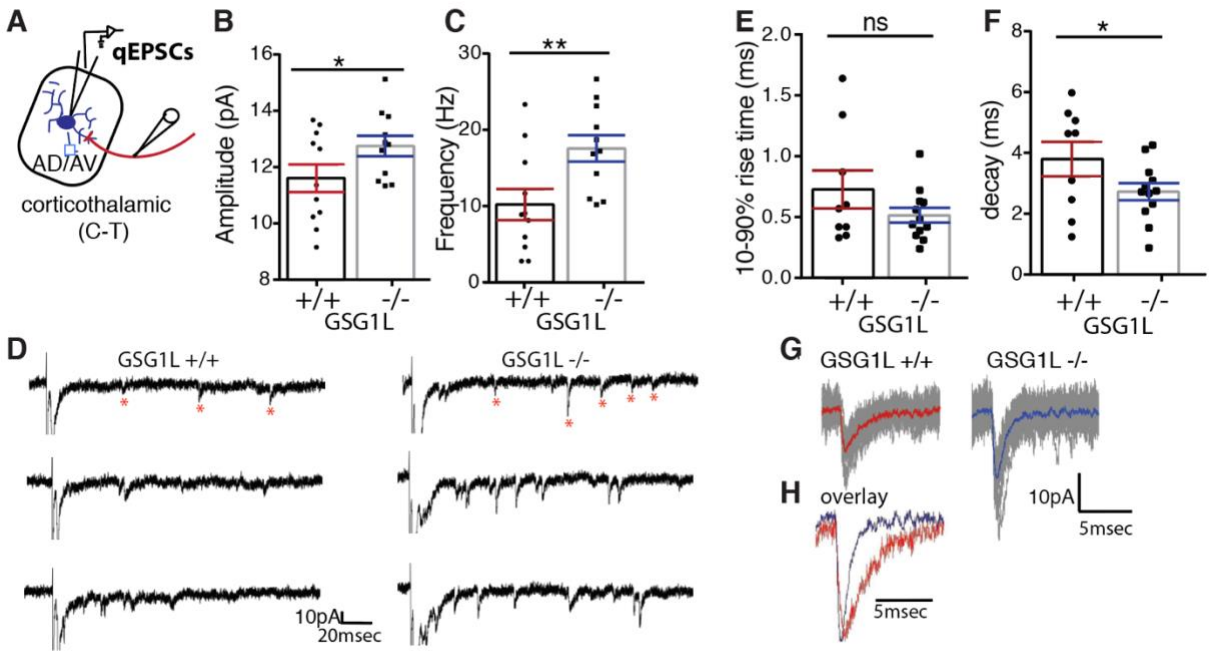

Figure 3-10.GSG1L is a negative AMPAR regulator at corticothalamic synapses in the AD/AV nuclei.

A. Asynchronous qEPSCs recorded at corticothalamic synapses at AD/AV nuclei in GSG1L WT and KO. B and C. Amplitude (P15-P30, p=0.0378, Mann-Whitney U test) and the frequency of qEPSCs (p=0.0060, Mann-Whitney U test) comparing GSG1L KO (n=11, N=4) and WT (n=11, N=5). D. Representative traces of qEPSCs. E and F. Pooled data for rise time (p=0.0900, Mann-Whitney U test) and decay kinetics (p=0.0413, Mann-Whitney U test). Each data point is an average obtained form one neuron. G. Representative traces of averaged qEPSCs from one neuron in GSG1L WT (red) and KO (blue), respectively. The raw traces are shown in gray. H. The averaged qEPSCs in K are normalized and overlaid for comparison.

Importantly, consistent with GSG1L having an input-specific function at AD/AV, there were no significant differences in the amplitude nor frequency of asynchronous qEPSCs between GSG1L KO and WT in mammillothalamic (Figure 3.11A-C) or subiculum-thalamic synapses (Figure 3.11G-I). The kinetics of qEPSCs in these two pathways were unaltered between GSG1L KO and WT (Figure 3.11). In line with the results obtained from characterization of short-term plasticity at these two pathways, we predict that GSG1L likely does not have a postsynaptic function in mammillothalamic and subiculum-thalamic synapses. The two signatures of GSG1L-based modulation, slowing of the recovery from desensitization and the reduction in the amplitude of AMPAR-mediated currents, are unchanged in mammillothalamic and subiculum-thalamic synapses in GSG1L KO mice.

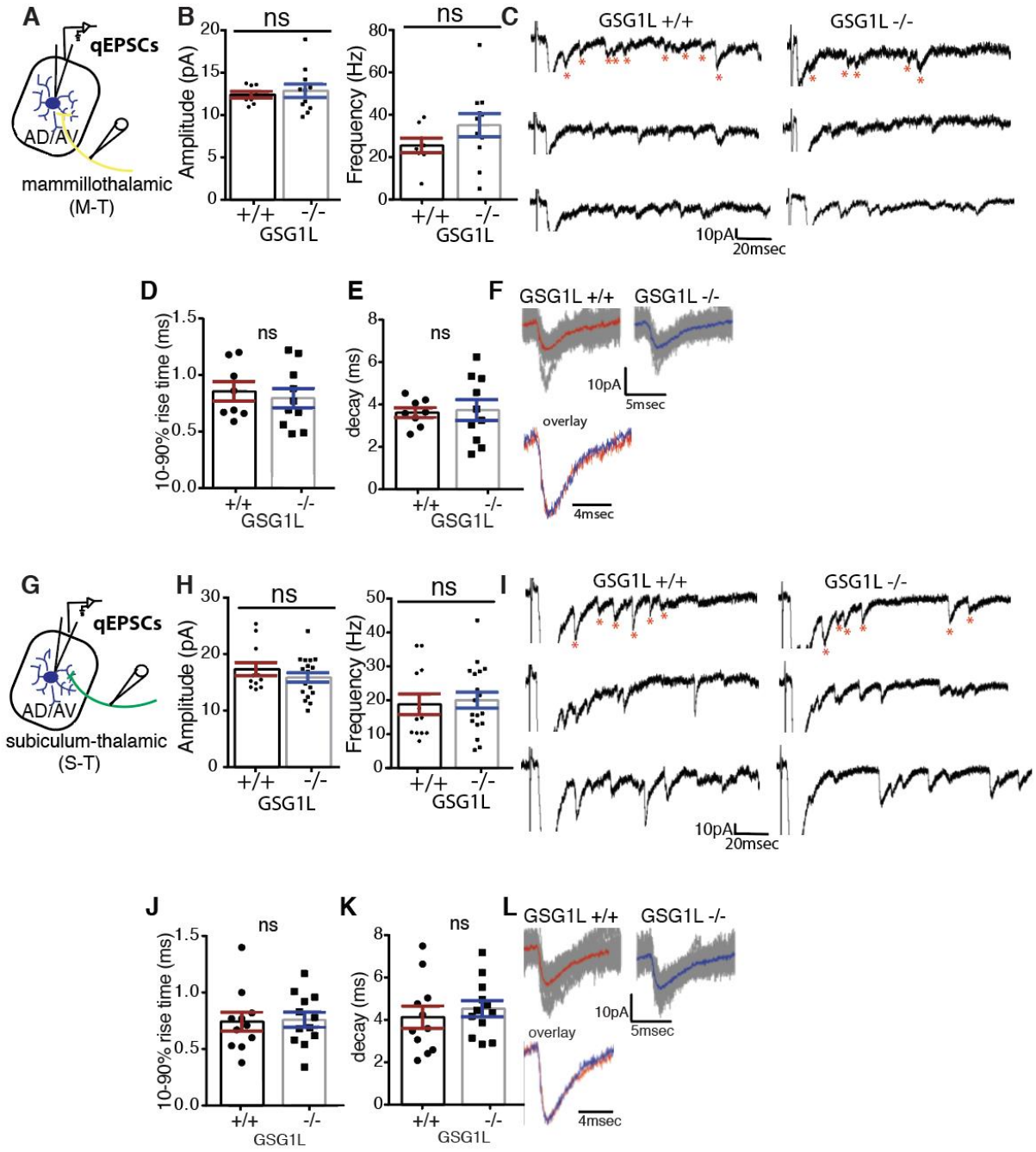

Figure 3-11. GSG1L does not have a postsynaptic effect on AMPAR activity at mammillothalamic and subiculum-thalamic synapses.

A and G. Asynchronous qEPSCs recorded at corticothalamic synapses at AD/AV nuclei in GSG1L WT and KO B. Amplitude (p=0.4455, Mann-Whitney U test) and frequency (p=0.0535, Mann-Whitney U test) of mammillothalamic qEPSCs comparing GSG1L KO (n=11, N=5) and

WT (n=8, N=6). D and E. Pooled data for rise time (p=0.7452, Mann-Whitney U test) and decay kinetics of M-T synapses (p=0.9355, Mann-Whitney U test). F. (top) Representative traces of averaged qEPSCs from GSG1L WT (red) and KO (blue) cells with the raw traces shown in gray. (bottom) The averages of individual qEPSCs are normalized and overlaid for comparison.

H. Amplitude (p=0.2184, Mann-Whitney U test) and the frequency (p=0.3269, Mann-Whitney U test) of S-T qEPSCs of GSG1L KO (n=18, N=5) WT (n=12, N=6). C and I. Representative traces of qEPSCs from the two pathways and corresponding genotypes. J and K. Pooled data for rise time (p=0.5956, Mann-Whitney U test) and decay kinetics of S-T synapses (p=0.4413, Mann-Whitney U test). L. (top) Representative traces of averaged qEPSCs from GSG1L WT (red) and KO (blue) cells with the raw traces shown in gray. (bottom) The averages of individual qEPSCs are normalized and overlaid for comparison.

3.8. GSG1L and stargazin compete in vivo for AMPAR regulation in AD/AV

Aforementioned results strongly indicate that GSG1L has an input-specific role in AD/AV, where it is only regulating a subset of synapses that receive inputs from the cortex and not the other two pathways. We next wondered why GSG1L is only functioning in a subset of synapses in AD/AV nuclei. One possibility is that there is another auxiliary subunit (s) co-expressed in these nuclei, that may be interfering and competing for AMPAR regulatory function. We reasoned that the one of the potential candidates for the interfering auxiliary subunit was stargazin. First of all, there is evidence for functional competition between GSG1L and stargazin in AMPAR gating modulation *in vitro*. Coexpression of GluA1 and GluA2 with GSG1L in *Xenopus* oocytes results in a slower recovery from AMPAR desensitization by almost 10-fold (Schwenk *et al.*, 2012). On the other hand, presence of stargazin has a minimal effect on the

recovery. Interestingly, coexpression of GSG1L and stargazin together with GluA1 and GluA2 in *Xenopus* oocytes results in stargazin fully outcompeting the AMPAR modulatory role. This may imply that two types auxiliary subunits compete for the same binding site on AMPAR but one is preferred over the other. Indeed, at the structural level, recent cryo-EM structures of AMPAR complexes suggest that GSG1L and stargazin bind to identical sites on AMPARs (Kamalova & Nakagawa, 2020). Therefore, if the two auxiliary subunits are co-expressed within a given neuronal population- they are likely competing for AMPAR binding and receptor modulation. The extent of functional co-interaction between GSG1L and stargazin and whether the functional competition holds true *in vivo* has not been studied yet and will be further explored in this chapter.

3.9. Functional co-expression of GSG1L and stargazin in AD/AV neurons

To explore potential functional co-expression of GSG1L and stargazin, we first wanted to determine whether stargazin is expressed in the AD/AV nuclei. Using Allen Brain Atlas as a reference, we inferred that stargazin is the only dominant type I TARP expressed in AD/AV neurons (Figure 3.12).

To test the hypothesis that stargazin and GSG1L both modulate AMPARs at synapses in AD/AV neurons, we investigated the effect of deleting stargazin using a γ-2 KO mouse generated in our lab (Figure 3.13). This mutant mouse line was generated with a CRISPR-Cas9 strategy. We first wanted to confirm the absence of stargazin protein expression in

our γ-2 KO mouse line, by pulling down GluA2-containing AMPAR complexes. Consistently, we find that stargazin protein expression is absent in γ-2 KO mice (Figure 3.13D-E). Similar to *stargazer* mutant mice (i.e. spontaneously occurred γ-2 KO mice), our γ-2 KO mice have behavioral phenotypes including severe ataxia, dyskinesia, and characteristic-head tossing behavior.

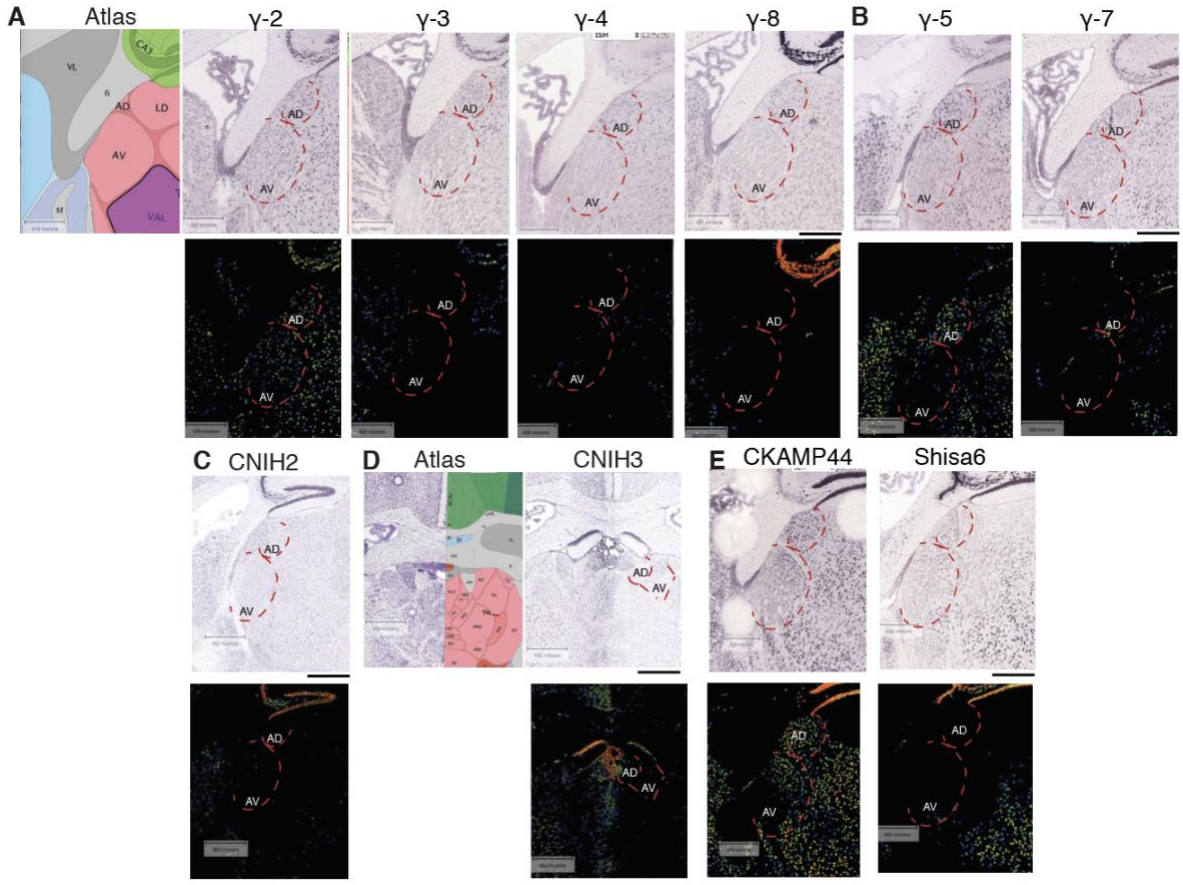

Figure 3-12. Expression profile of AMPAR auxiliary subunits in the AD/AV nuclei.

A. Allen Brain Atlas *in situ* hybridization data shows γ-2 is the only type I TARP that is highly expressed at the AD/AV (scale bar- 420 µm). B. Among type II TARPs, γ-5 is expressed in the AD/AV nuclei (scale bar- 420 µm). C and D. CNIH2 and CNIH3 are not expressed at the AD/AV (scale bar- 420 µm). E. CKAMP44 (shisa9), but not shisa6, is expressed in the AD/AV (scale bar- 420 µm).

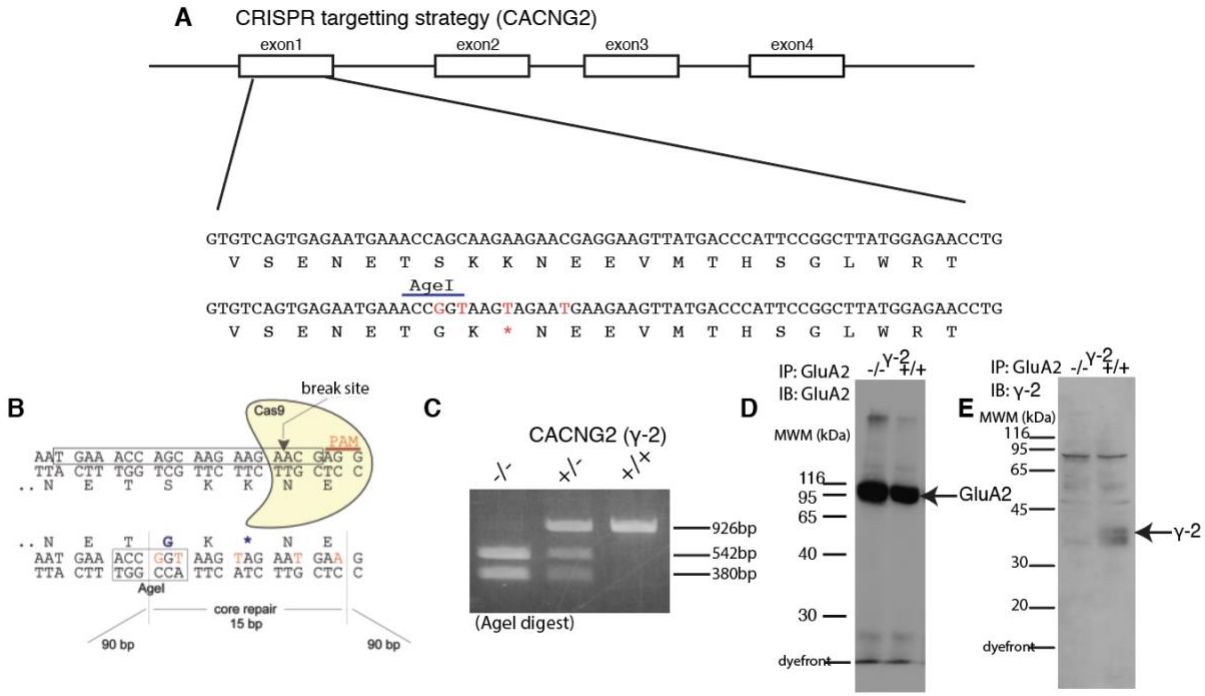

Figure 3-13. Characterization of transgenic γ-2 KO mouse line.

A and B. Diagram of CRISPR targeting strategy of CACNG2 (encoding γ-2). The resulting mutant mouse has a premature stop codon in the exon 1 and *AgeI* restriction enzyme site. C. PCR based genotyping demonstrating γ-2 WT, heterozygote, and homozygote KO respectively. D. The KO mouse was validated at protein level, by obtaining an immunoprecipitate of anti-GluA2CT antibody from 1% CHAPS-extracted total brain membrane. E. γ-2 protein is absent in γ-2 KO immunoprecipitate.

In *stargazer* mutant mice, there is a complete loss of functional synaptic AMPARs in cerebellar granule cells (Hashimoto *et al.*, 1999; Chen *et al.*, 2000). In contrast, we find that in the AD/AV neurons, there is a residual AMPAR activity in γ-2 KO mice. Consistent with stargazin being a positive AMPAR regulator, both the amplitude and the frequency of AMPAR mediated mEPSCs are significantly lower in γ-2 KO relative to WT control (Figure 3.14A-D). The residual mEPSCs indicate the existence of a subset of synapses with functional AMPARs. We predict that these are corticothalamic synapses that do not have stargazin regulation, but instead are controlled by GSG1L. Indeed, we find that there are no significant differences in the amplitude or the frequency of asynchronous qEPSCs between γ-2 KO and WT in corticothalamic synapses (Figure 3.14E-G). These results suggest that γ-2 plays a minimal role regulating cortico-thalamic synapses in AD/AV neurons in the presence of GSG1L.

We predict that stargazin is a dominant auxiliary subunit in mammillothalamic and subiculum-thalamic synapses; whereas, GSG1L exclusively regulates corticothalamic synapses where stargazin does not have a postsynaptic function. Consistent with this hypothesis, we find that removal of stargazin in the AD/AV neurons unmasks the basal postsynaptic modulatory effect of GSG1L in GSG1L/γ-2 double knockout (dKO) mice (Figure 3.15). Namely, both the amplitude and the frequency of mEPSCs are significantly increased in GSG1L/γ-2 dKO mice relative to GSG1LWT/γ-2KO and GSG1LHet/γ-2KO. Furthermore, consistent with the role of GSG1L in slowing AMPAR kinetics, both the rise time and decay time of mESPCs are significantly reduced in GSG1L/γ-2 dKO relative to GSG1LWT/γ-2KO neurons (Figure 3.15E-G). Together, these findings indicate that under basal conditions, stargazin outcompetes GSG1L in modulating AMPARs in

mammillothalamic and subiculum-thalamic synapses. The action of GSG1L on basal synaptic transmission is fully unmasked in GSG1L/γ-2 dKO mouse.

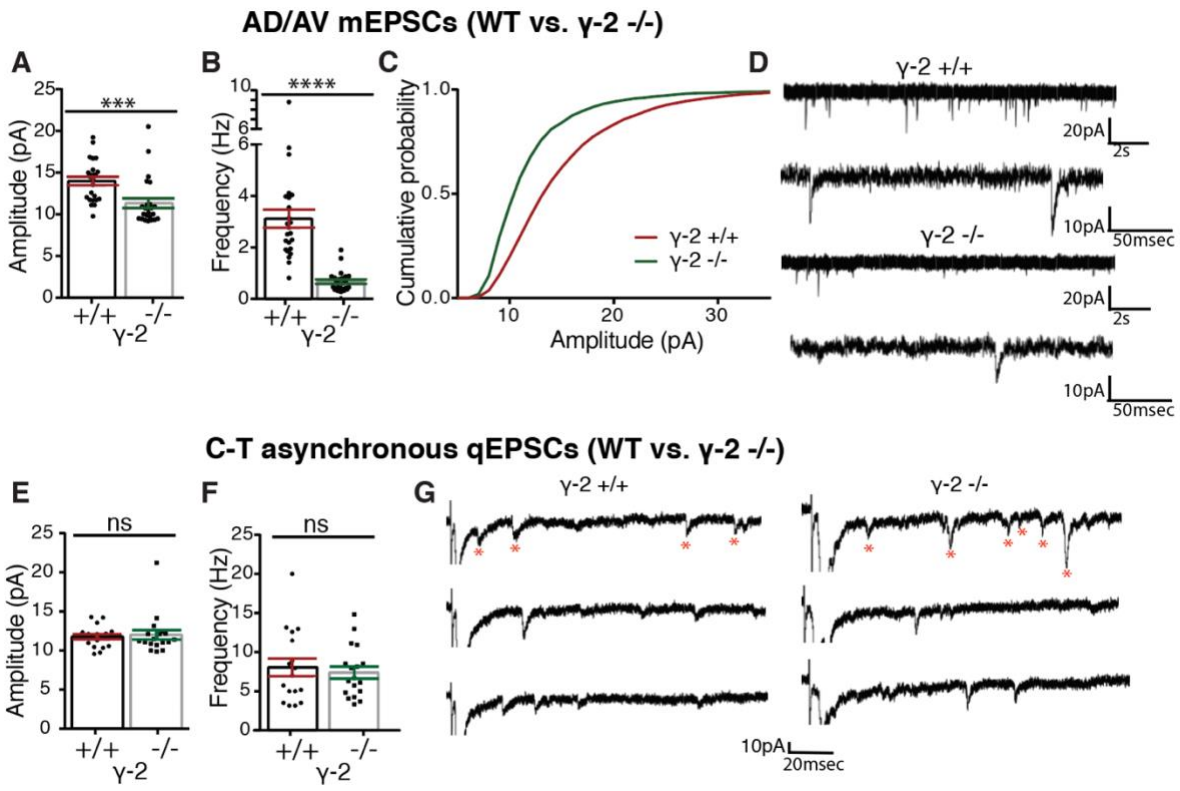

Figure 3-14. Stargazin does not have a postsynaptic role in corticothalamic synapses at AD/AV. A. Mean amplitude of AMPAR-mediated mEPSCs in the AD/AV of γ-2 KO and γ-2 WT (p=0.0006, Mann-Whitney U test; P15-22, γ-2 KO, n=24, N=3; γ-2 WT n=24, N=3). B. The frequency of mEPSCs (p<0.0001, Mann-Whitney U test). C. Cumulative plot of the amplitude distribution between γ-2 KO and WT animals (p=0.024, K-S test). D. Representative AMPAR-mediated mEPSCs traces of the AD/AV neurons. E and F. Asynchronous qEPSCs recorded at C-T synapses at AD/AV in γ-2 WT (P15-22, n=17, N=6) and KO (n=18, N=6). Mean amplitude (p=0.4123, Mann-Whitney U test) and frequency (p=0.4578, Mann-Whitney U test) of qEPSCs. G. Representative traces of qEPSCs at C-T synapses.

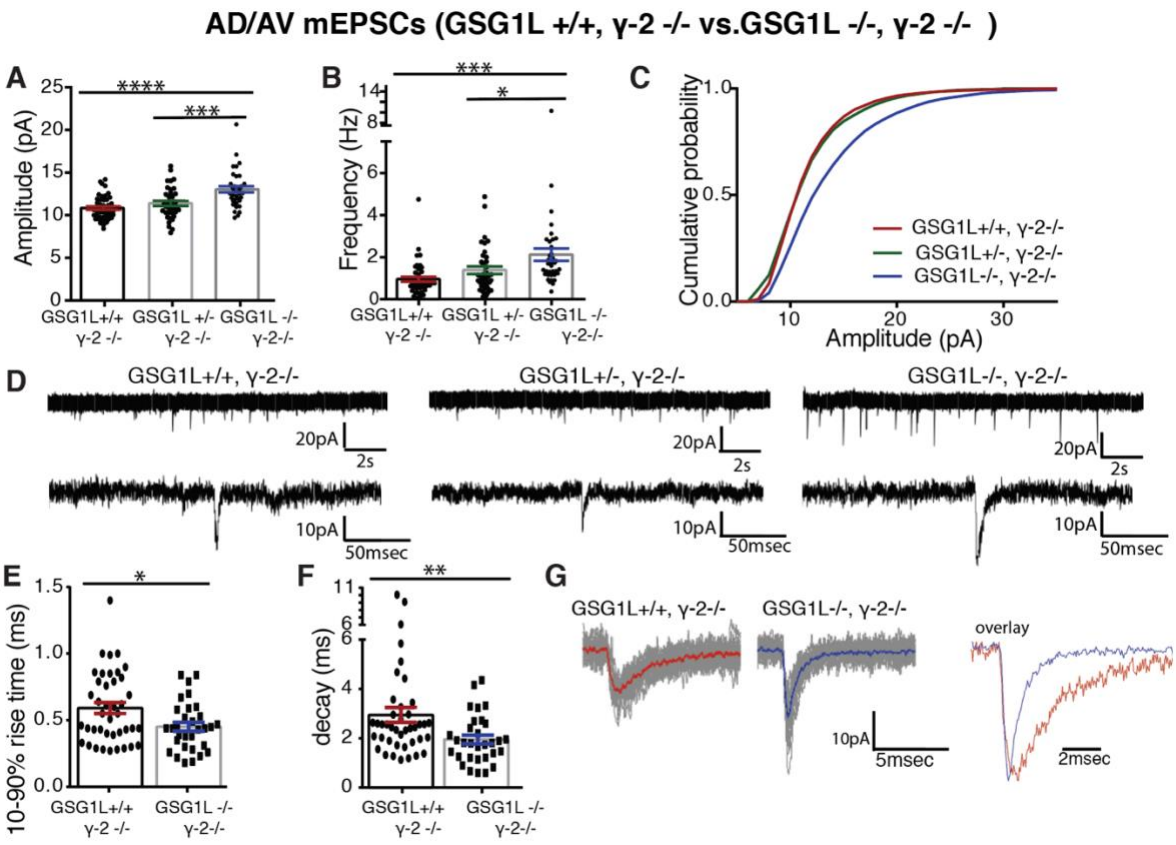

Figure 3-15. GSG1L and stargazin compete *in vivo.*

A. Mean amplitude of AMPAR-mediated mEPSCs in the AD/AV of GSG1L KO/ γ-2 KO mice relative to the GSG1L WT/ γ-2 KO and GSG1L Het/ γ-2 KO (P15-P22, p<0.0001,Two-Way ANOVA; GSG1L WT/ γ-2 KO n=45, N=6; GSG1L HET/ γ-2 KO n=37, N=5; GSG1L KO/ γ-2 KO n=36, N=5). B. Frequency of mEPSCs (p=0.0003, Two-Way ANOVA) C. Cumulative plot showing amplitude distribution (p= 0.0166, K-S test). D. Representative AMPAR-mediated mEPSCs traces from corresponding genotypes. E and F. Rise time (p=0.0277, Mann-Whitney U test) and decay (p=0.0058, Mann-Whitney U test) of mEPSCs in GSG1L KO/ γ-2 KO (blue) relative to GSG1L WT/ γ-2 KO (red). G. Representative traces of averaged mEPSCs with the averages shown in bold. The averages of individual mEPSCs are normalized and overlaid for comparison with GSG1L KO/ γ-2 KO in blue and GSG1LWT/ γ-2 KO in red. *Post hoc* Sidak comparisons: ** p<0.05, *** p<0.001, **** p<0.0001.*

3.8. Discussion

With the collective work presented In Chapter 3, we characterized the synaptic regulatory function of a unique auxiliary subunit, GSG1L. We utilized a transgenic lacZ reporter rat strain to determine the spatio-temporal expression pattern of GSG1L over the course of 9 months. GSG1L is highly expressed in the anterior thalamus throughout development, specifically in the AD and AV nuclei. We also determined that GSG1L has a postsynaptic function in these nuclei, where it regulates the recovery from AMPAR desensitization and negatively regulates AMPAR currents in synapses that receive inputs from the cortex. Our studies showed that GSG1L does not have a function in mammillothalamic and subiculum-thalamic synapses, where we predict stargazin is a dominant auxiliary subunit. Using GSG1L and γ-2 double KO mouse lines, we also showed that GSG1L and stargazin compete in AD/AV nuclei.

We report the first comprehensive expression profile of AMPAR regulatory subunit GSG1L in rats over the course of 8 months. The expression profile was deduced from X-gal histochemistry of a transgenic GSG1L KO rat that expresses a lacZ reporter under the endogenous GSG1L promoter. The GSG1L expression is dynamic during postnatal development with higher expression in adults. Our results are overall consistent with the in situ hybridization data of mouse brain in Allen Brain Atlas that was examined up to P56.

Previous studies have investigated the expression patterns of TARPs (Tomita et al. 2003, Fukaya et al. 2005) up to young adults. *In situ* hybridization analysis of TARPs other than TARP γ-4 showed no appreciable changes in expression during development (E13-P21). They were first detected in embryonic stages of development and persisted to the adult

stage. The TARP γ-4 subunit, on the other hand, showed high expression until P7, which decreased at P14 through P21, which was the latest time point tested in this study. Age-dependent changes in TARP expression beyond P60 were unclear. As such, our study is the first to investigate the temporal expression profile of AMPAR regulatory proteins, stargazin, CNIH2, and GSG1L, over a significant fraction of adult life. From this analysis we suggest that GSG1L exhibits a unique age dependent increase. The findings reported here will serve as a valuable resource for future functional studies of GSG1L in various brain regions throughout development

Previous investigations on the synaptic phenotypes of GSG1L KO rats in CA1 and DG neurons (Gu et al., 2016; Mao et al., 2017) were both conducted at time points when the expression of the lacZ reporter for GSG1L promoter activity is low (Figures 3.3). Specifically, GSG1L KO rat acute slices at postnatal day (P) 13–P19 were used. Although GSG1L protein is detectable in a subset of dendritic spines in older neurons (Schwenk et al., 2012; Shanks et al., 2012; Willems et al., 2020), the overall expression of GSG1L may be low in the hippocampus compared with the anterior thalamus at young age (i.e., P13–P19). In agreement with such a hypothesis, a previous study on GSG1L KO rat reported a substantial contribution of another auxiliary subunit, CNIH2, superimposed on the functional effect of GSG1L (Gu et al., 2016). However, because the lacZ reporter is an indirect indicator of GSG1L protein expression, future studies using more direct methods are necessary to determine whether its expression is low in young hippocampus.

The AD/AV nuclei, where GSG1L is abundantly expressed, are at the core of the extended hippocampal-diencephalic network with crucial roles in memory (Aggleton & Brown, 1999), and thus their damage is associated with severe anterograde amnesia

(Ghika-Schmid & Bogousslavsky, 2000; Gold & Squire, 2006). AD/AV nuclei also contain neurons that sense head direction during spatial navigation (Clark & Taube, 2012), and have been implicated in seizure initiation and/or propagation (Mirski & Ferrendelli, 1984; Kerrigan *et al.*, 2004). In contrast to the extensively studied LGN, molecular and functional characterization of the synapses of AD/AV nuclei is largely lacking.

Our studies, delineated in this chapter, show that GSG1L is functionally expressed at AD/AV nuclei, where it regulates AMPAR activity in a subset of synapses that receive inputs from the cortex, but not mammillary bodies or subiculum. In corticothalamic synapses, GSG1L reduces the amplitude and slows the kinetics of AMPAR mediated qEPSCs and further suppresses short-term facilitation by slowing the recovery from desensitization. Previous investigations have shown that GSG1L may play a role in trafficking of AMPARs, where its presence is associated with a reduction in surface expression of AMPARs in hippocampal neurons (Gu *et al.*, 2016), and such mechanism may partially contribute to the properties of corticothalamic synapses. However, we suggest that the effect of GSG1L on gating modulation plays a dominant role in regulating short-term plasticity given the CTZ sensitivity of these synapses in the wild type but not in GSG1L KO (Figure 3.8).

In contrast to GSG1L, stargazin plays a major role in regulating AMPAR activity in mammillothalamic or subiculum-thalamic synapses. The mechanism that restricts the functions of GSG1L and stargazin to specific afferent synapses remains to be determined. We speculate that presynaptic terminals may provide some trans-synaptic molecular cues, considering that GSG1L lacks a PDZ (PSD-95, dlg, ZO-1) domain binding motif in the cytoplasmic C terminus as it would normally facilitate synaptic anchoring. However,

future studies will be needed to more definitively determine the mechanisms underlying the segregations of AMPAR complexes.

Coexpression of GSG1L and stargazin in AD/AV nuclei is particularly interesting. In Xenopus oocytes, stargazin outcompetes GSG1L in AMPAR modulation (Schwenk et al., 2012), which agrees with GSG1L and stargazin sharing identical binding sites on AMPARs (Twomey et al., 2016, 2017b). These observations would suggest that the two auxiliary subunits would likely compete for AMPAR regulation in neuronal populations where they are co-expressed. Indeed, in AD/AV nuclei, we also found that under basal conditions, stargazin outcompetes GSG1L, functionally, in most synapses (Figures 3.15). The effect of GSG1L is unmasked in GSG1L/ γ-2 dKO mice, with changes in AMPAR-mediated mEPSCs amplitude and frequency, as well as changes in the kinetics of mEPSCs. These observations also indicate that in AD/AV, the corticothalamic synapses are the smaller population compared with the combined sets of mammillothalamic and subiculum-thalamic synapses.

Similar to GSG1L, CKAMP44 also slows the recovery from desensitization and has been previously shown to modulate short-term plasticity in hippocampal and retinogeniculate synapses (von Engelhardt *et al.*, 2010; Chen *et al.*, 2018). Based on the *in situ* hybridization data, CKAMP44 is highly expressed in AD/AV nuclei. We find that mammillothalamic synapses in the AD/AV nuclei undergo pronounced short-term depression (Figure 3.6C-E, Figure 3.7A-C), which is highly sensitive to CTZ (data not shown). Given that GSG1L does not modulate AMPAR function at mammillothalamic synapses, we speculate that CKAMP44 could be postsynaptically functional in these

synapses, which is yet to be investigated. Again, input specific functional expression of an AMPAR auxiliary subunit in the thalamus may extend to the case of CKAMP44.

AMPAR desensitization is critical for normal brain function (Christie *et al.*, 2010). Introduction of a mutation that abolishes AMPAR desensitization in knock-in, GluA2^{L483Y} mutant mice results in lethality of homozygous mice. Heterozygous mice carrying this mutation exhibit severe neurological phenotype, including seizures and early mortality (Christie *et al.*, 2010). These investigations highlight the critical importance of AMPAR desensitization *in vivo*.

4. Circuit-level and behavioral changes in GSG1L knockout mice

Adapted from Kamalova et al., “AMPA receptor auxiliary subunit GSG1L suppresses short-term facilitation in corticothalamic synapses and determines seizure susceptibility”

4.1. Introduction

A classic, longstanding, approach in elucidating the physiological role of a protein has been to disrupt the expression of the gene encoding the protein. Interestingly, besides mutant *stargazer* mouse behavioral phenotypes, other TARP, CNIH2/3, or shisa protein family KO mouse models do not present with any apparent gross behavioral defects (Jackson & Nicoll, 2011; Jacobi & von Engelhardt, 2020). However, the behavioral phenotypes can be better revealed by challenging animals with distinct behavioral paradigms.

It has been well confirmed experimentally, that damage to the anterior thalamus in human patients is associated with severe anterograde amnesia (Aggleton *et al.*, 2010). Furthermore, in rodents, damage to the nuclei themselves or their prominent input from the mammillary bodies is associated with deficits in spatial learning. Therefore, given the overall role of anterior thalamus in memory systems and postsynaptic function of GSG1L in this brain region, we predict that loss of function of GSG1L in the AD/AV could be accompanied with potential cognitive deficits.

In addition to their critical role for memory systems, AD/AV nuclei are also heavily implicated in seizure initiation and propagation (Mirski & Ferrendelli, 1984; Kerrigan *et al.*, 2004). Previous work had also established that DBS of anterior thalamus provides a therapeutic relieve for patients with intractable epilepsy (Hodaie *et al.*, 2002). The

molecular mechanisms underlying the connection between anterior thalamus and seizure is currently not well understood.

Given the loss of negative AMPAR regulation in GSG1L KO mice and inherent association of anterior thalamus with seizure states, we will perform behavioral analyses comparing GSG1L KO mice and WT control mice. In addition, we will also examine circuit level changes in excitability and spontaneous firing of AD/AV neurons in GSG1L KO. Finally, we will also perform seizure susceptibility tests to unambiguously determine whether loss of GSG1L is associated with increased seizure susceptibility.

4.2. Increased hyperexcitability in GSG1L KO AD/AV neurons

Having established the synaptic function of GSG1L in Chapter 3, we next sought to investigate whether the loss of GSG1L would result in circuit level changes in excitability. We first examined this in the AD/AV neurons, by recording spontaneous action potential firing in current clamp mode with no current injection. This would allows to determine whether GSG1L KO AD/AV neurons spontaneously fire action potentials at a higher rate relative to WT control. Remarkably, we find that GSG1L KO mice do indeed have increased spontaneous action potential firing rates, termed as “spiking”. We find that 60% of GSG1L KO AD/AV neurons spiked during a 3-minute recording period, whereas only 15% in WT neurons (Figure 4.1). This finding raises the question of whether GSG1L KO neurons are intrinsically more excitable. To determine this directly, we examined various aspects of intrinsic excitability.

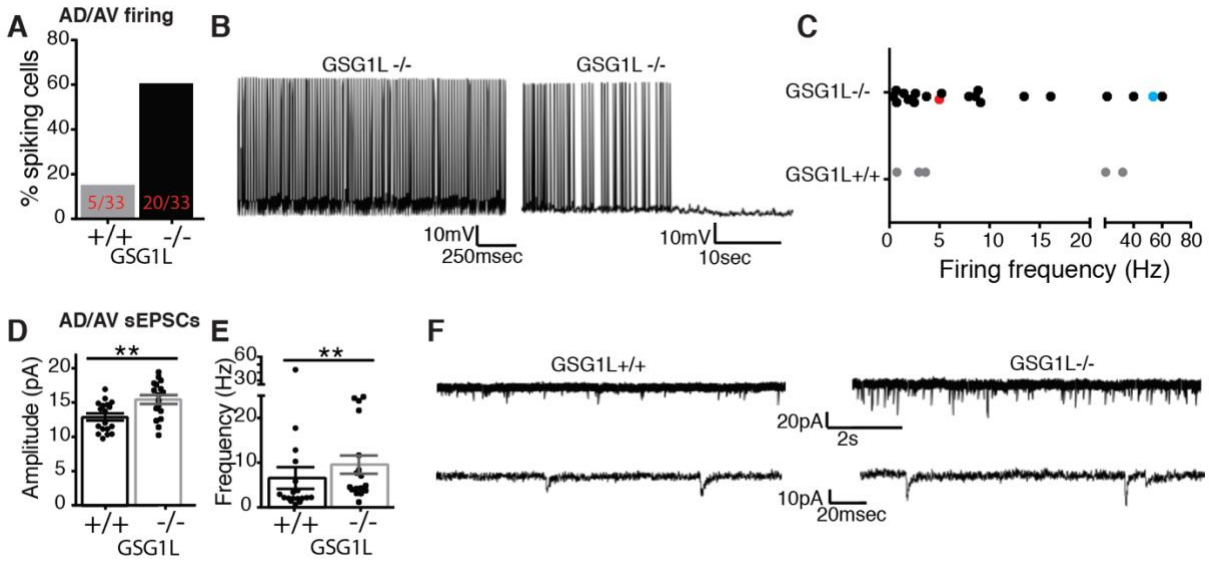

Figure 4-1. Loss of GSG1L results in enhanced excitability of AD/AV neurons in GSG1L KO mice.

A. Bar graph summarizing spontaneously firing AD/AV neurons in GSG1L KO (20/33 cells, N = 5) and WT control (5/33 cells, N = 5). B. Representative traces of two spiking GSG1L KO AD/AV neurons. C. Bar graph summarizing firing frequency distribution. Blue and red data points represent left and right traces in (B), respectively. D and E. Mean amplitude ($p = 0.0037$, Mann-Whitney U test) and frequency ($p = 0.0084$, Mann-Whitney U test) of AMPAR-mediated sEPSCs in AD/AV neurons of GSG1L KO (P15–P30, n = 17, N = 4) and WT (n = 18, N = 4). F. Representative sEPSC traces of GSG1L KO and WT

In the current clamp recording mode, we examined potential differences in the resting membrane potential, rheobase, firing rate, and input resistance in GSG1L KO relative to WT control. We find that there was no change in overall intrinsic excitability of neurons in GSG1L KO, with no differences in the resting membrane potential, rheobase, and neuronal firing rate between GSG1L KO and WT control (Figures 4.2A-D). However, the input resistance is significantly reduced in GSG1L KO mice (Figure 4.2E), which is consistent with increased synaptic activity, although it may not be the sole cause of the effect. Future investigations will be needed to definitively determine whether decreased input resistance is due to the increase in synaptic activity.

In line with the results of increased hyperexcitability of AD/AV neurons, we found that spontaneous excitatory synaptic transmission is also significantly enhanced in GSG1L KO mice (Figures 4.1D-F). Importantly, this phenotype was also observed in GSG1L/ γ-2 dKO mice (Figures 4.2F-I). Both the amplitude and the frequency of AMPAR-mediated spontaneous EPSCs (sEPSCs) are increased in GSG1L KO neurons. Altogether, neurons in AD/AV neurons of GSG1L KO mice are hyperactive overall. Collectively, these findings indicate that GSG1L KO AD/AV neurons exhibit enhanced hyperexcitability.

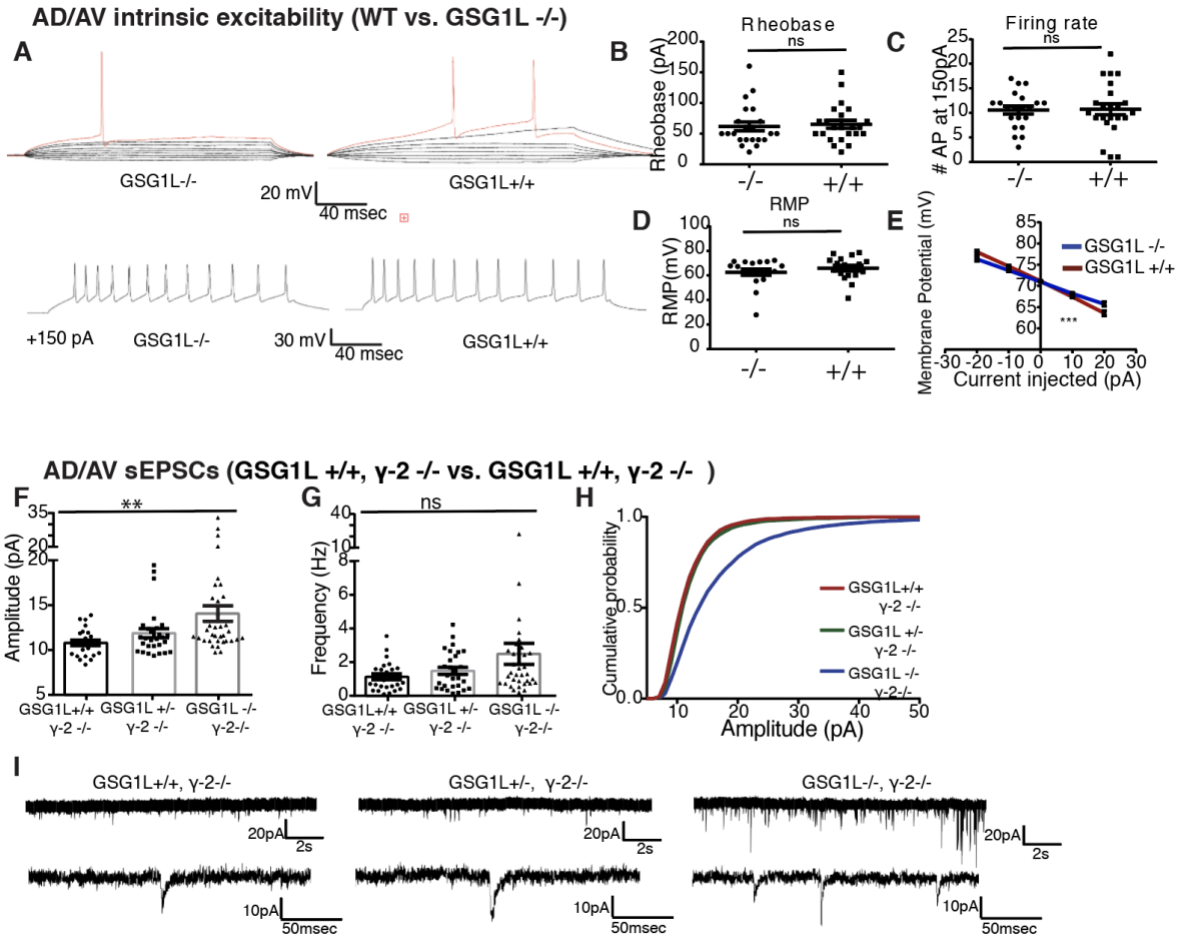

Figure 4-2. GSG1L KO AD/AV neurons exhibit increased input resistance.

A. Example traces of current clamp recordings from AD/AV in GSG1L KO and WT littermates. B, C, and D. There is no significant difference in the rheobase (P15-P30; p=0.4563, Mann Whitney U test, GSG1L KO n=22, N=5, GSG1L WT n=23, N=5), firing rate (p=0.9021, Mann-Whitney U test, GSG1L KO n=21, N=5, GSG1L WT n=23, N=5), or resting membrane potential, RMP (p=0.3953, Mann-Whitney U test, GSG1L KO n=18, N=5, GSG1L WT n=19, N=5). E. The input resistance is significantly lower in GSG1L KO neurons in the AD/AV nuclei (p<0.0001, Mann-Whitney U test, GSG1L KO n=22, N=5, GSG1L WT n=24, N=5). F. Bar graph summarizing the amplitude of sEPSCs in GSG1L/ γ-2 dKO (P15-22, n=36, N=6) mice relative to GSG1L WT/ γ-2 (n=25, N=4) and GSG1L Het/ γ-2 KO (n=28, N=5) (p=0.0032, Two-Way ANOVA). G. Bar graph of the frequency of sEPSCs (p=0.0914, Two-Way ANOVA). H. Cumulative plot showing a significant difference in the amplitude distribution between corresponding genotypes (p<0.0001,K-S test). I. Representative AMPAR-mediated sEPSCs traces of the AD/AV neurons from corresponding genotypes.

4.3. Increased hyperexcitability in L2/3 cortical neurons in GSG1L KO mice

We next sought to investigate whether aforementioned hyperactivity is observed in other brain regions downstream of anterior thalamus. AD/AV neurons send projections to the retrosplenial cortex (Van Groen & Wyss, 1995). In the process of acquiring various electrophysiological data from GSG1L KO mice and WT littermate L2/3 cortical neurons, that have high GSG1L expression (Figure 3.1), we came across a number of GSG1L KO neurons that exhibited spontaneous and persistent spiking, in the presence of 100 μM picrotoxin, while being voltage clamped at -70 mV (data not shown). To solidify this finding in a more systematic way, we patched >80 pyramidal L2/3 cortical neurons in the somatosensory cortex of GSG1L KO and WT mice. We find that approximately 9% of GSG1L KO neurons (8 cells out of 88 total) exhibited the spiking phenotype and only 2% WT controls (2 cells out of 83 total) spiked in the presence of 100μM picrotoxin and voltage clamped at -70mV (Figure 4.3). There are no changes in the intrinsic excitability of GSG1L KO L2/3 cortical neurons relative to WT control (Figure 4.4A-D). Furthermore, the basal synaptic transmission is unaltered with no differences in the amplitude or frequency of mEPSCs (Figure 4.4E-H).

On the other hand, the overall excitatory neurotransmission in L2/3 cortical neurons in GSG1L KO mice is similarly enhanced. Both the amplitude and the frequency of sEPSCs are significantly increased relative to WT controls (Figure 4.3C-G). These findings show that the absence of GSG1L results in circuit-level hyperexcitability phenotypes. LacZ expression and in situ hybridization from Allen Brain Atlas show that GSG1L is highly

expressed in L2/3 cortical neurons specifically in adult animals (Figure 3.3). We find that at basal conditions, there are no postsynaptic GSG1L-dependendent effects.

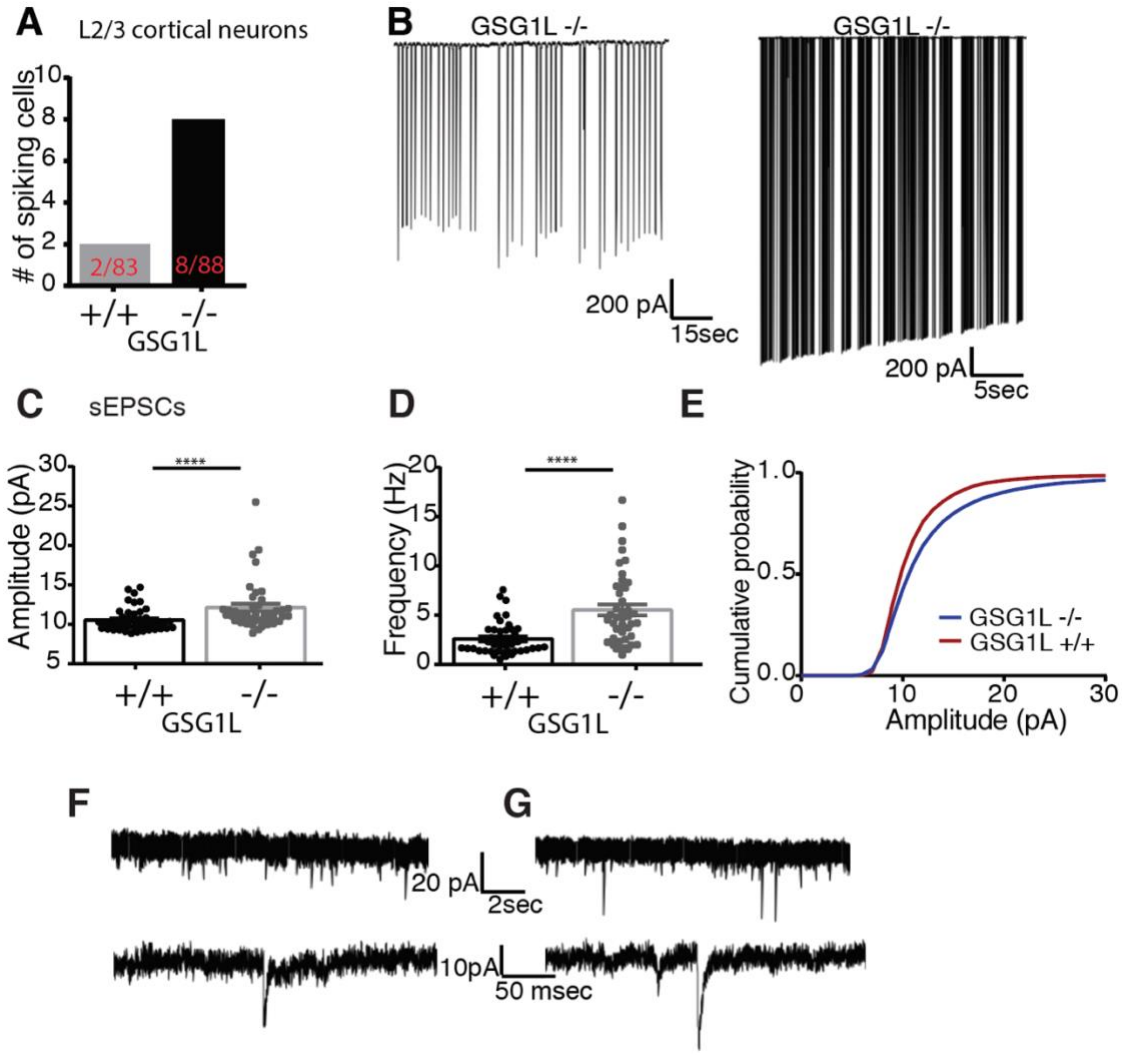

Figure 4-3. GSG1L KO L2/3 cortical neurons are hyperexcitable.

A. Systematic analysis revealed that 8 out of 88 GGS1L KO pyramidal L2/3 cortical neurons and only 2 out of 83 WT spiked at -70mV. B. Representative traces of spiking GSG1L L2/3 neurons. C-D. Excitatory neurotransmission is enhanced in GSG1L KO L2/3 cortical neurons (n=43, N=6) relative to WT control at P180 (WT n=43, N=6). Both the amplitude ($p<0.001$, Mann Whitney U test) and the frequency ($p<0.001$) are significantly increased. E**.** Cumulative plot showing a significant difference in the amplitude distribution between GSG1L KO and WT animals (K-S test, $p=0.0015$). F-G. Representative AMPAR-mediated sEPSCs traces of the L2/3 cortical neurons from the somatosensory cortex from corresponding genotypes.

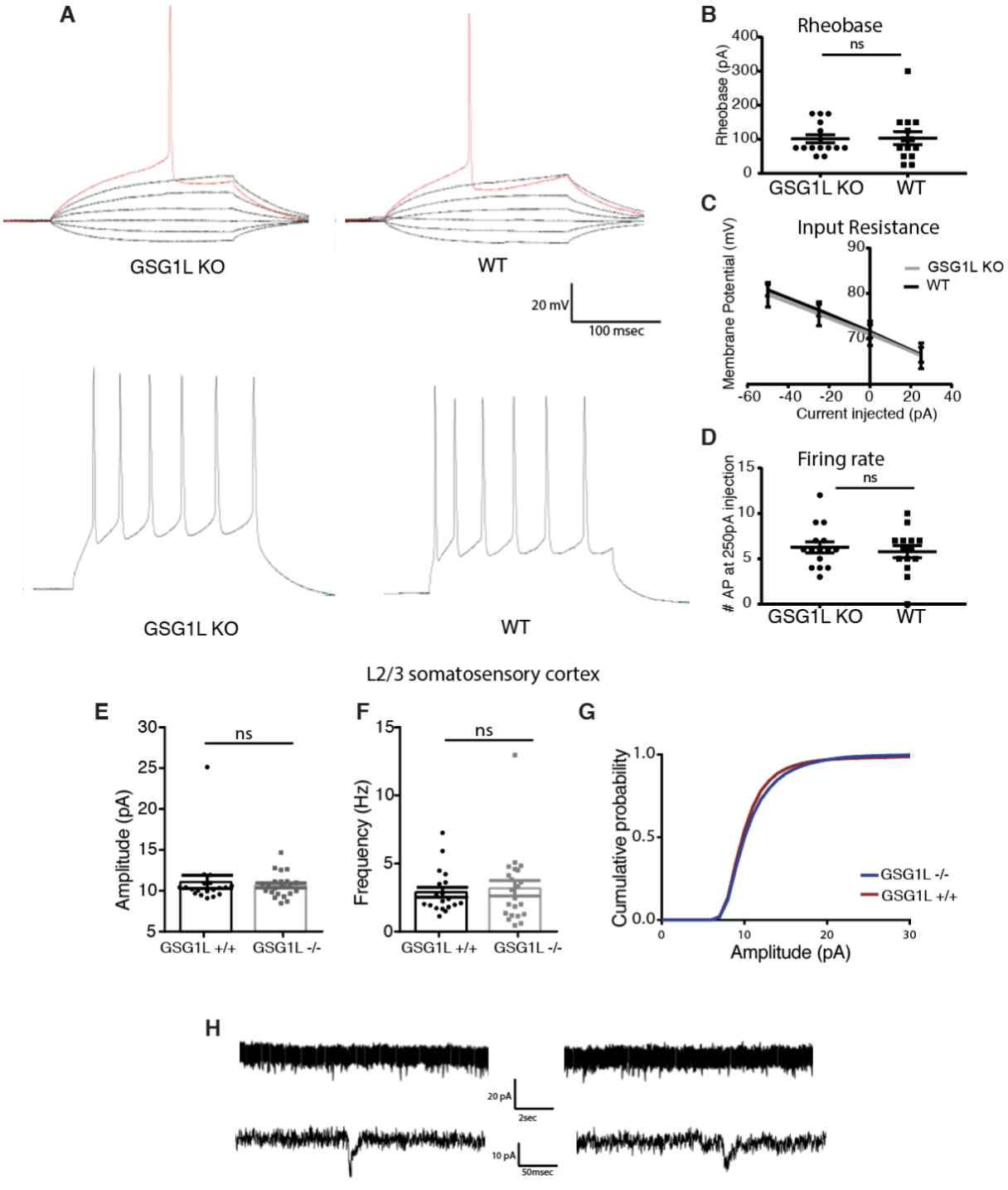

Figure 4-4. No changes in excitability of L2/3 cortical neurons in GSG1L KO.

A. Example traces of current clamp recordings from L2/3 cortical neurons in somatosensory cortex (P180, GSG1L n=16, N=3, GSG1L WT n=15, N=3). B-D The intrinsic excitability is unaltered in GSG1L KO. There are no significant differences in rheobase (Mann Whitney U test, p=0.7498), input resistance (p=1.1828), or firing rate (p=0.9211). ** p<0.05, ** p<0.01, *** p<0.001.* E**.** The amplitude of mEPSCs in L2/3 cortical neurons is not significantly different between GSG1L KO (n=22, N=3) and WT controls (n=19, N=3) (p=0.3222). F. The frequency of mEPSCs in L2/3 cortical neurons is not significantly different between GSG1L KO and WT controls (p=0.5000). G. Cumulative plot showing significant difference in the amplitude distribution between GSG1L KO and WT. H. Representative AMPAR-mediated mEPSCs traces of the L2/3 cortical neurons from corresponding genotypes.

4.4. GSG1L KO mice exhibit enhanced susceptibility to seizures

Next, we sought to investigate the effect of the loss of GSG1L at the whole organism level. Initial basic behavioral phenotyping of GSG1L KO mice revealed no differences in grip strength, rotarod performance, elevated zero maze, and gait parameters (Figures 4.5 A-D). However, we found that GSG1L KO mice show deficits in a novel object recognition (NOR) task (Figure 4.5E), similar to the findings of previous reports using GSG1L KO rats (Gu et al., 2016). These results are consistent with the known role of anterior thalamus in learning and memory (Parker and Gaffan, 1997), but a more drastic behavioral phenotype was revealed when the animals were challenged with seizure paradigm, a condition in which anterior thalamus plays a critical role (Mirski and Ferrendelli, 1984; Bittencourt et al.,2010).

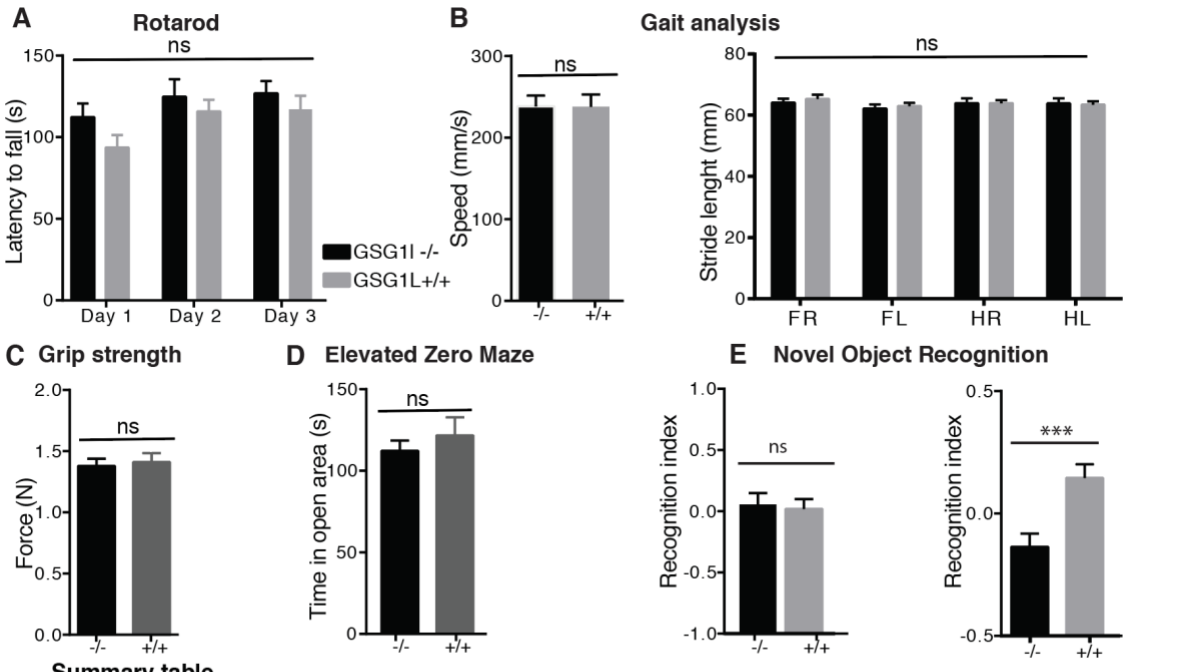

Summary table

Rotarod	no genotypic difference	GSG1L KO n=15, GSG1L W Tn=15	Latency to fall, p=0.0722, Two-Way ANOVa
Gait analysis	no genotypic difference	GSG1L KO n=14, GSG1L WT n=15	Running speed p=0.4921; Stride length p=0.9290
Grip strength	no genotypic difference	GSG1L KO n=15,GSG1L WT n=15	Grip strength p=0.3692
Elevated zero maze	no genotypic difference	GSG1L KO n=16, GSG1L WT n=14	Time in open arm area p=0.2308

Figure 4-5. GSG1L KO mice have deficits in Novel Object Recognition task.

A**.** Bar graph showing no significant difference in rotarod performance between GSG1L KO and WT littermate controls (p=0.0722, Two-Way ANOVA, KO n=16, WT n=16). B**.** Bar graph summarizing gait parameters, running speed (p=0.4921, Mann-Whitney U test, KO=14, WT=15) and stride length (p=0.9290,Two-Way ANOVA). C**.** Bar graph summarizing grip strength (p=0.3692, Mann-Whitney U test, KO n=15, WT n=15). D**.** Bar graph summarizing elevated zero maze performance (p=0.2308, Mann-Whitney U test, KO n=15, WT n=14). E**.** Bar graphs showing that GSG1L KO mice have significant deficits in novel object recognition task. During the test phase (right), GSG1L KO had lower recognition index relative to WT control littermates (p=0.0006, Mann-Whitney U test, KO n=15, WT n=15). Summary table (bottom).

Strikingly, we found that GSG1L KO mice exhibit enhanced susceptibility to kainate-induced seizures (Figures 4.6A-D). The seizure severity was determined on a scale of 0–7, a rating system with increasing severity in an ascending scale and with a score 7 denoting death (Morrison et al., 1996). At a lower-dose injection (15 mg/kg intraperitoneal [i.p.]) of kainate, GSG1L KO mice had a significantly higher seizure severity score than WT controls. Furthermore, 23% (3 of 13 mice) of GSG1L KO mice, and no GSG1L WT mice, died within 2 h after kainate administration. At a higher-dose injection (25 mg/kg i.p.) of kainate, 75% of GSG1L KO mice died within 2 h post injection and only 25% of WT mice. These results highlight the in vivo importance of GSG1L in protecting against kainate-induced neurotoxicity and pathological hyperexcitability. Consistent with GSG1L being a negative regulator of AMPAR function, GSG1L KO mice have enhanced excitatory neurotransmission and susceptibility to seizures, along with increased spontaneous firing of AD/AV neurons.

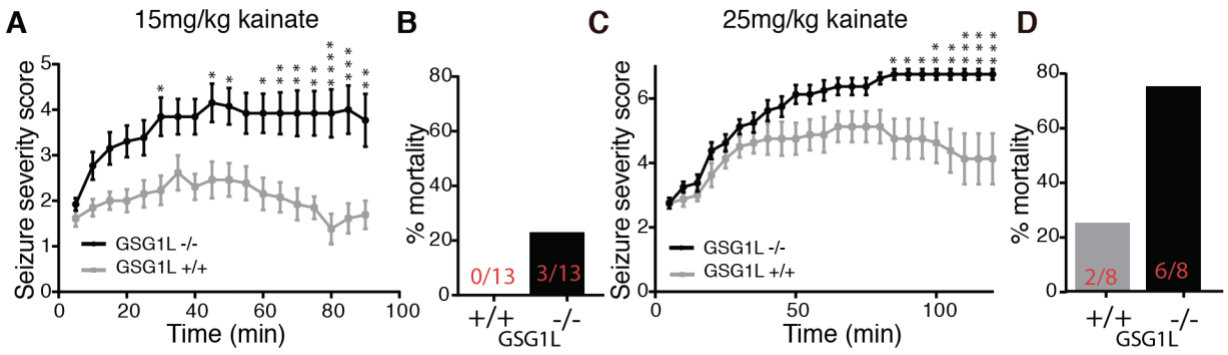

Figure 4-6. Loss of GSG1L results in enhanced seizure susceptibility.

A. Seizure severity over time (minutes) following i.p. injection of 15mg/kg of kainate (GSG1L KO n=13, GSG1L WT n=13). GSG1L KO (9-10 mo, both sexes) and WT mice (9-10 mo, both sexes) were scored on a previously described scale (Morrison *et al.*, 1996). Higher score corresponds to a more severe seizure status with 7 denoting death. B. 3 out of 13 GSG1L KO mice died within the two hours post-kainate injection and no WT did. C**.** Higher dose 25mg/kg kainate i.p. injection results in increased seizure severity scores for GSG1L KO mice relative to WT control (9-10 months old, both sexes, n=8 each). D**.** 6 out of 8 GSG1L KO mice died within the two hours post-kainate injection and only 2 out of 8 GSG1L WT mice did. The two groups were compared using Two-Way Anova ($p<0.0001$ for 15mg/kg and 25mg/kg) with Sidak post hoc analysis and the significance was established as follows: * *$p<0.05$, ** $p<0.01$, *** $p<0.001$*

4.5. Discussion

Consistent with GSG1L being a negative regulator of AMPAR function, loss of GSG1L results in hyperexcitability in the anterior thalamus, with its impact observed elsewhere in the brain, such as somatosensory cortex. The hyperexcitability is likely not due to the changes in intrinsic firing properties of GSG1L KO AD/AV neurons, as we didn't observe changes in most intrinsic excitability properties. The input resistance was reduced in AD/AV GSG1L KO neurons, which could be due to increased AMPAR activity and more channels being open. However, further experiments will be needed to defenitively support this hypothesis. Moreover, we determined that GSG1L KO mice have enhanced susceptibility and mortality in response to kainate-induced seizures, as well as, deficits in cognitive tasks such as novel object recognition.

While we do observe enhanced excitatory neurotransmission in somatosensory L2/3 cortical neurons, these neuronal populations are not directly downstream of AD/AV nuclei. Based on anatomical studies, it is known that AD/AV nuclei send projections to the deep layers of the retrosplenial cortex (Van Groen & Wyss, 1995). It would be interesting to speculate whether increased firing of AD/AV KO neurons is propagated downstream resulting in increased hyperexcitability of the retrosplenial cortical neurons. This needs to be tested experimentally.

While we observe increased hyperexcitability and seizure susceptibility in GSG1L KO mice, the underlying mechanisms are not known. We speculate that disturbed excitation/inhibition (E/I) balance in GSG1L KO could be associated with seizure states

(Bateup et al., 2013; Paz and Huguenard, 2015; Staley, 2015). For instance, KO mice lacking tuberous sclerosis complex (Tsc) 1 similarly exhibit hyperexcitability, increased E/I balance, and susceptibility to kainate-induced seizures. The proposed mechanism for this hyperexcitability phenotype is the overall imbalance in excitation and inhibition in the KO mice, where there is an overall reduction of inhibition onto Tsc-1 KO pyramidal neurons (Bateup *et al.*, 2013). To definitively determine whether the increased hyperexcitability and seizure susceptibility in GSG1L KO mice, future investigations will be needed. It is possible that loss of GSG1L negative regulation specifically in the AD/AV nuclei that are known to be implicated in seizure and epilepsy models, elicits the seizure phenotype in GSG1L KO mice. However, at the moment, there is no experimental evidence for direct connection of the postsynaptic action of GSG1L in the AD/AV nuclei and enhanced hyperexcitability and increased susceptibility in GSG1L KO mice. An immediate next important experiment would be to test the necessity of the loss of GSG1L in AD/AV nuclei for the seizure phenotype.

As discussed above, the anterior thalamus has been previously implicated in seizure initiation and propagation. First, lesion of the prominent mammillothalamic input onto the AD/AV results in the protection against convulsant actions of pentylenetetrazol (Mirski & Ferrendelli, 1984). Additionally, bilateral removal of the anterior thalamus also protects against seizure in animal models (Hamani *et al.*, 2004). Inhibition of the anterior thalamus through microinjections of GABAergic agonists, such as muscimol and bicuculline increases the latency to seizures and is overall protective (Bittencourt *et al.*, 2010). These observations emphasize that overall inhibition or complete removal of

ATN is protective against seizures, however, the underlying mechanisms are currently unknown. Importantly, our results indicate that GSG1L KO mice exhibit enhanced excitability and AMPAR activity in the ATN as well as enhanced susceptibility to kainate-induced seizures. Currently, these are all correlative speculations, however, there is evidence for a correlation of decreased anterior thalamic function and protection against seizures. Future studies will be needed to further support this claim and better understand the underlying mechanisms.

Interestingly, circumstantial evidence suggests GSG1L may serve a neuroprotective role against hyperexcitability and ischemia (Keum and Marchuk, 2009; Du et al., 2015). GSG1L was identified as one of the candidate genes at the locus that determines the extent of infarct volume in mouse models of focal cerebral ischemia (Keum and Marchuk, 2009). Furthermore, a suggestive single-nucleotide polymorphism in GSG1L was found to be associated with infarct volume upon ischemic stroke in mice and human patients (Du et al., 2015). However, these are correlative studies, and further investigation is warranted to the test the direct link between GSG1L and ischemia.

5. Conclusions and future directions

5.1. Summary of the results

The body of work presented in this dissertation established a physiological role of GSG1L in the anterior thalamus (summarized in Figure 5.1). Considering the critical role of auxiliary subunits for normal brain function and the uniqueness of a negative modulator GSG1L, I hope the cumulative findings of my dissertation work will provide a framework for subsequent investigations of GSG1L within and outside anterior thalamus.

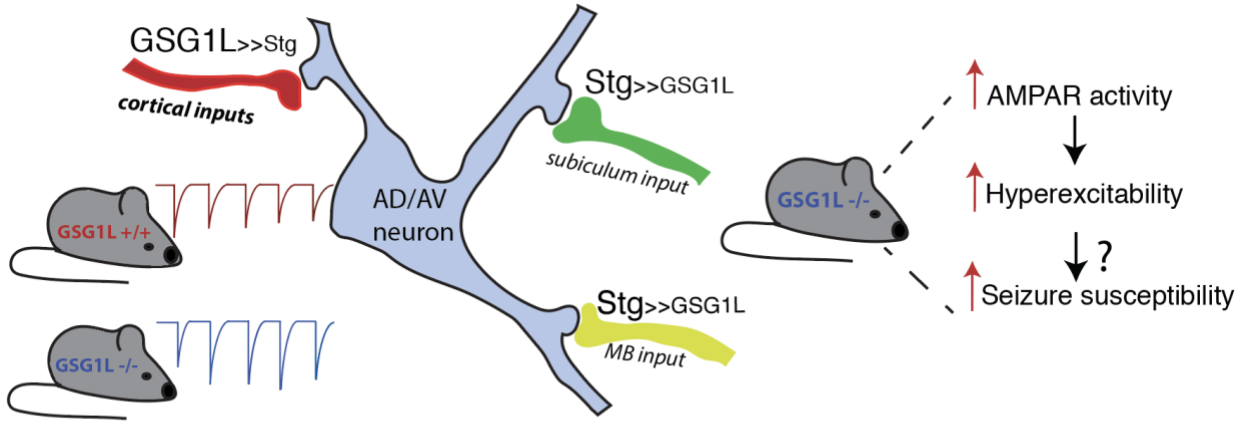

Figure 5-1. Summary of the dissertation work.

GSG1L is a dominant auxiliary subunit in corticothalamic synapses (red) of AD/AV neurons (blue). In these synapses, GSG1L suppresses short-term facilitation by slowing recovery from AMPAR desensitization. Stargazin (Stg) is a dominant auxiliary subunit in S-T synapses (green) and M-T synapses (yellow) in AD/AV. Consistent with GSG1L being a negative regulator of AMPARs, GSG1L KO mice have increased AMPAR-mediated quantal events in corticothalamic synapses. GSG1L KO mice have enhanced excitability in the AT. The enhanced hyperexcitability is accompanied by increased susceptibility to kainate-induced seizures in GSG1L KO mice.

5.2. GSG1L and short-term plasticity

Short-term plasticity entails changes that occur over milliseconds to minutes and is postulated to play an important role in synaptic computation and information processing (Zucker & Regehr, 2002; Abbott & Regehr, 2004). While the two prominent mechanisms of short-term plasticity are both presynaptic, changes in the recovery of postsynaptic AMPARs does constitute a postsynaptic mechanism in certain brain regions. Contribution of receptor desensitization to synaptic transmission is rare because, in most synapses, glutamate clearance is fast and precedes the entrance of receptors into the desensitized and nonconducting state (Jones & Westbrook, 1996). As such, the lifetime of glutamate within the synaptic cleft is very short. However, there are synapses that have distinct ultrastructure and general geometry which increases the overall lifetime of glutamate within the synaptic cleft. Under these circumstances, glutamate will be present in the cleft for a longer duration allowing for receptor desensitization to occur.

Synapses, such as retinogeniculate, mossy fiber to granule cell, and calyceal synapses, where desensitization has been shown to contribute to short-term plasticity (Trussell *et al.*, 1993; Chen *et al.*, 2002; Xu-Friedman & Regehr, 2003) often have an ultrastructure with multiple release sites next to each other and minimal astrocytic cytoplasm. This overall geometrical arrangement precludes fast glutamate clearance and allows for a prolonged activation of postsynaptic receptors (Xu-Friedman & Regehr, 2003). Retinogeniculate synapses are an excellent example of synapses with strong AMPAR desensitization component. Ultrastructural investigations using electron microscopy (EM)

analyses revealed that retinal inputs contact LGN with multiple release sites next to each other and overall minimal glial presence allowing for glutamate spillover and activation of neighboring receptors (Rafols & Valverde, 1973).

CKAMP44, similar to GSG1L, also slows the recovery from AMPAR desensitization (von Engelhardt *et al.*, 2010). CKAMP44 was shown to regulate short-term plasticity at retinogeniculate synapses by slowing the recovery from AMPAR desensitization (Chen *et al.*, 2018). As such, it was shown to contribute to the underlying mechanism of short-term depression in retinogeniculate synapses (Chen *et al.*, 2000; Kielland & Heggelund, 2002; Budisantoso *et al.*, 2012; Chen *et al.*, 2018). The glomerular structure of retinogeniculate synapse has large terminals and closely spaced release sites (Rafols & Valverde, 1973). The unique overall geometry prevents fast removal of glutamate and allows for a spillover resulting in AMPAR desensitization (Budisantoso *et al.*, 2012).

The corticogeniculate synapses, on the other hand, have single distant synaptic contacts (Erisir *et al.*, 1997; Narushima *et al.*, 2016) with low release probability (Granseth *et al.*, 2002). In these synapses, AMPAR desensitization is predicted not to contribute to short-term plasticity, such as that observed in the ventrobasal nucleus (Sun & Beierlein, 2011). In fact, CKAMP44 plays no role in short-term plasticity at corticogeniculate synapses in the LGN (Chen *et al.*, 2018). In contrast, we find that AMPAR desensitization substantially contributes to short-term plasticity at corticothalamic synapses in the AD/AV nuclei. GSG1L is highly expressed in the AD/AV but not in the LGN or ventrobasal nuclei of the thalamus (Lein *et al.*, 2007a). Hence, it is uniquely positioned to regulate short-term plasticity in corticothalamic synapses in the AD/AV.

The ultrastructure of corticothalamic synapses in the LGN allows for a fast glutamate clearance and hence AMPAR desensitization does not contribute to short-term plasticity. The ultrastructure of corticothalamic synapses in the AD/AV nuclei is currently unknown. An interesting avenue for future studies would be to investigate the ultrastructure of AD/AV synapses, where we observe strong contribution of receptor desensitization to synaptic transmission. This would allow us to investigate at the ultrastructural level, the geometry of corticothalamic synapses in the AD/AV.

5.3. Functional co-expression of GSG1L and stargazin

Native AMPAR complexes contain more than one type of auxiliary subunit and as introduced in Chapter 1, AMPARs auxiliary subunits are co-expressed in multiple brain regions and neuronal populations. For instance, CKAMP44 and TARP γ-8 are functionally co-expressed in the DG granule cells (von Engelhardt *et al.*, 2010). Removal of TARP γ-8 or CKAMP44 decreases the density of somatic AMPARs—deletion of both leads to an even further reduction (Khodosevich *et al.*, 2014). CKAMP44 and TARP γ-8 have opposing modulatory effects on the recovery from AMPAR desensitization, with CKAMP44 significantly slowing this parameter in DG neurons. Consistently, the PPR of AMPAR mediated EPSCs was increased in CKAMP44 KO mice and decreased in γ-8 KO mice (Khodosevich *et al.*, 2014). In this study, investigators similarly compared the extent of short-term plasticity in two distinct synapses within the DG, those receiving inputs from lateral perforant path and those that are activated by medial perforant path axons. Interestingly, the extent of short-term

plasticity changes upon deletion of γ-8 or CKAMP44 were similar when comparing stimulation of lateral perforant path inputs relative to medial perforant path inputs.
In our investigations, delineated in Chapter 3, we find that GSG1L and stargazin are similarly functionally co-expressed AD/AV nuclei. Consistent with the *in vitro* observations (Schwenk *et al.*, 2012), we find that the two auxiliary subunits compete for AMPAR modulation in AD/AV nuclei. We observe an input-specific function of GSG1L specifically in corticothalamic synapses, where stargazin does not have a postsynaptic function. One particularly intriguing question that we haven't addressed in our studies is the molecular mechanism (s) underlying the seperation of the two populations of AMPARs- those that are modulated by GSG1L in the corticothalamic synapses and others that are modulated predominantly by stargazin in mammillothalamic and subiculum-thalamic synapses.

One possible mechanism could be through distinct protein-protein interactions. As introduced in Chapter 1, stargazin contains a PDZ binding motif, whereas, GSG1L does not. It is therefore intriguing to speculate that distinct interactions of stargazin with scaffolding proteins through its PDZ binding motif could restrict the presence of stargazin-bound AMPARs to synapses receiving inputs from the mammillary bodies and the subiculum. Another possibility is that the presynaptic terminals may provide some transsynaptic molecular cues to selectively segregate GSG1L-bound AMPARs opposite of afferents arriving from the retrosplenial cortex. For instance, transsynaptic adhesion molecules such as leucine-rich repeat (LRR)-containing transmembrane proteins (LRRTMs) were shown to interact with presynaptic neurexins- an interaction, which is

critical for excitatory synapse development (de Wit & Ghosh, 2014). Similarly, cell adhesion proteins neuroligins at the postsynaptic site form a transsynaptic connection with their presynaptic neurexin counterparts (Krueger *et al.*, 2012). One possibility could be that the transsynaptic molecular cues selectively segregate GSG1L-bound AMPARs to one population of synapses and stargazin-bound AMPARs to other synapses within the AD/AV. However, future experiments are needed to test this hypothesis.

GSG1L and stargazin are both distant homologs of claudin proteins (Shanks *et al.*, 2012), which were originally identified in liver tight junctions (Furuse *et al.*, 1998). Claudins are critical components of tight junctions and interactions between claudins on adjacent membranes facilitate cell adhesion (Gunzel & Yu, 2013). It is intriguing to speculate, given the evolutionary similarity between GSG1L, stargazin, and claudins, whether there is a possibility of transsynaptic interactions with presynaptic proteins and formation of “synaptic junctions” by stargazin- a possibility that has previously been discussed (Tomita *et al.*, 2001) and/or GSG1L. However, currently there is no experimental evidence in support of this hypothesis.

Despite GSG1L and stargazin binding to identical sites on AMPAR, co-assembly of the two onto one receptor complex is plausible. Consistent with this viewpoint, CNIHs and TARPs share binding sites and previous studies have shown that CNIH2 and TARP γ-8 can interact with common hippocampal AMPARs (Kato *et al.*, 2010). Future studies will be needed to evaluate potential co-assembly of GSG1L with other auxiliary subunits

onto a given synaptic receptor populations. Co-assembly would, in turn, further amplify the rich diversity of functional properties of AMPARs within the brain.

Finally, another exciting avenue for future studies would be to investigate potential activity-dependent changes in GSG1L function. It is possible that GSG1L levels, activity and the proportion of GSG1L-bound AMPARs could be regulated by activity or modified by various signaling mechanisms. For instance, visual experience alters stargazin expression and phosphorylation in the LGN (Louros *et al.*, 2014). Visual deprivation during critical period led to a significant increase in stargazin protein levels and phosphorylation levels. AMPAR auxiliary subunits have also been previously implicated in inflammatory pain induced plasticity (Sullivan *et al.*, 2017). Stargazin is expressed in the lamina II of the spinal cord horn and is essential for CP-AMPAR plasticity following inflammatory hyperalgesia. In fact, previous studies have shown that knockdown of stargazin in the spinal cord is associated with decreased pain following inflammation and postoperative pain (Tao *et al.*, 2006; Guo *et al.*, 2014). While the model of postooperative pain didn’t change the levels of stargazin, it did increase the stargazin-AMPAR interaction in the dorsal horn (Guo *et al.*, 2014). Currently, it is unknown whether GSG1L is regulated in an activity-dependent manner. It will therefore be interesting to determine the biological circumstances that are accompanied with changes in GSG1L levels and/or function.

At the gene level, there is evidence for changes in GSG1L levels in Huntington's disease (HD) mutant mice (Becanovic *et al.*, 2010). Interestingly, GSG1L gene

expression levels were downregulated in the caudate putamen specifically in aged YAC128, mouse model of HD, mice. This is particularly interesting given that, according to lacZ expression data, GSG1L expression significantly increases in older animals. Importantly, GSG1L levels are similarly downregulated in HD human patients specifically in the caudate (Becanovic *et al.*, 2010). Currently, the link between GSG1L and HD has not been investigated yet. This could also be an exciting avenue for future research.

5.4. Potential implication of GSG1L in spatial navigation

Results presented in Chapter 4 show that GSG1L KO mice exhibit some form of memory impairment as evidenced by deficits in novel object recognition task performance. This is in agreement with previous report of GSG1L KO rats, which also showed impairement in this particular memory task (Gu *et al.*, 2016). While the retrosplenial cortex, which is reciprocally connected with the AD/AV nuclei, has previously been implicated in object recency memory in rats (Powell *et al.*, 2017), anterior thalamic nuclei are more heavily associated with spatial memory tasks (Jankowski *et al.*, 2013). Given the implication of anterior thalamus in spatial memory, it will be interesting to test whether there are any deficits specifically in spatial memory tasks in GSG1L KO mice. Currently, the connection between GSG1L and spatial memory has not been investigated.

As introduced in Chapter 1, the anterior thalamus contains high concentration of head direction cells, that are specifically tuned to an animal's head direction in space (Taube, 1995). These cells selectively fire when an animal's head is facing one particular direction. Besides anterior thalamus, head direction cells have also been found in the retrosplenial cortex, mammillary bodies and in their prominent input dorsal tegmental nucleus of the Gudden within the brainstem (Sharp *et al.*, 2001). The head direction information itself is generated based on the vestibular signals arriving at the dorsal tegmental nucleus of the Gudden and the mammillary nuclei and further getting relayed to the anterior thalamus and downstream to the subiculum (Sharp *et al.*, 2001). One possible avenue for future studies is to determine whether loss of GSG1L is associated with disruptions in head direction system. Another possibility is to directly look at spatial memory tasks, which could be influenced by the head direction system (Vantomme *et al.*, 2020), comparing GSG1L KO and WT control littermates. For instance, previous studies have shown that performance of mice in Morris water maze is determined by visual as well as vestibular cues (Stackman *et al.*, 2012). Selective inactivation of the anterior thalamus can disrupt how animals respond in the Morris water maze (Stackman *et al.*, 2012). Furthermore, lesions of the anterior thalamus are also associated with an impairment in radial-arm maze performance (Mair *et al.*, 2003). We could, therefore, also investigate potential deficits in spatial learning through Morris water maze and radial-arm maze performances of GSG1L KO mice.

5.5. Emerging neuroprotective role of GSG1L

Stroke is the second leading cause of death, accounting for approximately 5.5 million deaths worldwide every year (Mukherjee & Patil, 2011; Feigin *et al.*, 2014). No notable therapeutic intervention to promote recovery currently exists. One of the dominant cellular mechanisms underlying massive neuronal death following ischemia is excitotoxicity (Clarkson & Carmichael, 2009). Indeed, supraphysiological concentrations of glutamate have been previously reported in human patients and animal models of ischemic stroke (Akins & Atkinson, 2002). Excitotoxicity is one of the principal mechanisms driving neuronal death following ischemic stroke. Elevated glutamate levels activate postsynaptic glutamate receptors leading to prolonged depolarization, ultimately resulting in calcium overload and cell death.

Multiple studies have shown that GluA2 levels are downregulated following ischemia, resulting in increased intracellular Ca^{2+} levels, ultimately causing cell death (Pellegrini-Giampietro *et al.*, 1992; Liu *et al.*, 2004; Noh *et al.*, 2005). On the other hand, expression of calcium-impermeable unedited GluA2 (R) results in decreased neurodegeneration (Pellegrini-Giampietro *et al.*, 1992). In line with these results, overexpression of calcium-permeable GluA2 (Q) confers increased sensitivity to global ischemia (Pellegrini-Giampietro *et al.*, 1992). Numerous clinical trials aimed at blocking overall AMPAR function with potent antagonists have been unsuccessful due to detrimental side effects as a result of blockade of physiological function in non-injured neurons (Sheardown *et al.*, 1990; Gill *et al.*, 1992). Thus, a more targeted approach to suppressing subset of AMPARs may yield new therapies with minimal side effects.

GSG1L reduces single-channel conductance and calcium permeability of CP-AMPARs (McGee *et al.*, 2015). Furthermore, GSG1L increases polyamine-dependent rectification. Given the negative regulatory properties of GSG1L on CP-AMPAR function, it is intriguing to speculate its role, if any, in dynamically controlling CP-AMPAR function, thereby mitigating potential excitotoxic effects of excess calcium-entry.

Additionally, there is circumstantial evidence in support of GSG1L playing a neuroprotective role following ischemic stroke (Keum and Marchuk, 2009; Du et al., 2015). In fact, GSG1L was determined as one of the candidate genes at the genetic locus that determines the extent of infarct volume in mouse models of focal cerebral ischemia (Keum and Marchuk, 2009). Similarly, a suggestive single-nucleotide polymorphism (SNP) in GSG1L was found to be associated with infarct volume upon ischemic stroke in mice and human patients (Du et al., 2015). However, these are correlative studies, and further investigation is warranted to the test the direct link between GSG1L and ischemia. It is currently unknown what aspect of GSG1L function is associated overall infarct volume following ischemic stroke.

The neuroprotective role of GSG1L has also been suggested from characterization of Huntington's disease mouse models and human patient studies. As aforementioned, GSG1L gene expression levels are significantly downregulated in the caudate of aged mutant mice and HD human patients (Becanovic *et al.*, 2010). Interestingly, GSG1L has also been associated with HD age of onset (Genetic Modifiers of Huntington's Disease Consortium. Electronic address & Genetic Modifiers of Huntington's Disease, 2019). Future investigations will be needed to directly interrogate the potential neuroprotective role of GSG1L in HD model.

5.6. Concluding remarks

The collective work presented in this dissertation thesis highlights an important aspect of AMPAR regulation *in vivo.* Among all of the known auxiliary subunits, GSG1L stands out for its prominent net negative regulatory function. These studies revelead GSG1L as a critical AMPAR regulator within the anterior thalamus with potential implications for its function on input integration and information processing. We identified a novel input-specific role for GSG1L in the AD/AV nuclei. We also established functional competition between GSG1L and stargazin. GSG1L is a dominant auxiliary subunit in corticothalamic synapses, whereas, stargazin is dominant in subiculum- and mammillothalamic synapses. Future investigations will be needed to solve the mechanisms of functional modulation of AMPARs by their auxiliary subunits at the synapse, neuron and circuit levels. Collectively, this would give us a better understanding of the rich functional diversity and molecular mechanisms of AMPAR function in the CNS. And thus, would inform us for better development of optimal therapeautic approaches targetting AMPAR dysfunction in various neurological disease states.

References

Abbott LF & Regehr WG. (2004). Synaptic computation. *Nature* **431,** 796-803.

Aggleton JP & Brown MW. (1999). Episodic memory, amnesia, and the hippocampal-anterior thalamic axis. *Behav Brain Sci* **22,** 425-444; discussion 444-489.

Aggleton JP, O'Mara SM, Vann SD, Wright NF, Tsanov M & Erichsen JT. (2010). Hippocampal-anterior thalamic pathways for memory: uncovering a network of direct and indirect actions. *Eur J Neurosci* **31,** 2292-2307.

Akins PT & Atkinson RP. (2002). Glutamate AMPA receptor antagonist treatment for ischaemic stroke. *Curr Med Res Opin* **18 Suppl 2,** s9-13.

Armstrong N & Gouaux E. (2000). Mechanisms for activation and antagonism of an AMPA-sensitive glutamate receptor: crystal structures of the GluR2 ligand binding core. *Neuron* **28,** 165-181.

Armstrong N, Sun Y, Chen GQ & Gouaux E. (1998). Structure of a glutamate-receptor ligand-binding core in complex with kainate. *Nature* **395,** 913-917.

Ayalon G & Stern-Bach Y. (2001). Functional assembly of AMPA and kainate receptors is mediated by several discrete protein-protein interactions. *Neuron* **31,** 103-113.

Azumaya CM, Days EL, Vinson PN, Stauffer S, Sulikowski G, Weaver CD & Nakagawa T. (2017). Screening for AMPA receptor auxiliary subunit specific modulators. *PLoS One* **12,** e0174742.

Barria A, Muller D, Derkach V, Griffith LC & Soderling TR. (1997). Regulatory phosphorylation of AMPA-type glutamate receptors by CaM-KII during long-term potentiation. *Science* **276,** 2042-2045.

Bateup HS, Johnson CA, Denefrio CL, Saulnier JL, Kornacker K & Sabatini BL. (2013). Excitatory/inhibitory synaptic imbalance leads to hippocampal hyperexcitability in mouse models of tuberous sclerosis. *Neuron* **78,** 510-522.

Becanovic K, Pouladi MA, Lim RS, Kuhn A, Pavlidis P, Luthi-Carter R, Hayden MR & Leavitt BR. (2010). Transcriptional changes in Huntington disease identified using genome-wide expression profiling and cross-platform analysis. *Hum Mol Genet* **19,** 1438-1452.

Bedoukian MA, Weeks AM & Partin KM. (2006). Different domains of the AMPA receptor direct stargazin-mediated trafficking and stargazin-mediated modulation of kinetics. *J Biol Chem* **281,** 23908-23921.

Ben-Yaacov A, Gillor M, Haham T, Parsai A, Qneibi M & Stern-Bach Y. (2017). Molecular Mechanism of AMPA Receptor Modulation by TARP/Stargazin. *Neuron*.

Berl S & Waelsch H. (1958). Determination of glutamic acid, glutamine, glutathione and gamma-aminobutyric acid and their distribution in brain tissue. *J Neurochem* **3,** 161-169.

Bittencourt S, Dubiela FP, Queiroz C, Covolan L, Andrade D, Lozano A, Mello LE & Hamani C. (2010). Microinjection of GABAergic agents into the anterior nucleus of the thalamus modulates pilocarpine-induced seizures and status epilepticus. *Seizure* **19,** 242-246.

Bliss TV & Lomo T. (1973). Long-lasting potentiation of synaptic transmission in the dentate area of the anaesthetized rabbit following stimulation of the perforant path. *J Physiol* **232,** 331-356.

Bonnet C, Leheup B, Beri M, Philippe C, Gregoire MJ & Jonveaux P. (2009). Aberrant GRIA3 transcripts with multi-exon duplications in a family with X-linked mental retardation. *Am J Med Genet A* **149A,** 1280-1289.

Boudkkazi S, Brechet A, Schwenk J & Fakler B. (2014). Cornichon2 dictates the time course of excitatory transmission at individual hippocampal synapses. *Neuron* **82,** 848-858.

Bowie D. (2008). Ionotropic glutamate receptors & CNS disorders. *CNS Neurol Disord Drug Targets* **7,** 129-143.

Bowie D & Mayer ML. (1995). Inward rectification of both AMPA and kainate subtype glutamate receptors generated by polyamine-mediated ion channel block. *Neuron* **15,** 453-462.

Budisantoso T, Matsui K, Kamasawa N, Fukazawa Y & Shigemoto R. (2012). Mechanisms underlying signal filtering at a multisynapse contact. *J Neurosci* **32,** 2357-2376.

Cais O, Herguedas B, Krol K, Cull-Candy SG, Farrant M & Greger IH. (2014). Mapping the interaction sites between AMPA receptors and TARPs reveals a role for the receptor N-terminal domain in channel gating. *Cell Rep* **9,** 728-740.

Calton JL, Stackman RW, Goodridge JP, Archey WB, Dudchenko PA & Taube JS. (2003). Hippocampal place cell instability after lesions of the head direction cell network. *J Neurosci* **23,** 9719-9731.

Chang PK, Verbich D & McKinney RA. (2012). AMPA receptors as drug targets in neurological disease--advantages, caveats, and future outlook. *Eur J Neurosci* **35,** 1908-1916.

Chen C, Blitz DM & Regehr WG. (2002). Contributions of receptor desensitization and saturation to plasticity at the retinogeniculate synapse. *Neuron* **33,** 779-788.

Chen C & Regehr WG. (2000). Developmental remodeling of the retinogeniculate synapse. *Neuron* **28,** 955-966.

Chen L, Chetkovich DM, Petralia RS, Sweeney NT, Kawasaki Y, Wenthold RJ, Bredt DS & Nicoll RA. (2000). Stargazin regulates synaptic targeting of AMPA receptors by two distinct mechanisms. *Nature* **408,** 936-943.

Chen S & Gouaux E. (2019). Structure and mechanism of AMPA receptor - auxiliary protein complexes. *Curr Opin Struct Biol* **54,** 104-111.

Chen S, Zhao Y, Wang Y, Shekhar M, Tajkhorshid E & Gouaux E. (2017). Activation and Desensitization Mechanism of AMPA Receptor-TARP Complex by Cryo-EM. *Cell* **170,** 1234-1246 e1214.

Chen X, Aslam M, Gollisch T, Allen K & von Engelhardt J. (2018). CKAMP44 modulates integration of visual inputs in the lateral geniculate nucleus. *Nat Commun* **9,** 261.

Chiyonobu T, Hayashi S, Kobayashi K, Morimoto M, Miyanomae Y, Nishimura A, Nishimoto A, Ito C, Imoto I, Sugimoto T, Jia Z, Inazawa J & Toda T. (2007). Partial tandem duplication of GRIA3 in a male with mental retardation. *Am J Med Genet A* **143A,** 1448-1455.

Cho CH, St-Gelais F, Zhang W, Tomita S & Howe JR. (2007). Two families of TARP isoforms that have distinct effects on the kinetic properties of AMPA receptors and synaptic currents. *Neuron* **55,** 890-904.

Christie LA, Russell TA, Xu J, Wood L, Shepherd GM & Contractor A. (2010). AMPA receptor desensitization mutation results in severe developmental phenotypes and early postnatal lethality. *Proc Natl Acad Sci U S A* **107,** 9412-9417.

Clark BJ & Taube JS. (2012). Vestibular and attractor network basis of the head direction cell signal in subcortical circuits. *Front Neural Circuits* **6,** 7.

Clarkson AN & Carmichael ST. (2009). Cortical excitability and post-stroke recovery. *Biochem Soc Trans* **37,** 1412-1414.

Collingridge GL, Kehl SJ & McLennan H. (1983). Excitatory amino acids in synaptic transmission in the Schaffer collateral-commissural pathway of the rat hippocampus. *J Physiol* **334,** 33-46.

Collingridge GL, Olsen RW, Peters J & Spedding M. (2009). A nomenclature for ligand-gated ion channels. *Neuropharmacology* **56,** 2-5.

Constals A, Penn AC, Compans B, Toulme E, Phillipat A, Marais S, Retailleau N, Hafner AS, Coussen F, Hosy E & Choquet D. (2015). Glutamate-induced AMPA receptor desensitization increases their mobility and modulates short-term plasticity through unbinding from Stargazin. *Neuron* **85,** 787-803.

Coombs ID, Soto D, Zonouzi M, Renzi M, Shelley C, Farrant M & Cull-Candy SG. (2012). Cornichons modify channel properties of recombinant and glial AMPA receptors. *J Neurosci* **32,** 9796-9804.

Cull-Candy S, Kelly L & Farrant M. (2006). Regulation of Ca2+-permeable AMPA receptors: synaptic plasticity and beyond. *Curr Opin Neurobiol* **16,** 288-297.

Curtis DR, Phillis JW & Watkins JC. (1959). Chemical excitation of spinal neurones. *Nature* **183,** 611-612.

Curtis DR, Phillis JW & Watkins JC. (1960). The chemical excitation of spinal neurones by certain acidic amino acids. *J Physiol* **150,** 656-682.

Dawe GB, Kadir MF, Venskutonyte R, Perozzo AM, Yan Y, Alexander RPD, Navarrete C, Santander EA, Arsenault M, Fuentes C, Aurousseau MRP, Frydenvang K, Barrera NP, Kastrup JS, Edwardson JM & Bowie D. (2019). Nanoscale Mobility of the Apo State and TARP Stoichiometry Dictate the Gating Behavior of Alternatively Spliced AMPA Receptors. *Neuron* **102,** 976-992 e975.

Dawe GB, Musgaard M, Aurousseau MR, Nayeem N, Green T, Biggin PC & Bowie D. (2016). Distinct Structural Pathways Coordinate the Activation of AMPA Receptor-Auxiliary Subunit Complexes. *Neuron* **89,** 1264-1276.

de Wit J & Ghosh A. (2014). Control of neural circuit formation by leucine-rich repeat proteins. *Trends Neurosci* **37,** 539-550.

Diaz-Alonso J, Morishita W, Incontro S, Simms J, Holtzman J, Gill M, Mucke L, Malenka RC & Nicoll RA. (2020). Long-term potentiation is independent of the C-tail of the GluA1 AMPA receptor subunit. *Elife* **9**.

Diaz-Alonso J, Sun YJ, Granger AJ, Levy JM, Blankenship SM & Nicoll RA. (2017). Subunit-specific role for the amino-terminal domain of AMPA receptors in synaptic targeting. *Proc Natl Acad Sci U S A* **114,** 7136-7141.

Erisir A, Van Horn SC, Bickford ME & Sherman SM. (1997). Immunocytochemistry and distribution of parabrachial terminals in the lateral geniculate nucleus of the cat: a comparison with corticogeniculate terminals. *J Comp Neurol* **377,** 535-549.

Erlenhardt N, Yu H, Abiraman K, Yamasaki T, Wadiche JI, Tomita S & Bredt DS. (2016). Porcupine Controls Hippocampal AMPAR Levels, Composition, and Synaptic Transmission. *Cell Rep* **14,** 782-794.

Everett KV, Chioza B, Aicardi J, Aschauer H, Brouwer O, Callenbach P, Covanis A, Dulac O, Eeg-Olofsson O, Feucht M, Friis M, Goutieres F, Guerrini R, Heils A, Kjeldsen M, Lehesjoki AE, Makoff A, Nabbout R, Olsson I, Sander T, Siren A, McKeigue P, Robinson R, Taske N, Rees M & Gardiner M. (2007). Linkage and association analysis of CACNG3 in childhood absence epilepsy. *Eur J Hum Genet* **15,** 463-472.

Feigin VL, Forouzanfar MH, Krishnamurthi R, Mensah GA, Connor M, Bennett DA, Moran AE, Sacco RL, Anderson L, Truelsen T, O'Donnell M, Venketasubramanian N, Barker-Collo S, Lawes CM, Wang W, Shinohara Y, Witt E, Ezzati M, Naghavi M, Murray C, Global Burden of Diseases I, Risk Factors S & the GBDSEG. (2014). Global and regional burden of stroke during 1990-2010: findings from the Global Burden of Disease Study 2010. *Lancet* **383,** 245-254.

Fisher R, Salanova V, Witt T, Worth R, Henry T, Gross R, Oommen K, Osorio I, Nazzaro J, Labar D, Kaplitt M, Sperling M, Sandok E, Neal J, Handforth A, Stern J, DeSalles A, Chung S, Shetter A, Bergen D, Bakay R, Henderson J, French J, Baltuch G, Rosenfeld W, Youkilis A, Marks W, Garcia P, Barbaro N, Fountain N, Bazil C, Goodman R, McKhann G, Babu Krishnamurthy K, Papavassiliou S, Epstein C, Pollard J, Tonder L, Grebin J, Coffey R, Graves N & Group SS. (2010). Electrical stimulation of the anterior nucleus of thalamus for treatment of refractory epilepsy. *Epilepsia* **51,** 899-908.

Floor K, Baroy T, Misceo D, Kanavin OJ, Fannemel M & Frengen E. (2012). A 1 Mb de novo deletion within 11q13.1q13.2 in a boy with mild intellectual disability and minor dysmorphic features. *Eur J Med Genet* **55,** 695-699.

Fonnum F. (1984). Glutamate: a neurotransmitter in mammalian brain. *J Neurochem* **42,** 1-11.

Fukaya M, Yamazaki M, Sakimura K & Watanabe M. (2005). Spatial diversity in gene expression for VDCCgamma subunit family in developing and adult mouse brains. *Neurosci Res* **53,** 376-383.

Furuse M, Fujita K, Hiiragi T, Fujimoto K & Tsukita S. (1998). Claudin-1 and -2: novel integral membrane proteins localizing at tight junctions with no sequence similarity to occludin. *J Cell Biol* **141,** 1539-1550.

Garcia-Nafria J, Herguedas B, Watson JF & Greger IH. (2016). The dynamic AMPA receptor extracellular region: a platform for synaptic protein interactions. *J Physiol* **594,** 5449-5458.

Gardinier KM, Gernert DL, Porter WJ, Reel JK, Ornstein PL, Spinazze P, Stevens FC, Hahn P, Hollinshead SP, Mayhugh D, Schkeryantz J, Khilevich A, De Frutos O, Gleason SD, Kato AS, Luffer-Atlas D, Desai PV, Swanson S, Burris KD, Ding C, Heinz BA, Need AB, Barth VN, Stephenson GA, Diseroad BA, Woods TA, Yu H, Bredt D & Witkin JM. (2016). Discovery of the First alpha-Amino-3-hydroxy-5-methyl-4-

isoxazolepropionic Acid (AMPA) Receptor Antagonist Dependent upon Transmembrane AMPA Receptor Regulatory Protein (TARP) gamma-8. *J Med Chem* **59,** 4753-4768.

Genetic Modifiers of Huntington's Disease Consortium. Electronic address ghmhe & Genetic Modifiers of Huntington's Disease C. (2019). CAG Repeat Not Polyglutamine Length Determines Timing of Huntington's Disease Onset. *Cell* **178,** 887-900 e814.

Ghika-Schmid F & Bogousslavsky J. (2000). The acute behavioral syndrome of anterior thalamic infarction: a prospective study of 12 cases. *Ann Neurol* **48,** 220-227.

Gill MB, Kato AS, Roberts MF, Yu H, Wang H, Tomita S & Bredt DS. (2011). Cornichon-2 modulates AMPA receptor-transmembrane AMPA receptor regulatory protein assembly to dictate gating and pharmacology. *J Neurosci* **31,** 6928-6938.

Gill R, Nordholm L & Lodge D. (1992). The neuroprotective actions of 2,3-dihydroxy-6-nitro-7-sulfamoyl-benzo(F)quinoxaline (NBQX) in a rat focal ischaemia model. *Brain Res* **580,** 35-43.

Goda Y & Stevens CF. (1994). Two components of transmitter release at a central synapse. *Proc Natl Acad Sci U S A* **91,** 12942-12946.

Gold JJ & Squire LR. (2006). The anatomy of amnesia: neurohistological analysis of three new cases. *Learn Mem* **13,** 699-710.

Granger AJ, Shi Y, Lu W, Cerpas M & Nicoll RA. (2013). LTP requires a reserve pool of glutamate receptors independent of subunit type. *Nature* **493,** 495-500.

Granseth B, Ahlstrand E & Lindstrom S. (2002). Paired pulse facilitation of corticogeniculate EPSCs in the dorsal lateral geniculate nucleus of the rat investigated in vitro. *J Physiol* **544,** 477-486.

Greger IH, Watson JF & Cull-Candy SG. (2017). Structural and Functional Architecture of AMPA-Type Glutamate Receptors and Their Auxiliary Proteins. *Neuron* **94,** 713-730.

Gu X, Mao X, Lussier MP, Hutchison MA, Zhou L, Hamra FK, Roche KW & Lu W. (2016). GSG1L suppresses AMPA receptor-mediated synaptic transmission and uniquely modulates AMPA receptor kinetics in hippocampal neurons. *Nat Commun* **7,** 10873.

Gunzel D & Yu AS. (2013). Claudins and the modulation of tight junction permeability. *Physiol Rev* **93,** 525-569.

Guo R, Zhao Y, Zhang M, Wang Y, Shi R, Liu Y, Xu J, Wu A, Yue Y, Wu J, Guan Y & Wang Y. (2014). Down-regulation of Stargazin inhibits the enhanced surface delivery of alpha-amino-3-hydroxy-5-methyl-4-isoxazole propionate receptor GluR1 subunit in rat dorsal horn and ameliorates postoperative pain. *Anesthesiology* **121,** 609-619.

Hackmann K, Matko S, Gerlach EM, von der Hagen M, Klink B, Schrock E, Rump A & Di Donato N. (2013). Partial deletion of GLRB and GRIA2 in a patient with intellectual disability. *Eur J Hum Genet* **21,** 112-114.

Hafner AS, Penn AC, Grillo-Bosch D, Retailleau N, Poujol C, Philippat A, Coussen F, Sainlos M, Opazo P & Choquet D. (2015). Lengthening of the Stargazin Cytoplasmic Tail Increases Synaptic Transmission by Promoting Interaction to Deeper Domains of PSD-95. *Neuron* **86,** 475-489.

Hamani C, Ewerton FI, Bonilha SM, Ballester G, Mello LE & Lozano AM. (2004). Bilateral anterior thalamic nucleus lesions and high-frequency stimulation are protective against pilocarpine-induced seizures and status epilepticus. *Neurosurgery* **54,** 191-195; discussion 195-197.

Hamdan FF, Gauthier J, Araki Y, Lin DT, Yoshizawa Y, Higashi K, Park AR, Spiegelman D, Dobrzeniecka S, Piton A, Tomitori H, Daoud H, Massicotte C, Henrion E, Diallo O, Group SD, Shekarabi M, Marineau C, Shevell M, Maranda B, Mitchell G, Nadeau A, D'Anjou G, Vanasse M, Srour M, Lafreniere RG, Drapeau P, Lacaille JC, Kim E, Lee JR, Igarashi K, Huganir RL, Rouleau GA & Michaud JL. (2011). Excess of de novo deleterious mutations in genes associated with glutamatergic systems in nonsyndromic intellectual disability. *Am J Hum Genet* **88,** 306-316.

Han W, Li J, Pelkey KA, Pandey S, Chen X, Wang YX, Wu K, Ge L, Li T, Castellano D, Liu C, Wu LG, Petralia RS, Lynch JW, McBain CJ & Lu W. (2019). Shisa7 is a GABAA receptor auxiliary subunit controlling benzodiazepine actions. *Science* **366,** 246-250.

Harding A, Halliday G, Caine D & Kril J. (2000). Degeneration of anterior thalamic nuclei differentiates alcoholics with amnesia. *Brain* **123 (Pt 1),** 141-154.

Hashimoto K, Fukaya M, Qiao X, Sakimura K, Watanabe M & Kano M. (1999). Impairment of AMPA receptor function in cerebellar granule cells of ataxic mutant mouse stargazer. *J Neurosci* **19,** 6027-6036.

Hawken NM, Zaika EI & Nakagawa T. (2017a). Engineering defined membrane-embedded elements of AMPA receptor induces opposing gating modulation by cornichon 3 and stargazin. *J Physiol*.

Hawken NM, Zaika EI & Nakagawa T. (2017b). Engineering defined membrane-embedded elements of AMPA receptor induces opposing gating modulation by cornichon 3 and stargazin. *J Physiol* **595,** 6517-6539.

Heine M, Groc L, Frischknecht R, Beique JC, Lounis B, Rumbaugh G, Huganir RL, Cognet L & Choquet D. (2008). Surface mobility of postsynaptic AMPARs tunes synaptic transmission. *Science* **320,** 201-205.

Henley JM & Wilkinson KA. (2016). Synaptic AMPA receptor composition in development, plasticity and disease. *Nat Rev Neurosci* **17,** 337-350.

Herguedas B, Watson JF, Ho H, Cais O, Garcia-Nafria J & Greger IH. (2019). Architecture of the heteromeric GluA1/2 AMPA receptor in complex with the auxiliary subunit TARP gamma8. *Science* **364**.

Herring BE, Shi Y, Suh YH, Zheng CY, Blankenship SM, Roche KW & Nicoll RA. (2013). Cornichon proteins determine the subunit composition of synaptic AMPA receptors. *Neuron* **77,** 1083-1096.

Higuchi M, Maas S, Single FN, Hartner J, Rozov A, Burnashev N, Feldmeyer D, Sprengel R & Seeburg PH. (2000). Point mutation in an AMPA receptor gene rescues lethality in mice deficient in the RNA-editing enzyme ADAR2. *Nature* **406,** 78-81.

Hodaie M, Wennberg RA, Dostrovsky JO & Lozano AM. (2002). Chronic anterior thalamus stimulation for intractable epilepsy. *Epilepsia* **43,** 603-608.

Hollmann M & Heinemann S. (1994). Cloned glutamate receptors. *Annu Rev Neurosci* **17,** 31-108.

Hollmann M, Maron C & Heinemann S. (1994). N-glycosylation site tagging suggests a three transmembrane domain topology for the glutamate receptor GluR1. *Neuron* **13,** 1331-1343.

Hollmann M, O'Shea-Greenfield A, Rogers SW & Heinemann S. (1989). Cloning by functional expression of a member of the glutamate receptor family. *Nature* **342,** 643-648.

Hsieh H, Boehm J, Sato C, Iwatsubo T, Tomita T, Sisodia S & Malinow R. (2006). AMPAR removal underlies Abeta-induced synaptic depression and dendritic spine loss. *Neuron* **52,** 831-843.

Huganir RL & Nicoll RA. (2013). AMPARs and synaptic plasticity: the last 25 years. *Neuron* **80,** 704-717.

Inamura M, Itakura M, Okamoto H, Hoka S, Mizoguchi A, Fukazawa Y, Shigemoto R, Yamamori S & Takahashi M. (2006). Differential localization and regulation of stargazin-like protein, gamma-8 and stargazin in the plasma membrane of hippocampal and cortical neurons. *Neurosci Res* **55,** 45-53.

Izsvak Z, Frohlich J, Grabundzija I, Shirley JR, Powell HM, Chapman KM, Ivics Z & Hamra FK. (2010). Generating knockout rats by transposon mutagenesis in spermatogonial stem cells. *Nat Methods* **7,** 443-445.

Jackson AC & Nicoll RA. (2011). The expanding social network of ionotropic glutamate receptors: TARPs and other transmembrane auxiliary subunits. *Neuron* **70,** 178-199.

Jacobi E & von Engelhardt J. (2018). AMPA receptor complex constituents: Control of receptor assembly, membrane trafficking and subcellular localization. *Mol Cell Neurosci* **91,** 67-75.

Jacobi E & von Engelhardt J. (2020). Modulation of information processing by AMPA receptor auxiliary subunits. *J Physiol*.

Jankowski MM, Ronnqvist KC, Tsanov M, Vann SD, Wright NF, Erichsen JT, Aggleton JP & O'Mara SM. (2013). The anterior thalamus provides a subcortical circuit supporting memory and spatial navigation. *Front Syst Neurosci* **7,** 45.

Jones MV & Westbrook GL. (1996). The impact of receptor desensitization on fast synaptic transmission. *Trends Neurosci* **19,** 96-101.

Kamalova A, Futai K, Delpire E & Nakagawa T. (2020). AMPA Receptor Auxiliary Subunit GSG1L Suppresses Short-Term Facilitation in Corticothalamic Synapses and Determines Seizure Susceptibility. *Cell Rep* **32,** 107921.

Kamalova A & Nakagawa T. (2020). AMPA receptor structure and auxiliary subunits. *J Physiol*.

Kamboj SK, Swanson GT & Cull-Candy SG. (1995). Intracellular spermine confers rectification on rat calcium-permeable AMPA and kainate receptors. *J Physiol* **486 (Pt 2),** 297-303.

Karataeva AR, Klaassen RV, Stroder J, Ruiperez-Alonso M, Hjorth JJ, van Nierop P, Spijker S, Mansvelder HD & Smit AB. (2014). C-terminal interactors of the AMPA receptor auxiliary subunit Shisa9. *PLoS One* **9,** e87360.

Kato AS, Burris KD, Gardinier KM, Gernert DL, Porter WJ, Reel J, Ding C, Tu Y, Schober DA, Lee MR, Heinz BA, Fitch TE, Gleason SD, Catlow JT, Yu H, Fitzjohn SM, Pasqui F, Wang H, Qian Y, Sher E, Zwart R, Wafford KA, Rasmussen K, Ornstein PL, Isaac JT, Nisenbaum ES, Bredt DS & Witkin JM. (2016). Forebrain-selective AMPA-receptor antagonism guided by TARP gamma-8 as an antiepileptic mechanism. *Nat Med* **22,** 1496-1501.

Kato AS, Gill MB, Ho MT, Yu H, Tu Y, Siuda ER, Wang H, Qian YW, Nisenbaum ES, Tomita S & Bredt DS. (2010). Hippocampal AMPA receptor gating controlled by both TARP and cornichon proteins. *Neuron* **68,** 1082-1096.

Kato AS, Siuda ER, Nisenbaum ES & Bredt DS. (2008). AMPA receptor subunit-specific regulation by a distinct family of type II TARPs. *Neuron* **59,** 986-996.

Keinanen K, Wisden W, Sommer B, Werner P, Herb A, Verdoorn TA, Sakmann B & Seeburg PH. (1990). A family of AMPA-selective glutamate receptors. *Science* **249,** 556-560.

Kerrigan JF, Litt B, Fisher RS, Cranstoun S, French JA, Blum DE, Dichter M, Shetter A, Baltuch G, Jaggi J, Krone S, Brodie M, Rise M & Graves N. (2004). Electrical stimulation of the anterior nucleus of the thalamus for the treatment of intractable epilepsy. *Epilepsia* **45,** 346-354.

Kessels HW, Kopec CD, Klein ME & Malinow R. (2009). Roles of stargazin and phosphorylation in the control of AMPA receptor subcellular distribution. *Nat Neurosci* **12,** 888-896.

Khodosevich K, Jacobi E, Farrow P, Schulmann A, Rusu A, Zhang L, Sprengel R, Monyer H & von Engelhardt J. (2014). Coexpressed auxiliary subunits exhibit distinct modulatory profiles on AMPA receptor function. *Neuron* **83,** 601-615.

Kielland A & Heggelund P. (2002). AMPA and NMDA currents show different short-term depression in the dorsal lateral geniculate nucleus of the rat. *J Physiol* **542,** 99-106.

Kim E & Sheng M. (2004). PDZ domain proteins of synapses. *Nat Rev Neurosci* **5,** 771-781.

Klaassen RV, Stroeder J, Coussen F, Hafner AS, Petersen JD, Renancio C, Schmitz LJ, Normand E, Lodder JC, Rotaru DC, Rao-Ruiz P, Spijker S, Mansvelder HD, Choquet D & Smit AB. (2016). Shisa6 traps AMPA receptors at postsynaptic sites and prevents their desensitization during synaptic activity. *Nat Commun* **7,** 10682.

Koh DS, Burnashev N & Jonas P. (1995). Block of native Ca(2+)-permeable AMPA receptors in rat brain by intracellular polyamines generates double rectification. *J Physiol* **486 (Pt 2),** 305-312.

Kott S, Sager C, Tapken D, Werner M & Hollmann M. (2009). Comparative analysis of the pharmacology of GluR1 in complex with transmembrane AMPA receptor regulatory proteins gamma2, gamma3, gamma4, and gamma8. *Neuroscience* **158,** 78-88.

Krueger DD, Tuffy LP, Papadopoulos T & Brose N. (2012). The role of neurexins and neuroligins in the formation, maturation, and function of vertebrate synapses. *Curr Opin Neurobiol* **22,** 412-422.

Kunde SA, Rademacher N, Zieger H & Shoichet SA. (2017). Protein kinase C regulates AMPA receptor auxiliary protein Shisa9/CKAMP44 through interactions with neuronal scaffold PICK1. *FEBS Open Bio* **7,** 1234-1245.

Lee HK, Takamiya K, Han JS, Man H, Kim CH, Rumbaugh G, Yu S, Ding L, He C, Petralia RS, Wenthold RJ, Gallagher M & Huganir RL. (2003). Phosphorylation of the AMPA

receptor GluR1 subunit is required for synaptic plasticity and retention of spatial memory. *Cell* **112,** 631-643.

Lee KJ, Shon YM & Cho CB. (2012). Long-term outcome of anterior thalamic nucleus stimulation for intractable epilepsy. *Stereotact Funct Neurosurg* **90,** 379-385.

Lee MR, Gardinier KM, Gernert DL, Schober DA, Wright RA, Wang H, Qian Y, Witkin JM, Nisenbaum ES & Kato AS. (2017). Structural Determinants of the gamma-8 TARP Dependent AMPA Receptor Antagonist. *ACS Chem Neurosci* **8,** 2631-2647.

Lein ES, Hawrylycz MJ, Ao N, Ayres M, Bensinger A, Bernard A, Boe AF, Boguski MS, Brockway KS, Byrnes EJ, Chen L, Chen L, Chen T-M, Chin MC, Chong J, Crook BE, Czaplinska A, Dang CN, Datta S, Dee NR, Desaki AL, Desta T, Diep E, Dolbeare TA, Donelan MJ, Dong H-W, Dougherty JG, Duncan BJ, Ebbert AJ, Eichele G, Estin LK, Faber C, Facer BA, Fields R, Fischer SR, Fliss TP, Frensley C, Gates SN, Glattfelder KJ, Halverson KR, Hart MR, Hohmann JG, Howell MP, Jeung DP, Johnson RA, Karr PT, Kawal R, Kidney JM, Knapik RH, Kuan CL, Lake JH, Laramee AR, Larsen KD, Lau C, Lemon TA, Liang AJ, Liu Y, Luong LT, Michaels J, Morgan JJ, Morgan RJ, Mortrud MT, Mosqueda NF, Ng LL, Ng R, Orta GJ, Overly CC, Pak TH, Parry SE, Pathak SD, Pearson OC, Puchalski RB, Riley ZL, Rockett HR, Rowland SA, Royall JJ, Ruiz MJ, Sarno NR, Schaffnit K, Shapovalova NV, Sivisay T, Slaughterbeck CR, Smith SC, Smith KA, Smith BI, Sodt AJ, Stewart NN, Stumpf K-R, Sunkin SM, Sutram M, Tam A, Teemer CD, Thaller C, Thompson CL, Varnam LR, Visel A, Whitlock RM, Wohnoutka PE, Wolkey CK, Wong VY, Wood M, Yaylaoglu MB, Young RC, Youngstrom BL, Yuan XF, Zhang B, Zwingman TA & Jones AR. (2007a). Genome-wide atlas of gene expression in the adult mouse brain. *Nature* **445,** 168-176.

Lein ES, Hawrylycz MJ, Ao N, Ayres M, Bensinger A, Bernard A, Boe AF, Boguski MS, Brockway KS, Byrnes EJ, Chen L, Chen L, Chen TM, Chin MC, Chong J, Crook BE, Czaplinska A, Dang CN, Datta S, Dee NR, Desaki AL, Desta T, Diep E, Dolbeare TA, Donelan MJ, Dong HW, Dougherty JG, Duncan BJ, Ebbert AJ, Eichele G, Estin LK, Faber C, Facer BA, Fields R, Fischer SR, Fliss TP, Frensley C, Gates SN, Glattfelder KJ, Halverson KR, Hart MR, Hohmann JG, Howell MP, Jeung DP, Johnson RA, Karr PT, Kawal R, Kidney JM, Knapik RH, Kuan CL, Lake JH, Laramee AR, Larsen KD, Lau C, Lemon TA, Liang AJ, Liu Y, Luong LT, Michaels J, Morgan JJ, Morgan RJ, Mortrud MT, Mosqueda NF, Ng LL, Ng R, Orta GJ, Overly CC, Pak TH, Parry SE, Pathak SD, Pearson OC, Puchalski RB, Riley ZL, Rockett HR, Rowland SA, Royall JJ, Ruiz MJ, Sarno NR, Schaffnit K, Shapovalova NV, Sivisay T, Slaughterbeck CR, Smith SC, Smith KA, Smith BI, Sodt AJ, Stewart NN, Stumpf KR, Sunkin SM, Sutram M, Tam A, Teemer CD, Thaller C, Thompson CL, Varnam LR, Visel A, Whitlock RM, Wohnoutka PE, Wolkey CK, Wong VY, Wood M, Yaylaoglu MB, Young RC, Youngstrom BL, Yuan XF, Zhang B, Zwingman TA & Jones AR. (2007b). Genome-wide atlas of gene expression in the adult mouse brain. *Nature* **445,** 168-176.

Letts VA, Felix R, Biddlecome GH, Arikkath J, Mahaffey CL, Valenzuela A, Bartlett FS, 2nd, Mori Y, Campbell KP & Frankel WN. (1998). The mouse stargazer gene encodes a neuronal Ca2+-channel gamma subunit. *Nat Genet* **19,** 340-347.

Lisman J, Yasuda R & Raghavachari S. (2012). Mechanisms of CaMKII action in long-term potentiation. *Nat Rev Neurosci* **13,** 169-182.

Liu S, Lau L, Wei J, Zhu D, Zou S, Sun HS, Fu Y, Liu F & Lu Y. (2004). Expression of Ca(2+)-permeable AMPA receptor channels primes cell death in transient forebrain ischemia. *Neuron* **43,** 43-55.

Liu YL, Fann CS, Liu CM, Chen WJ, Wu JY, Hung SI, Chen CH, Jou YS, Liu SK, Hwang TJ, Hsieh MH, Chang CC, Yang WC, Lin JJ, Chou FH, Faraone SV, Tsuang MT & Hwu HG. (2008). RASD2, MYH9, and CACNG2 genes at chromosome 22q12 associated with the subgroup of schizophrenia with non-deficit in sustained attention and executive function. *Biol Psychiatry* **64,** 789-796.

Lledo PM, Zhang X, Sudhof TC, Malenka RC & Nicoll RA. (1998). Postsynaptic membrane fusion and long-term potentiation. *Science* **279,** 399-403.

Lodge D. (2009). The history of the pharmacology and cloning of ionotropic glutamate receptors and the development of idiosyncratic nomenclature. *Neuropharmacology* **56,** 6-21.

Louros SR, Hooks BM, Litvina L, Carvalho AL & Chen C. (2014). A role for stargazin in experience-dependent plasticity. *Cell Rep* **7,** 1614-1625.

Lu W, Man H, Ju W, Trimble WS, MacDonald JF & Wang YT. (2001). Activation of synaptic NMDA receptors induces membrane insertion of new AMPA receptors and LTP in cultured hippocampal neurons. *Neuron* **29,** 243-254.

Lu W, Shi Y, Jackson AC, Bjorgan K, During MJ, Sprengel R, Seeburg PH & Nicoll RA. (2009). Subunit composition of synaptic AMPA receptors revealed by a single-cell genetic approach. *Neuron* **62,** 254-268.

Maher MP, Matta JA, Gu S, Seierstad M & Bredt DS. (2017). Getting a Handle on Neuropharmacology by Targeting Receptor-Associated Proteins. *Neuron* **96,** 989-1001.

Mair RG, Burk JA & Porter MC. (2003). Impairment of radial maze delayed nonmatching after lesions of anterior thalamus and parahippocampal cortex. *Behav Neurosci* **117,** 596-605.

Malenka RC & Bear MF. (2004). LTP and LTD: an embarrassment of riches. *Neuron* **44,** 5-21.

Mao X, Gu X & Lu W. (2017). GSG1L regulates the strength of AMPA receptor-mediated synaptic transmission but not AMPA receptor kinetics in hippocampal dentate granule neurons. *J Neurophysiol* **117,** 28-35.

Mayer ML, Westbrook GL & Guthrie PB. (1984). Voltage-dependent block by Mg2+ of NMDA responses in spinal cord neurones. *Nature* **309,** 261-263.

McGee TP, Bats C, Farrant M & Cull-Candy SG. (2015). Auxiliary Subunit GSG1L Acts to Suppress Calcium-Permeable AMPA Receptor Function. *J Neurosci* **35,** 16171-16179.

Menuz K, Kerchner GA, O'Brien JL & Nicoll RA. (2009). Critical role for TARPs in early development despite broad functional redundancy. *Neuropharmacology* **56,** 22-29.

Menuz K, O'Brien JL, Karmizadegan S, Bredt DS & Nicoll RA. (2008). TARP redundancy is critical for maintaining AMPA receptor function. *J Neurosci* **28,** 8740-8746.

Milstein AD & Nicoll RA. (2009). TARP modulation of synaptic AMPA receptor trafficking and gating depends on multiple intracellular domains. *Proc Natl Acad Sci U S A* **106,** 11348-11351.

Milstein AD, Zhou W, Karimzadegan S, Bredt DS & Nicoll RA. (2007). TARP subtypes differentially and dose-dependently control synaptic AMPA receptor gating. *Neuron* **55,** 905-918.

Mirski MA & Ferrendelli JA. (1984). Interruption of the mammillothalamic tract prevents seizures in guinea pigs. *Science* **226,** 72-74.

Morrison RS, Wenzel HJ, Kinoshita Y, Robbins CA, Donehower LA & Schwartzkroin PA. (1996). Loss of the p53 tumor suppressor gene protects neurons from kainate-induced cell death. *J Neurosci* **16,** 1337-1345.

Mukherjee D & Patil CG. (2011). Epidemiology and the global burden of stroke. *World Neurosurg* **76,** S85-90.

Nakagawa T. (2019). Structures of the AMPA receptor in complex with its auxiliary subunit cornichon. *Science* **366,** 1259-1263.

Nakagawa T, Cheng Y, Ramm E, Sheng M & Walz T. (2005). Structure and different conformational states of native AMPA receptor complexes. *Nature* **433,** 545-549.

Nakamura S, Irie K, Tanaka H, Nishikawa K, Suzuki H, Saitoh Y, Tamura A, Tsukita S & Fujiyoshi Y. (2019). Morphologic determinant of tight junctions revealed by claudin-3 structures. *Nat Commun* **10,** 816.

Nakanishi N, Shneider NA & Axel R. (1990). A family of glutamate receptor genes: evidence for the formation of heteromultimeric receptors with distinct channel properties. *Neuron* **5,** 569-581.

Narushima M, Uchigashima M, Yagasaki Y, Harada T, Nagumo Y, Uesaka N, Hashimoto K, Aiba A, Watanabe M, Miyata M & Kano M. (2016). The Metabotropic Glutamate Receptor Subtype 1 Mediates Experience-Dependent Maintenance of Mature Synaptic Connectivity in the Visual Thalamus. *Neuron* **91,** 1097-1109.

Newpher TM & Ehlers MD. (2008). Glutamate receptor dynamics in dendritic microdomains. *Neuron* **58,** 472-497.

Niciu MJ, Kelmendi B & Sanacora G. (2012). Overview of glutamatergic neurotransmission in the nervous system. *Pharmacol Biochem Behav* **100,** 656-664.

Noh KM, Yokota H, Mashiko T, Castillo PE, Zukin RS & Bennett MV. (2005). Blockade of calcium-permeable AMPA receptors protects hippocampal neurons against global ischemia-induced death. *Proc Natl Acad Sci U S A* **102,** 12230-12235.

Nomura T, Kakegawa W, Matsuda S, Kohda K, Nishiyama J, Takahashi T & Yuzaki M. (2012). Cerebellar long-term depression requires dephosphorylation of TARP in Purkinje cells. *Eur J Neurosci* **35,** 402-410.

Oh SW, Harris JA, Ng L, Winslow B, Cain N, Mihalas S, Wang Q, Lau C, Kuan L, Henry AM, Mortrud MT, Ouellette B, Nguyen TN, Sorensen SA, Slaughterbeck CR, Wakeman W, Li Y, Feng D, Ho A, Nicholas E, Hirokawa KE, Bohn P, Joines KM, Peng H, Hawrylycz MJ, Phillips JW, Hohmann JG, Wohnoutka P, Gerfen CR, Koch C, Bernard A, Dang C, Jones AR & Zeng H. (2014). A mesoscale connectome of the mouse brain. *Nature* **508,** 207-214.

Opazo P, Labrecque S, Tigaret CM, Frouin A, Wiseman PW, De Koninck P & Choquet D. (2010). CaMKII triggers the diffusional trapping of surface AMPARs through phosphorylation of stargazin. *Neuron* **67,** 239-252.

Park J, Chavez AE, Mineur YS, Morimoto-Tomita M, Lutzu S, Kim KS, Picciotto MR, Castillo PE & Tomita S. (2016). CaMKII Phosphorylation of TARPgamma-8 Is a Mediator of LTP and Learning and Memory. *Neuron* **92,** 75-83.

Pellegrini-Giampietro DE, Zukin RS, Bennett MV, Cho S & Pulsinelli WA. (1992). Switch in glutamate receptor subunit gene expression in CA1 subfield of hippocampus following global ischemia in rats. *Proc Natl Acad Sci U S A* **89,** 10499-10503.

Petrof I & Sherman SM. (2009). Synaptic properties of the mammillary and cortical afferents to the anterodorsal thalamic nucleus in the mouse. *J Neurosci* **29,** 7815-7819.

Philippe A, Malan V, Jacquemont ML, Boddaert N, Bonnefont JP, Odent S, Munnich A, Colleaux L & Cormier-Daire V. (2013). Xq25 duplications encompassing GRIA3 and STAG2 genes in two families convey recognizable X-linked intellectual disability with distinctive facial appearance. *Am J Med Genet A* **161A,** 1370-1375.

Phillips JW, Schulmann A, Hara E, Winnubst J, Liu C, Valakh V, Wang L, Shields BC, Korff W, Chandrashekar J, Lemire AL, Mensh B, Dudman JT, Nelson SB & Hantman AW. (2019). A repeated molecular architecture across thalamic pathways. *Nat Neurosci* **22,** 1925-1935.

Potier MC, Spillantini MG & Carter NP. (1992). The human glutamate receptor cDNA GluR1: cloning, sequencing, expression and localization to chromosome 5. *DNA Seq* **2,** 211-218.

Powell AL, Vann SD, Olarte-Sanchez CM, Kinnavane L, Davies M, Amin E, Aggleton JP & Nelson AJD. (2017). The retrosplenial cortex and object recency memory in the rat. *Eur J Neurosci* **45,** 1451-1464.

Priel A, Kolleker A, Ayalon G, Gillor M, Osten P & Stern-Bach Y. (2005). Stargazin reduces desensitization and slows deactivation of the AMPA-type glutamate receptors. *J Neurosci* **25,** 2682-2686.

Puckett C, Gomez CM, Korenberg JR, Tung H, Meier TJ, Chen XN & Hood L. (1991). Molecular cloning and chromosomal localization of one of the human glutamate receptor genes. *Proc Natl Acad Sci U S A* **88,** 7557-7561.

Rafols JA & Valverde F. (1973). The structure of the dorsal lateral geniculate nucleus in the mouse. A Golgi and electron microscopic study. *J Comp Neurol* **150,** 303-332.

Riva I, Eibl C, Volkmer R, Carbone AL & Plested AJ. (2017). Control of AMPA receptor activity by the extracellular loops of auxiliary proteins. *Elife* **6**.

Rodriguez CI, Buchholz F, Galloway J, Sequerra R, Kasper J, Ayala R, Stewart AF & Dymecki SM. (2000). High-efficiency deleter mice show that FLPe is an alternative to Cre-loxP. *Nat Genet* **25,** 139-140.

Rogawski MA. (2011). Revisiting AMPA receptors as an antiepileptic drug target. *Epilepsy Curr* **11,** 56-63.

Rogers SW, Andrews PI, Gahring LC, Whisenand T, Cauley K, Crain B, Hughes TE, Heinemann SF & McNamara JO. (1994). Autoantibodies to glutamate receptor GluR3 in Rasmussen's encephalitis. *Science* **265,** 648-651.

Rossmann M, Sukumaran M, Penn AC, Veprintsev DB, Babu MM & Greger IH. (2011). Subunit-selective N-terminal domain associations organize the formation of AMPA receptor heteromers. *EMBO J* **30,** 959-971.

Rouach N, Byrd K, Petralia RS, Elias GM, Adesnik H, Tomita S, Karimzadegan S, Kealey C, Bredt DS & Nicoll RA. (2005). TARP gamma-8 controls hippocampal AMPA receptor number, distribution and synaptic plasticity. *Nat Neurosci* **8,** 1525-1533.

Roy B, Ahmed KT, Cunningham ME, Ferdous J, Mukherjee R, Zheng W, Chen XZ & Ali DW. (2016). Zebrafish TARP Cacng2 is required for the expression and normal development of AMPA receptors at excitatory synapses. *Dev Neurobiol* **76,** 487-506.

Rueter SM, Burns CM, Coode SA, Mookherjee P & Emeson RB. (1995). Glutamate receptor RNA editing in vitro by enzymatic conversion of adenosine to inosine. *Science* **267,** 1491-1494.

Saitoh Y, Suzuki H, Tani K, Nishikawa K, Irie K, Ogura Y, Tamura A, Tsukita S & Fujiyoshi Y. (2015). Tight junctions. Structural insight into tight junction disassembly by Clostridium perfringens enterotoxin. *Science* **347,** 775-778.

Sakimura K, Bujo H, Kushiya E, Araki K, Yamazaki M, Yamazaki M, Meguro H, Warashina A, Numa S & Mishina M. (1990). Functional expression from cloned cDNAs of glutamate receptor species responsive to kainate and quisqualate. *FEBS Lett* **272,** 73-80.

Salpietro V, Dixon CL, Guo H, Bello OD, Vandrovcova J, Efthymiou S, Maroofian R, Heimer G, Burglen L, Valence S, Torti E, Hacke M, Rankin J, Tariq H, Colin E, Procaccio V, Striano P, Mankad K, Lieb A, Chen S, Pisani L, Bettencourt C, Mannikko R, Manole A, Brusco A, Grosso E, Ferrero GB, Armstrong-Moron J, Gueden S, Bar-Yosef O, Tzadok M, Monaghan KG, Santiago-Sim T, Person RE, Cho MT, Willaert R, Yoo Y, Chae JH, Quan Y, Wu H, Wang T, Bernier RA, Xia K, Blesson A, Jain M, Motazacker MM, Jaeger B, Schneider AL, Boysen K, Muir AM, Myers CT, Gavrilova RH, Gunderson L, Schultz-Rogers L, Klee EW, Dyment D, Osmond M, Parellada M, Llorente C, Gonzalez-Penas J, Carracedo A, Van Haeringen A, Ruivenkamp C, Nava C, Heron D, Nardello R, Iacomino M, Minetti C, Skabar A, Fabretto A, Group SS, Raspall-Chaure M, Chez M, Tsai A, Fassi E, Shinawi M, Constantino JN, De Zorzi R, Fortuna S, Kok F, Keren B, Bonneau D, Choi M, Benzeev B, Zara F, Mefford HC, Scheffer IE, Clayton-Smith J, Macaya A, Rothman JE, Eichler EE, Kullmann DM & Houlden H. (2019). AMPA receptor GluA2 subunit defects are a cause of neurodevelopmental disorders. *Nat Commun* **10,** 3094.

Schmitz LJM, Klaassen RV, Ruiperez-Alonso M, Zamri AE, Stroeder J, Rao-Ruiz P, Lodder JC, van der Loo RJ, Mansvelder HD, Smit AB & Spijker S. (2017). The AMPA receptor-associated protein Shisa7 regulates hippocampal synaptic function and contextual memory. *Elife* **6**.

Schnell E, Sizemore M, Karimzadegan S, Chen L, Bredt DS & Nicoll RA. (2002). Direct interactions between PSD-95 and stargazin control synaptic AMPA receptor number. *Proc Natl Acad Sci U S A* **99,** 13902-13907.

Schwenk J, Baehrens D, Haupt A, Bildl W, Boudkkazi S, Roeper J, Fakler B & Schulte U. (2014a). Regional diversity and developmental dynamics of the AMPA-receptor proteome in the mammalian brain. *Neuron* **84,** 41-54.

Schwenk J, Baehrens D, Haupt A, Bildl W, Boudkkazi S, Roeper J, Fakler B & Schulte U. (2014b). Regional Diversity and Developmental Dynamics of the AMPA-Receptor Proteome in the Mammalian Brain. *Neuron*.

Schwenk J, Boudkkazi S, Kocylowski MK, Brechet A, Zolles G, Bus T, Costa K, Kollewe A, Jordan J, Bank J, Bildl W, Sprengel R, Kulik A, Roeper J, Schulte U & Fakler B. (2019). An ER Assembly Line of AMPA-Receptors Controls Excitatory Neurotransmission and Its Plasticity. *Neuron*.

Schwenk J & Fakler B. (2019). Folding unpredicted. *Science* **366,** 1194-1195.

Schwenk J, Harmel N, Brechet A, Zolles G, Berkefeld H, Muller CS, Bildl W, Baehrens D, Huber B, Kulik A, Klocker N, Schulte U & Fakler B. (2012). High-resolution proteomics unravel architecture and molecular diversity of native AMPA receptor complexes. *Neuron* **74,** 621-633.

Schwenk J, Harmel N, Zolles G, Bildl W, Kulik A, Heimrich B, Chisaka O, Jonas P, Schulte U, Fakler B & Klöcker N. (2009). Functional proteomics identify cornichon proteins as auxiliary subunits of AMPA receptors. *Science* **323,** 1313-1319.

Shanks NF, Maruo T, Farina AN, Ellisman MH & Nakagawa T. (2010). Contribution of the global subunit structure and stargazin on the maturation of AMPA receptors. *J Neurosci* **30,** 2728-2740.

Shanks NF, Savas JN, Maruo T, Cais O, Hirao A, Oe S, Ghosh A, Noda Y, Greger IH, Yates JR, 3rd & Nakagawa T. (2012). Differences in AMPA and kainate receptor interactomes facilitate identification of AMPA receptor auxiliary subunit GSG1L. *Cell Rep* **1,** 590-598.

Sharp PE, Blair HT & Cho J. (2001). The anatomical and computational basis of the rat head-direction cell signal. *Trends Neurosci* **24,** 289-294.

Sheardown MJ, Nielsen EO, Hansen AJ, Jacobsen P & Honore T. (1990). 2,3-Dihydroxy-6-nitro-7-sulfamoyl-benzo(F)quinoxaline: a neuroprotectant for cerebral ischemia. *Science* **247,** 571-574.

Sheng N, Bemben MA, Diaz-Alonso J, Tao W, Shi YS & Nicoll RA. (2018). LTP requires postsynaptic PDZ-domain interactions with glutamate receptor/auxiliary protein complexes. *Proc Natl Acad Sci U S A* **115,** 3948-3953.

Sherman SM & Guillery RW. (2004). Thalamus. In *The Synaptic Organization of the Brain*, ed. Shepherd GM, pp. pp. 311–359. Oxford University Press.

Shi W, Xianyu A, Han Z, Tang X, Li Z, Zhong H, Mao T, Huang K & Shi SH. (2017). Ontogenetic establishment of order-specific nuclear organization in the mammalian thalamus. *Nat Neurosci* **20,** 516-528.

Shi Y, Lu W, Milstein AD & Nicoll RA. (2009). The stoichiometry of AMPA receptors and TARPs varies by neuronal cell type. *Neuron* **62,** 633-640.

Shibata H. (1998). Organization of projections of rat retrosplenial cortex to the anterior thalamic nuclei. *Eur J Neurosci* **10,** 3210-3219.

Shonesy BC, Jalan-Sakrikar N, Cavener VS & Colbran RJ. (2014). CaMKII: a molecular substrate for synaptic plasticity and memory. *Prog Mol Biol Transl Sci* **122,** 61-87.

Sia GM, Beique JC, Rumbaugh G, Cho R, Worley PF & Huganir RL. (2007). Interaction of the N-terminal domain of the AMPA receptor GluR4 subunit with the neuronal pentraxin NP1 mediates GluR4 synaptic recruitment. *Neuron* **55,** 87-102.

Silbereis J, Heintz T, Taylor MM, Ganat Y, Ment LR, Bordey A & Vaccarino F. (2010). Astroglial cells in the external granular layer are precursors of cerebellar granule neurons in neonates. *Mol Cell Neurosci* **44,** 362-373.

Sobolevsky AI, Rosconi MP & Gouaux E. (2009). X-ray structure, symmetry and mechanism of an AMPA-subtype glutamate receptor. *Nature* **462,** 745-756.

Sommer B, Keinanen K, Verdoorn TA, Wisden W, Burnashev N, Herb A, Kohler M, Takagi T, Sakmann B & Seeburg PH. (1990). Flip and flop: a cell-specific functional switch in glutamate-operated channels of the CNS. *Science* **249,** 1580-1585.

Soto D, Coombs ID, Kelly L, Farrant M & Cull-Candy SG. (2007). Stargazin attenuates intracellular polyamine block of calcium-permeable AMPA receptors. *Nat Neurosci* **10,** 1260-1267.

Stackman RW, Jr., Lora JC & Williams SB. (2012). Directional responding of C57BL/6J mice in the Morris water maze is influenced by visual and vestibular cues and is dependent on the anterior thalamic nuclei. *J Neurosci* **32,** 10211-10225.

Studniarczyk D, Coombs I, Cull-Candy SG & Farrant M. (2013). TARP gamma-7 selectively enhances synaptic expression of calcium-permeable AMPARs. *Nat Neurosci* **16,** 1266-1274.

Sullivan SJ, Farrant M & Cull-Candy SG. (2017). TARP gamma-2 Is Required for Inflammation-Associated AMPA Receptor Plasticity within Lamina II of the Spinal Cord Dorsal Horn. *J Neurosci* **37,** 6007-6020.

Sumioka A, Brown TE, Kato AS, Bredt DS, Kauer JA & Tomita S. (2011). PDZ binding of TARPgamma-8 controls synaptic transmission but not synaptic plasticity. *Nat Neurosci* **14,** 1410-1412.

Sumioka A, Yan D & Tomita S. (2010). TARP phosphorylation regulates synaptic AMPA receptors through lipid bilayers. *Neuron* **66,** 755-767.

Sun W, Ferrer-Montiel AV, Schinder AF, McPherson JP, Evans GA & Montal M. (1992). Molecular cloning, chromosomal mapping, and functional expression of human brain glutamate receptors. *Proc Natl Acad Sci U S A* **89,** 1443-1447.

Sun YG & Beierlein M. (2011). Receptor saturation controls short-term synaptic plasticity at corticothalamic synapses. *J Neurophysiol* **105,** 2319-2329.

Suzuki H, Nishizawa T, Tani K, Yamazaki Y, Tamura A, Ishitani R, Dohmae N, Tsukita S, Nureki O & Fujiyoshi Y. (2014). Crystal structure of a claudin provides insight into the architecture of tight junctions. *Science* **344,** 304-307.

Takebayashi S, Hashizume K, Tanaka T & Hodozuka A. (2007). The effect of electrical stimulation and lesioning of the anterior thalamic nucleus on kainic acid-induced focal cortical seizure status in rats. *Epilepsia* **48,** 348-358.

Tao F, Skinner J, Su Q & Johns RA. (2006). New role for spinal Stargazin in alpha-amino-3-hydroxy-5-methyl-4-isoxazolepropionic acid receptor-mediated pain sensitization after inflammation. *J Neurosci Res* **84,** 867-873.

Taube JS. (1995). Head direction cells recorded in the anterior thalamic nuclei of freely moving rats. *J Neurosci* **15,** 70-86.

Tomita S, Adesnik H, Sekiguchi M, Zhang W, Wada K, Howe JR, Nicoll RA & Bredt DS. (2005a). Stargazin modulates AMPA receptor gating and trafficking by distinct domains. *Nature* **435,** 1052-1058.

Tomita S, Chen L, Kawasaki Y, Petralia RS, Wenthold RJ, Nicoll RA & Bredt DS. (2003). Functional studies and distribution define a family of transmembrane AMPA receptor regulatory proteins. *J Cell Biol* **161,** 805-816.

Tomita S, Nicoll RA & Bredt DS. (2001). PDZ protein interactions regulating glutamate receptor function and plasticity. *J Cell Biol* **153,** F19-24.

Tomita S, Stein V, Stocker TJ, Nicoll RA & Bredt DS. (2005b). Bidirectional synaptic plasticity regulated by phosphorylation of stargazin-like TARPs. *Neuron* **45,** 269-277.

Traynelis J, Silk M, Wang Q, Berkovic SF, Liu L, Ascher DB, Balding DJ & Petrovski S. (2017). Optimizing genomic medicine in epilepsy through a gene-customized approach to missense variant interpretation. *Genome Res* **27,** 1715-1729.

Traynelis SF, Wollmuth LP, McBain CJ, Menniti FS, Vance KM, Ogden KK, Hansen KB, Yuan H, Myers SJ & Dingledine R. (2010). Glutamate receptor ion channels: structure, regulation, and function. *Pharmacol Rev* **62,** 405-496.

Trussell LO, Zhang S & Raman IM. (1993). Desensitization of AMPA receptors upon multiquantal neurotransmitter release. *Neuron* **10,** 1185-1196.

Twomey EC, Yelshanskaya MV, Grassucci RA, Frank J & Sobolevsky AI. (2016). Elucidation of AMPA receptor–stargazin complexes by cryo–electron microscopy. *Science* **353,** 83-86.

Twomey EC, Yelshanskaya MV, Grassucci RA, Frank J & Sobolevsky AI. (2017a). Channel opening and gating mechanism in AMPA-subtype glutamate receptors. *Nature* **549,** 60-65.

Twomey EC, Yelshanskaya MV, Grassucci RA, Frank J & Sobolevsky AI. (2017b). Channel opening and gating mechanism in AMPA-subtype glutamate receptors. *Nature*.

Twomey EC, Yelshanskaya MV, Grassucci RA, Frank J & Sobolevsky AI. (2017c). Structural Bases of Desensitization in AMPA Receptor-Auxiliary Subunit Complexes. *Neuron* **94,** 569-580 e565.

Twomey EC, Yelshanskaya MV & Sobolevsky AI. (2019). Structural and functional insights into transmembrane AMPA receptor regulatory protein complexes. *J Gen Physiol*.

Tzschach A, Menzel C, Erdogan F, Istifli ES, Rieger M, Ovens-Raeder A, Macke A, Ropers HH, Ullmann R & Kalscheuer V. (2010). Characterization of an interstitial 4q32 deletion in a patient with mental retardation and a complex chromosome rearrangement. *Am J Med Genet A* **152A,** 1008-1012.

Van Groen T & Wyss JM. (1995). Projections from the anterodorsal and anteroventral nucleus of the thalamus to the limbic cortex in the rat. *J Comp Neurol* **358,** 584-604.

Vandenberghe W, Nicoll RA & Bredt DS. (2005). Stargazin is an AMPA receptor auxiliary subunit. *Proc Natl Acad Sci U S A* **102,** 485-490.

Vann SD, Saunders RC & Aggleton JP. (2007). Distinct, parallel pathways link the medial mammillary bodies to the anterior thalamus in macaque monkeys. *Eur J Neurosci* **26,** 1575-1586.

Vantomme G, Rovo Z, Cardis R, Beard E, Katsioudi G, Guadagno A, Perrenoud V, Fernandez LMJ & Luthi A. (2020). A Thalamic Reticular Circuit for Head Direction Cell Tuning and Spatial Navigation. *Cell Rep* **31,** 107747.

von Engelhardt J, Mack V, Sprengel R, Kavenstock N, Li KW, Stern-Bach Y, Smit AB, Seeburg PH & Monyer H. (2010). CKAMP44: a brain-specific protein attenuating short-term synaptic plasticity in the dentate gyrus. *Science* **327,** 1518-1522.

Walker CS, Brockie PJ, Madsen DM, Francis MM, Zheng Y, Koduri S, Mellem JE, Strutz-Seebohm N & Maricq AV. (2006). Reconstitution of invertebrate glutamate receptor function depends on stargazin-like proteins. *Proc Natl Acad Sci U S A* **103,** 10781-10786.

Wang R, Walker CS, Brockie PJ, Francis MM, Mellem JE, Madsen DM & Maricq AV. (2008). Evolutionary conserved role for TARPs in the gating of glutamate receptors and tuning of synaptic function. *Neuron* **59,** 997-1008.

Watson JF, Ho H & Greger IH. (2017). Synaptic transmission and plasticity require AMPA receptor anchoring via its N-terminal domain. *Elife* **6**.

Wenthold RJ, Petralia RS, Blahos J, II & Niedzielski AS. (1996). Evidence for multiple AMPA receptor complexes in hippocampal CA1/CA2 neurons. *J Neurosci* **16,** 1982-1989.

Wolff M, Gibb SJ & Dalrymple-Alford JC. (2006). Beyond spatial memory: the anterior thalamus and memory for the temporal order of a sequence of odor cues. *J Neurosci* **26,** 2907-2913.

Wright NF, Erichsen JT, Vann SD, O'Mara SM & Aggleton JP. (2010). Parallel but separate inputs from limbic cortices to the mammillary bodies and anterior thalamic nuclei in the rat. *J Comp Neurol* **518,** 2334-2354.

Wu G, Lu ZH, Wang J, Wang Y, Xie X, Meyenhofer MF & Ledeen RW. (2005). Enhanced susceptibility to kainate-induced seizures, neuronal apoptosis, and death in mice lacking gangliotetraose gangliosides: protection with LIGA 20, a membrane-permeant analog of GM1. *J Neurosci* **25,** 11014-11022.

Wu Y, Arai AC, Rumbaugh G, Srivastava AK, Turner G, Hayashi T, Suzuki E, Jiang Y, Zhang L, Rodriguez J, Boyle J, Tarpey P, Raymond FL, Nevelsteen J, Froyen G, Stratton M, Futreal A, Gecz J, Stevenson R, Schwartz CE, Valle D, Huganir RL & Wang T. (2007). Mutations in ionotropic AMPA receptor 3 alter channel properties and are associated with moderate cognitive impairment in humans. *Proc Natl Acad Sci U S A* **104,** 18163-18168.

Xu-Friedman MA & Regehr WG. (2003). Ultrastructural contributions to desensitization at cerebellar mossy fiber to granule cell synapses. *J Neurosci* **23,** 2182-2192.

Yamazaki M, Fukaya M, Hashimoto K, Yamasaki M, Tsujita M, Itakura M, Abe M, Natsume R, Takahashi M, Kano M, Sakimura K & Watanabe M. (2010). TARPs gamma-2 and gamma-7 are essential for AMPA receptor expression in the cerebellum. *Eur J Neurosci* **31,** 2204-2220.

Yamazaki M, Le Pichon CE, Jackson AC, Cerpas M, Sakimura K, Scearce-Levie K & Nicoll RA. (2015). Relative contribution of TARPs gamma-2 and gamma-7 to cerebellar excitatory synaptic transmission and motor behavior. *Proc Natl Acad Sci U S A* **112,** E371-379.

Zeng M, Diaz-Alonso J, Ye F, Chen X, Xu J, Ji Z, Nicoll RA & Zhang M. (2019a). Phase Separation-Mediated TARP/MAGUK Complex Condensation and AMPA Receptor Synaptic Transmission. *Neuron*.

Zeng M, Diaz-Alonso J, Ye F, Chen X, Xu J, Ji Z, Nicoll RA & Zhang M. (2019b). Phase Separation-Mediated TARP/MAGUK Complex Condensation and AMPA Receptor Synaptic Transmission. *Neuron* **104,** 529-543 e526.

Zhao Y, Chen S, Swensen AC, Qian WJ & Gouaux E. (2019). Architecture and subunit arrangement of native AMPA receptors elucidated by cryo-EM. *Science* **364,** 355-362.

Zhao Y, Chen S, Yoshioka C, Baconguis I & Gouaux E. (2016). Architecture of fully occupied GluA2 AMPA receptor-TARP complex elucidated by cryo-EM. *Nature* **536,** 108-111.

Zheng CY, Chang K, Suh YH & Roche KW. (2015). TARP gamma-8 glycosylation regulates the surface expression of AMPA receptors. *Biochem J* **465,** 471-477.

Zucker RS. (1999). Calcium- and activity-dependent synaptic plasticity. *Curr Opin Neurobiol* **9,** 305-313.

Zucker RS & Regehr WG. (2002). Short-term synaptic plasticity. *Annu Rev Physiol* **64,** 355-405.